The Effect of High Tibial Osteotomy Correction Angle on Cartilage and Meniscus Loading Using Finite Element Analysis

KEKE ZHENG, B.E. (Hon)

THE UNIVERSITY OF SYDNEY

Sydney Orthopaedic Research Institute
www.sori.org.au

A thesis submitted in fulfilment of the requirements for the degree of Master of Philosophy

School of Aerospace, Mechanical and Mechatronic Engineering

The University of Sydney

2014

Declaration

This thesis is not being submitted in any form for another degree at any other university or institution of tertiary education. This thesis contains no material previously published by another person, except where due reference is made in the text of thesis.

Supervisory Committee

Prof. Qing Li, School of Aerospace, Mechanical and Mechatronic Engineering

Supervisor

Dr. Corey Scholes, Sydney Orthopaedic Research Institute

Co-Supervisor

Acknowledgements

First and foremost I offer my sincerest gratitude to my families for giving me so much encouragement and support throughout all my studies at University, providing a home in which to complete my writing up and taking care of my health and daily diet.

I would like to sincerely to give thanks to my thesis supervisor, Professor Qing Li, who has given me so much assistance and direction throughout this thesis, especially on the biomechanical aspects. Without his support and assistance in conducting my finite element analysis, this thesis would not have been possible.

I would like especially to give thanks to my external supervisor, Dr. Corey Scholes, who has supported me throughout my thesis with his patience and knowledge. Without his encouragement and effort, this thesis would not have been completed.

I would also take the opportunity to thank the PhD students from the school of AMME and Sydney Orthopaedic Research Institute, John Chen and Joe, in particular, for their supports, guidance and insights into the work conducted for this thesis, as well as providing me with valuable suggestions and certain technical support on both finite element analysis and gait analysis.

Lastly, I would like to thank my girlfriend, who has been through the hard time with me. She has given me so much power and happiness, without all your support, I would not have gotten this far.

Abstract

For knees afflicted by osteoarthritis (OA) progression in the medial compartment, a high tibial osteotomy (HTO) can be an important adjunct to conservative management in interrupting disease development. A medial opening wedge HTO allows shifting load from the affected medial compartment to the lateral compartment with intact cartilage by correcting the Hip-Knee-Ankle (HKA) angle. The current literature unfortunately lacks consensus with regards to the ideal correction angle based on tibiofemoral loading distribution to maximize osteotomy survival and post-operative knee function. To fill this knowledge gap, this study aimed to determine the biomechanical effects of simulated medial open-wedge HTO at varying correction angles on stress distribution in the tibiofemoral soft tissues by introducing a patient-specific modelling method.

In this study, a 3D knee finite element (FEA) model developed from MRI images of a healthy living subject was used to simulate different medial open-wedge HTO correction angles as 2.5°, 5°, 7.5° and 10° valgus(which is equivalent to the HKA angle of 0.2, 2.7, 3.9 and 6.6 valgus, respectively). The femur, tibia and fibula and articular cartilage were modelled as linear elastic, isotropic and homogenous, whereas the menisci and ligaments were modelled as nonlinear hyperelastic material. Loading and boundary condition assignments were based on the subject-specific kinematic and kinetic data recorded during gait analysis.

The compressive and shear stress distributions in the femoral cartilage and tibia cartilage of each angular case were quantified for the first time. Both the peak compressive and peak shear stresses in the medial compartment decreased as the loading axis shifted laterally but the lateral compartment increased the peak stresses. 3D finite element analysis (FEA) demonstrated that a simulated medial opening wedge HTO with 7.5° correction angle (equivalent to HKA of 3.9°) from neutral effectively reduced the loads in the medial compartment and achieved a more ideal situation with stresses most uniformly distributed between these two compartments.

More importantly, this patient-specific non-invasive analysis of stress distribution that provided a quantitative insight to evaluate the mechanical responses of the soft tissue within knee joint as a result of adjusting the loading axis, may be used as a preoperative assessment tool to predict the consequential mechanical loading information for surgeon to decide the patient specific optimal angle.

Table of Contents

List of Figures

List of Tables

Chapter 1 Introduction

Osteoarthritis (OA) is a common disease globally and it imposes a considerable ongoing health and economic burden on socioeconomic system [1]. In Australia, approximately 15% of the population is adversely affected by OA [2], with the knee most affected [1]. While it is recognised that etiology of OA is multi-factorial and complicated, biomechanics is amongst the most critical factors in its pathogenesis [3]. An unfavourable biomechanical environment or condition, such as overloading by obesity, overuse, and malalignment etc, is considered a significant risk factor attributable to the incidence of OA[4]. As more and more biomechanical factors been explored, malalignment of the lower limb has been found to influence load distribution across the articular surface of the knee joint very substantially.

The role of the loading axis in the progression of knee OA has been well recognised. Clinically, the interventions that alter the excessive forces related to position of loading axis acting on damaged tissues, such as articular cartilage, have been employed to relieve OA symptoms [5]. For knees afflicted by OA progression in the medial compartment, a medial opening wedge HTO can be an effective adjunct to conservative management of interrupting disease progression[6, 7]. By correcting the Hip-Knee-Ankle (HKA) angle, HTO shifts the mechanical load from the affected medial compartment to the lateral compartment with intact cartilage.

Although HTO significantly unloads the medial compartment and arrests the progression of OA, the literature lacks consensus on the ideal alignment to maximize osteotomy survival and post-operative knee function. While some have examined

this issue with survival studies [8-11], others have predicted the effect of correction on tibiofemoral load through cadaveric studies [12, 13]. On the other hand, finite element analysis (FEA) methods have been widely used to predict the local stress and strain distribution at the tibiofemoral joint to quantify soft tissue mechanics under different loading conditions [14-22]. Unfortunately, there have been no studies available on assessing the effect of variation in knee alignment (in terms of correction angle) using FEA. For this reason, this study adopted FEA to explore the effect of medial open-wedge HTO on the stress redistributions in femoral cartilage, tibia cartilage and menisci.

Following this introductory Chapter (Chapter 1), the thesis includes: Chapter 2, a thorough literature review by introducing the background knowledge of present study and commenting on the related studies published in literature; Chapter 3, describing the methodology with all techniques employed in this study; Chapter 4 and 5 quantifying the results with all stress distribution simulated from this study; Chapter 6, discussing the key finding and its clinical implication and Chapter 7, drawing major conclusions and recommending some critical areas for the further studies.

Publications and conference presentations raised from this MPhil study include:

Journal papers:

Zheng K, Chen J, Scholes C, Li Q (2013). **Magnetic Resonance Imaging (MRI) Based Finite Element Modeling for Analyzing the   Influence**

of Material   Properties on Menisci Responses. *Applied   Mechanics   and Materials*, 2014. 553: p.   305-09.

Journal Paper (To be submitted):

<u>**Zheng K, Scholes C, Chen J, Smith R, Lynch J, Parker D, Li Q**</u> . **The effect of high tibial osteotomy correction angle on articular cartilage and   meniscus loading using finite element   analysis.** Aim   for Journal of   Orthopaedics research.

Conference presentation:

Zheng K, Fatima M, Scholes C, Lynch J, Parker D, Li Q, An MRI-derived subject-specific finite element model of the stress and strain distributions in knee cartilage during stance phase of gait. 19th Australian & New Zealand Orthopaedic Research Society, Sept. 2013, Sydney, Australia.

Zheng K, Scholes C, Lynch J. Parker D, Li Q, The effect of high tibial osteotomy correction angle on articular cartilage loading using finite element analysis. 19th Australian & New Zealand Orthopaedic Research Society, Sept. 2013, Sydney, Australia.

Zheng K, Scholes C, Lynch J, Chen J, Parker D, Li Q, Finite element analysis of time-dependent stress and strain distribution at knee cartilage during the stance phase of gait. 8th Combined Meeting of Orthopaedic Research Sociality, Oct. 2013, Venice, Italy.

Chapter 2 Literature Review

In this Chapter, the background knowledge of the cause of OA is firstly introduced and followed by the biomechanical consideration in the progression of OA. After that, an overview of HTO and its surgical procedure are described, and then a thorough review on the published studies focusing on the optimal HTO correction angle in literature is conducted. At the last, the up-to-date FEA techniques used in knee joint biomechanics study are introduced followed by another thorough review on the applications of FEA in the area of knee joint diseases. By targeting the research gap in literature for HTO, the aim and hypothesis of this study are established to conclude this Chapter.

2.1 Medial compartment Osteoarthritis of knee

In OA, cartilage breaks down and subsequently degenerates, causing pain and stiffening in the joint from normal movements. Despite its nature of chronological aging which is considered the most important risk factor of OA, other risk factors of knee OA in young patients are related to an unfavourable biomechanical conditions, such as overloading by obesity, overuse, malalignment and genetics [23]. Of them, the malalignment of lower limb has been found to substantially influence load distribution across the articular surface of the knee joint [3, 24-27], which is therefore considered as a critical risk factor for OA progression. In this section, the varus and valgus malalignment is introduced followed by background knowledge of biomechanics in relation to knee OA.

2.1.1 Varus and valgus malalignment

Lower-limb alignment is typically defined as the hip-knee-ankle (HKA) angle and it represents a key determinant of load distribution in the knee joint [28]. The HKA angle is the lateral angle between the mechanical axes of the femur and tibia. As illustrated in Figure 1, the femoral mechanical axis is a line from the centre of the femoral head to the centre of the tibial spines, while the tibial mechanical axis (which happens to be the tibial anatomical axis as well) is the line from the centre of the tibial spines to the centre of the talus. A neutrally aligned knee is indicated with an HKA equal to 180°, whereas a valgus and varus knee position is typically indicated by an HKA >180° and HKA <180° respectively. In general, normal knee alignment is in-between 180°and 178° [29]. As a convention the HKA can also be expressed as

its angular deviation from 180° [30], i.e. 185° of HKA angle equal to 5° valgus. In addition, the Weight Bearing Line (WBL) illustrated in Figure 1 (the red line) is the mechanical axis (contacting centre of femoral head to the centre of ankle) measured as distance from the centre of the knee or as percentage of tibial width [31].
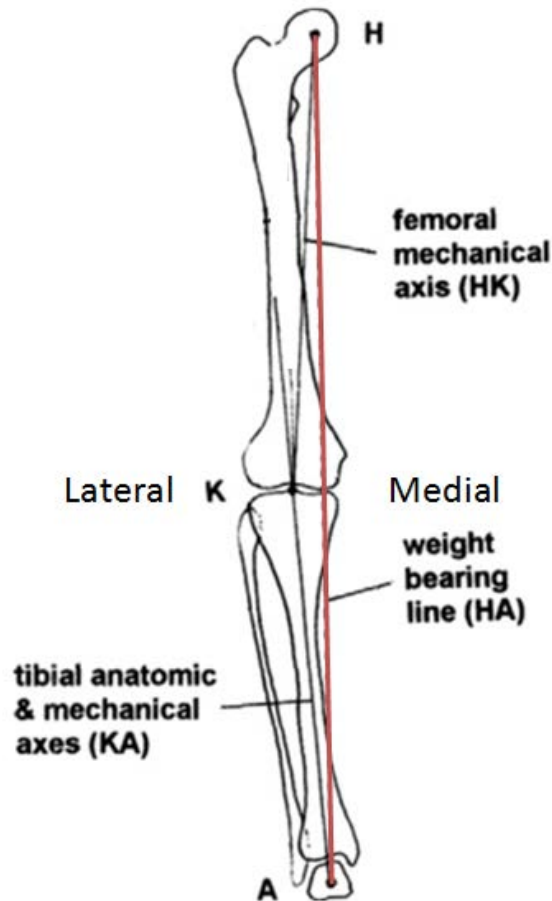
Figure 1 The mechanical axes of the femur and tibia [31]

In the normally aligned ambulating knee, load is disproportionately transmitted to the medial compartment [24] due to (1) alignment is considered as normal under 2° varus, and (2) the different anatomical structure between the medial and lateral compartment. For example, a 6° varus in single-leg stance, leads to a stress on the medial compartment to withstand 95% of the total body weight [32]. Therefore, it is

reasonable to associate the increased incidence of medial compartment OA with mechanical loading [10]. This is the reason why the medial opening wedge HTO (i.e. one of the HTO treatments for medial compartment OA) is considered in this study.

While limited quantitative evidence exists regarding the possible relationship between OA incidence and axial malalignment, the clinical correlation between the progression of early OA to advanced stages of degeneration and axial malalignment has been established [24]. The excessive compressive loading on either medial or lateral compartment may impair joint repair and maintenance. More importantly, the loss (degeneration) of articular cartilage and change of subchondral bone may in turn further increase malalignment.

2.1.2 Osteoarthritis as a mechanically driven disease

In order to understand how excessive loads result from lower limb malalignment influence the OA, a brief overview of the biomechanics of knee cartilage OA is provided in this section. The primary changes with OA typically occur in the articular cartilage, followed by the associated changes in subchondral bone [3]. The unique mechanical properties of articular cartilage depend on the extracellular matrix which consists of tissue fluid and framework of structural molecules. These highly organised molecular structures (Figure 2) were assembled by type II collagen fibres, non-collagenous proteins, proteoglycans and glycoproteins which are produced by chrondrocyte and give the cartilage its form and tensile strength [33].
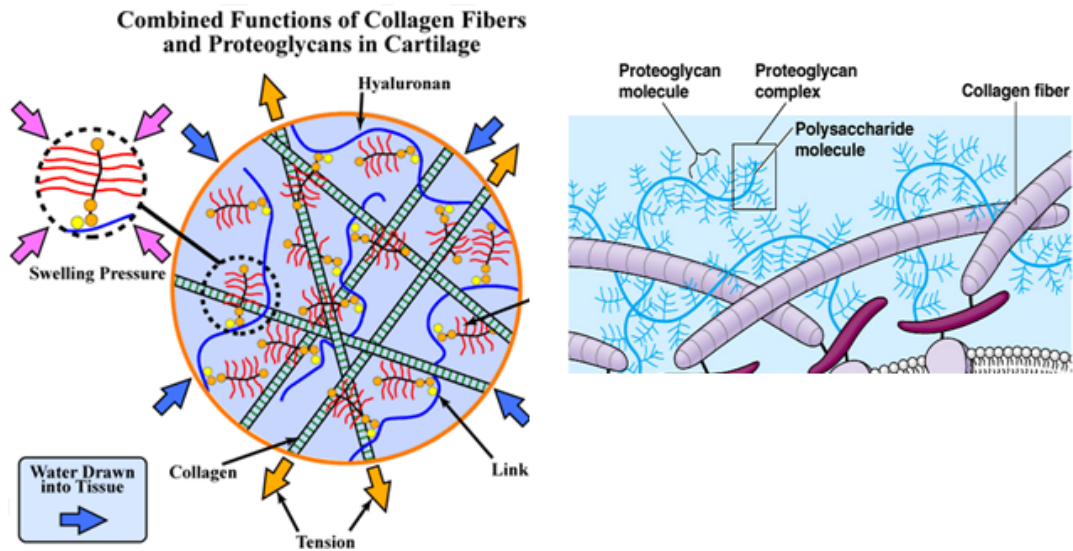
Figure 2.Molecular structure within cartilage [3]

It is claimed that the failure [3]of chrondrocyte to maintain the homeostasis between synthesis and degradation of such extracellular matrix components is one of the key reasons to trigger OA. The main cause of the chrondrocyte is the repetitively excessive loading. As a result, the water content in the matrix increases, but the proteoglucan content decreases. The collagen network is also weakened due to decreased synthesis of type II collagen. Furthermore, even the compensatory mechanism, in which the synthesis of matrix molecular and proliferation of chrondrocyte in deep layer of cartilage should increase to maintain the integrity of the articular cartilage, will eventually fail due to the loss of chrondrocyte after disruption of homeostasis (e.g. caused by excessive loading). Consequently, the OA starts.

Since the excessive loading caused by varus moment may increase the magnitude of compressive stress and strain in the cartilage, varus deformity can hasten progression of medial compartment knee OA. Shear stress induced by compression is associated with increased catabolic factors and decreased cartilage biosynthetic activity, leading

to cartilage damage [34]. Therefore, some surgical interventions may be necessary to correct the alignment of knee joint in the early stage of OA.

2.2 Medial Opening Wedge High Tibial Osteotomy

Treatment of knee OA can be fairly challenging, particularly in younger and more active patients. The role of mechanical loading in the progression of knee OA has been recognised in the previous studies [3], therefore interventions that shift the loads acting on the damaged tissues demonstrated considerable success in relieving symptoms. For a knee afflicted by OA progression in the medial compartment, the high tibial osteotomy (for short HTO) can be an important adjunct to conservative management in an effort to interrupt disease progression. The aim of an HTO is to shift load from the affected area to other areas with intact cartilage thereby providing considerable advantages over conventionally used total knee replacement in this population group by well preserving the biological knee structures [28]. Due to the increased incidence of medial compartment OA with loading as described in Section 2.1.1., this study focused on the HTO to treat the medial OA. In the following sections, an overview of high tibial osteotomy followed by a review of long term and short term clinical studies is provided.

2.2.1 Overview of medial opening wedge HTO

HTO is a surgical realignment procedure (Figure 3) designed to reduce the load acting on the degenerated medial knee compartment, thereby relieving pain and improving joint function[7]. The realignment reduces the varus moment, which also reduces the compressive loading related to knee pain and self-reported OA symptoms [1]. HTO has considerable advantages over total knee replacement (TKR) since it well preserves the native bone structure, as well as the durability and degree of

functional recovery particularly for young and active patients [26]. Therefore, osteotomy is recommended to younger and more active patients who require high knee function and wish to postpone the need for total knee replacement.
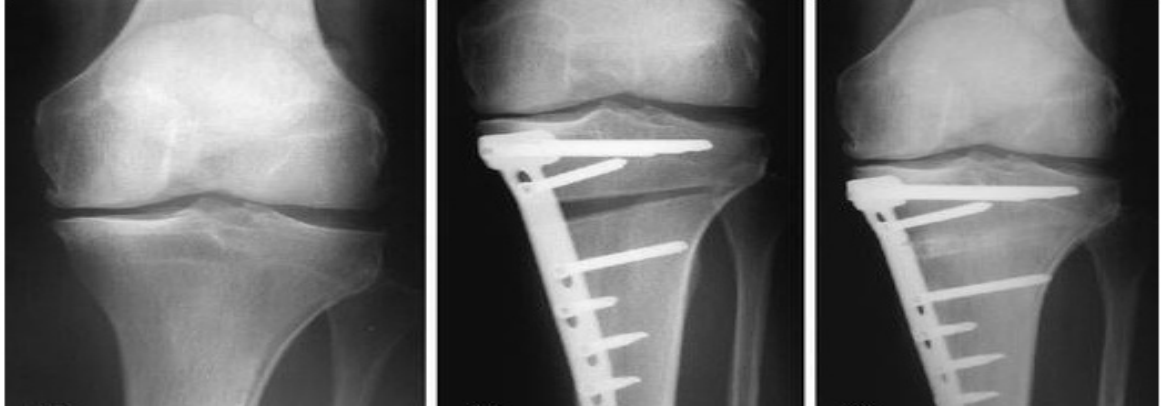
Figure 3.Radiographic results of HTO: a) preoperative, b) instant postoperative and c) 2 years postoperative[35]

One of debated issues of HTO is to decide whether to choose lateral closing wedge or medial opening wedge HTO for treating the medial compartment OA [36]. Recently, the medial opening wedge HTO has gained notable popularity and becomes a widely acceptable surgical option comparing to the lateral closing wedge HTO for treating medial knee OA, mainly due to several limitations of lateral closing HTO as follows [25, 27]:

1) Fibular osteotomy or proximal tibiofibular joint distruption,

2) Lateral muscle detachment,

3) Personal nerve dissection,

4) Bone stock loss,

5) More demanding subsequent TKR.

In a standard medial opening wedge HTO, the frontal angle (HKA) between the femur mechanical axis and the tibial mechanical axis is reduced, which corrects a

varus alignment to slight varus alignment by rotating the distal part of tibia laterally. During the rotation, the distal portion of the tibia is rotated about an anterior-posterior axis that runs through the hinge point (Figure 4b) of the osteotomy to maintain the posterior tibial slope [30]. After inserting the graft into the osteotomy gap (Figure 4a), a solid metallic plate will be used to fix the sectioned bone at the anteriomedial surface of tibia [35]. However, the position of fixation can be varied and will largely depend on other considerations, such as increasing the tibial slope to maintain joint stability.
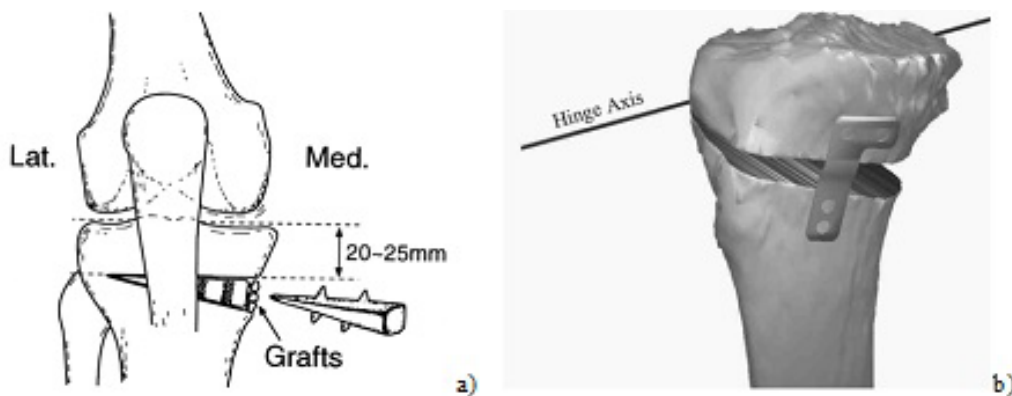
Figure 4.a) Incision is normally 20-25mm superior to proximal end of tibial and grafts are inserted into the gap, b) rotation is based on the hinge axis.[30, 35]

2.2.2 Long term and short term clinical outcome

While the HTO treatment has successfully proven to have the great short term effect on pain reduction [25, 37], the clinical outcome (e.g. survivorship) deteriorate with time. Despite a number of studies available, comparison and pooling of the clinical outcome are somewhat challenging because of the different evaluation systems and techniques used. The evaluation of clinical outcome of HTO has centred on survival analysis in which failure was defined as the need for conversion of HTO to TKR or if the osteotomy fail to reduce pain, follow-up evaluation system (various scoring

system of knee joint) and radiography for tibiofemoral angle measurement. Due to a large number of published studies on the survivorship of HTO, a summary is provided in Table 1. From this table, it is confirmed that the outcomes of HTO gradually deteriorate with time. Although Koshino et al [38] and Akizuki et al [5] reported some extraordinary high survival rate of HTO, most studies showed good results within the first 5 years and poor results after 15 years.

Table 1.Survivorship of HTO in literature

Reference	Year	Survival rate (5 Years)	Survival rate (10 Years)	Survival rate (15 Years+)
Naudie et al [39]	1999	75%	51%	39%
Billings et al [40]	2000	85%	53%	38%
Sprenger and Doerzbacher [10]	2003	86%	65-74%	N/A
Koshino et al [38]	2004	97.3%	95.1%	86.9%
Tang and Henderson [8]	2005	89.5%	74.7%	66.9%
Flecher et al [41]	2006	95%	93%	85%
Gstottner et al [42]	2008	94%	79.9%	70.5%
Akizuki et al [5]	2008	N/A	97.6%	90.4%
Hui et al [43]	2011	95%	79%	68
Efe et al [44]	2011	98%	84%	N/A

Various factors are believed to be responsible for the failure of HTO over long term (e.g. ten years or longer), such as under and over correction, advanced age, failure of fixation, patellofemoral arthritis joint instability and lateral thrust. Most of such factors can be avoided by ensuring adequate patient selection and preoperative planning, thereby improving surgical techniques. This explains why more recent

studies reported better long term outcome (Table 1), suggesting that the HTO procedure has been improved due to better patient selection, adequate preoperative planning and improved surgical techniques. Of the preoperative planning, deciding the optimal correction angle is considered to have significantly affect on the long term clinical outcome of the HTO treatment [24]. Nevertheless, an optimal correction angle remains controversial. In the following section, a detailed review of the selection of correction angle is provided.

2.3 Optimisation of correction angle

Of those preoperative planning factors, the optimal correction angle is generally considered most critical to the long term success of a HTO treatment. Despite the research in relation to the long term clinical outcome with an optimal angle, the conclusion of such topic is controversially debatable. Failure of targeting a desire alignment is responsible for poor outcomes, since alignment valgus associates with patellar subluxation, medial joint opening and rapid degeneration of the lateral cartilage, and correction leaned to neutral leads to re-progression of medial OA and patient dissatisfaction. Most of previous studies aimed to establish an optimal range of correction angle based on surgical outcomes empirically, such as survival rate [9, 10, 38, 45-49], knee scoring system [10, 36], cartilage wearing rate [50], motion analysis [51] and radiographical examination [11], etc, while few studies correlated the effect of correction angle to biomechanics, such as *in vitro* contact pressure on the cartilage [12, 13] and kinematic analysis [51].

2.3.1 Current clinical studies on optimizing correction angle

Achieving the appropriate alignment is a critical determinant of success for an HTO to treat medial compartment knee OA. However, it is surprising after several decades of osteotomy that there is little agreement between studies on the ideal alignment. In some studies [7, 52, 53], the target is a lateral shift of the weight bearing line to a maximum of 62.5% of the medial to lateral width of the tibia plateau (Fujisawa point) [54], equivalent to 3.5° of valgus [11]. The exact position of the correction was dependent upon the magnitude of mal-alignment and status of the articular cartilage

in the lateral tibiofemoral compartment as assessed by intraoperative arthroscopy. For those patients with good quality cartilage in the lateral compartment, an HKA angle of 3.5° valgus was sought, otherwise the target was towards 0°.However, after large number of clinical studies focusing on the ideal correction angle, the recommended angles vary from 1° valgus up to 10° valgus. In order to better understand the up-to-date investigation of optimal alignment following HTO, Table 2 summarised all the published clinical studies available in literature with a focus on an ideal post-operative alignment. Although some of them used the anatomical axis rather than mechanical axis (i.e. HKA angle measurement used in this study) to measure the alignment, it is possible to convert between anatomical alignment and mechanical alignment (also known as HKA) by considering an offset of 5° between them [55].

Table 2. Summary of up-to-date clinical studies in literature on optimal correction angle

Author	Year	Post-op alignment (Anatomical)(in degree)	Post-op alignment (Mechanical, i.e. HKA angle)(in degree)
Coventry et al [28]	1979		10
Inall et al [56]	1984	5-14	
Hernigou et al [50]	1987		3-6
Dugdales	1989		0-5
Valenti et al [9]	1990		3-8
Hsu et al [57]	1990		4.9
Yasuda et al [49]	1991	12-16	
Nakhostine et al [47]	1993	5-7	
Rinonapoli et al [45]	1998	10-12	
Korovessis et al [46]	1999	6-10	
Rudan et al [11]	1999	10.8	
Aglietti et al [58]	2003	8-14	
Sprenger et al [10]	2003	8-16	
Koshino et al [38]	2004	9	
Takeuchi et al [59]	2009	10.4	
Birmingham et al [60]	2009		1
Benzakour et al [36]	2010		2-4

Among these studies, we noticed that the recommended optimal alignment following HTO varies significantly by different authors; some of them even have contradictory results. Sprenger et al. investigated the correlation between various clinical radiographic factors and the long term results after HTO for medial compartment OA [10]. In their study, the radiographic valgus alignment between 3° and 11° had a significantly positive effect on survivorship for all end points (p<0.01) compared with the other parameters after an average 10 year follow-up study (n = 76 knees), with 90% survival. Similarly, Valenti et al [9] and Agletti et al [58]suggested an ideal correction angle of 3° to 8° and 3° to 9°, respectively, based on the highest survivorship in their study. However, this is still quite a big range to determine the optimal post-operative alignment.

Hernigou et al's study [50] examined an average 10 year follow-up on 93 HTO patients and they found that 3° to 6° generated the best outcome, which narrowed Sprenger et al's ideal correction range of 3° to 11° [10]. In Hernigou et al's study[50], 50 of the 93 knees had reverted to varus at the point of follow up, while there were only 5 of the 93 knees resulted in greater than 6° valgus. The standard used in their study to define unsuccessful correction was based on the lateral cartilage wear rate, even though 60% still exhibited a good, pain free result compared to 18% in the under-corrected group. Therefore, their result were interpreted in a manner that is somewhat self confirming, and while the 3° to 6° range may be a good target for post-operative alignment at follow up, greater overcorrection in surgery is ideal to ensure that this target range is actually reached and maintained by the majority of the knees in the long term. From Table 2, this narrowed range fits most of the clinical studies in literature.

On the other hand, there were some published studies that suggested an optimal alignment from 0° to 4°valgus, which is close to neutral alignment [36, 47, 60]. Benzakour et al[36] conducted an average 15 year's follow-up on 224 knees with HTO treatments, in which the excellent and good results were 75% in the group with an angle less than 4°. This result seems to be completely contradictory to those from other studies attempted to establish the correlation between correction angle and clinical results. However, Benzakour et al's study is the most recent clinical study investigating the optimal correction in HTO but unfortunately remains determination of ideal HTO alignment to be controversial.

2.3.2 Current biomechanical studies on optimizing correction angle

Other than purely investigating the effect of the amount of frontal plane knee alignment correction following HTO on clinical outcome, Briem et al [51] investigated the correlation between alignment angle and joint moment and muscle co-contraction. However, the results seemed lack of scrutiny, since they used the mean correction angles to define the under-correction and over-correction groups and found that overcorrection led to high adduction moment and muscle co-contraction which are associated with poor HTO survival rate. Although their findings narrowed the optimal alignment to smaller than 5° valgus, the lack of relating the kinematics and kinetic findings to the knee joint internal loading, limited this study to further explore the effect of changing alignment on knee joint internal loading, as the actual loading on the soft tissues (i.e. cartilages and menisci) is more relative to OA progression. Therefore, some mechanical testing experiments (as shown in Figure 5)

of HTO were conducted to investigate pressure distribution at the knee joint following a HTO surgery.

Figure 5.Mechanical testing for knee to simulate functional activities[12]

Mina et al [13] attempted to directly relate the correction angles to the contact loading pattern of the knee joint by using electronic pressure sensor inserted into the cartilage of cadaveric knee specimen under a specific mechanical testing system simulating functional activity of knee joint. 8 specimens had been used and each leg was tested through 10 different adduction angles using an osteotomy spreader in replication of real HTO treatment. Based on achieving equal stress distribution between the medial and lateral compartments which is considered most closely approximating idealised physiologic loading, Mina et al recommended an alignment of 0° – 4° of valgus, regardless of condylar width, baseline tibiofemoral alignment, body weight and the chrondral defect size. Although this recommendation somewhat narrowed the optimal HTO alignment, they[13] encapsulated one of the major challenges in HTO research that the *in vivo* measurement of stress and strain at the knee cartilage following HTO treatment is difficult during a dynamic loading cycle.

Another study [12] used pressure-sensitive film in mounted cadaveric specimens (6 specimens) to observe increased medial compartment pressure at 8°valgus with a compressive load of 1000N applied with a hydraulic apparatus. The reason for the discrepancy between this study and the Mina et al's study [13] may be due to differences in the location of the osteotomy. In their study, the osteotomy was superior to the distal attachment region of MCL, which led to a superiorly directed force on the medial tibial plateau, due to ligament tension caused by MCL.

2.3.3 Summary of the limitations and challenges of current studies

Although deciding an optimal angle of valgus correction is critical for achieving the long term survival result, many studies on clinical outcome have been linked to pursuit of such an empirical optimal angle, with as many conclusions as authors[9-11, 28, 36, 38, 41-46, 53-56] drawn. Most of the above studies were largely clinical based and lacked biomechanical insights into the causes of such controversy recommendations. Although the recommended alignment range has been narrowed by some cadaver mechanical testing which directly investigated the effect of changing alignment and loading in cartilage, the need to insert electronic pressure sensors, particularly under the menisci, limits this approach to *in-vivo* studies. Despite the difficulty of *in-vivo* measurement, the intra-patient variability of knee anatomy and difference of loading, particularly during functional tasks [21], have suggested a need for patient-specific quantification of tibiofemoral contact loading.

Although HTO has been employed widely in the past half century, optimising the correction angle of medial opening wedge HTO pre-operatively based on patient-

specific knee anatomy and subsequent biomechanics can increase survival rate of the procedure and restoration of patient function post-operatively. Facing the key challenge of quantifying the effects of varying correction angles on patient-specific knee load distribution non-invasively prior to surgery, it is worthwhile employing a new approach to optimising the HTO alignment based on knee biomechanics pre-operatively. This method should be able to provide the insightful understandings comparable to those derived from the experiments of mechanical testing or follow-up assessment of clinical studies.

2.4 Introduction to Finite Element Analysis in Knee joint biomechanical study

While the *in vitro* mechanical testing method provides some experimental results of loading distribution at the knee joint, there are still some limitations to impede detailed study on the quantitative investigation into the mechanism at the knee joint. Of those studies reviewed in the previous sections, only the surface pressures were recorded by placing the pressure-sensor film in-between cartilage and meniscus. The shear stress and strain within the cartilage structure, which are more significantly related to the progression of OA, however, could not be determined directly and precisely. The complexity of anatomical structure of the knee joint makes it very difficult (if not impossible) to use theoretical approaches, such as geometric abstraction and free body diagrams [61], for the biomechanics analysis. It is for this reason that numerical techniques have now become more and more popular in biomechanics. Computer-assisted design (CAD) and finite element analysis (FEA) provide an opportunity to simulate surgical effects in a patient-specific setting. In this section, an overview of Finite Element Method (FEM) is provided and some applications of FEA on knee joint are reviewed.

2.4.1 Overview of Finite Element Analysis

FEA is a promising method to overcome the challenge of performing direct measurement of stress/strain within such a complicated anatomy as knee joint *in vivo* by developing 3D finite element (FE) models for estimating the mechanical responses of the joint internal structures, where direct or indirect *in vivo* or *in-vitro*

22

measurement is difficult or impossible. The principle behind this numerical method is to perform the quantitative analysis of complex structure by modelling its anatomical geometry in a finite number of fine elements with relatively simple geometries. Then each element is processed individually by choosing adequate functions for interpolation to set up elemental stiffness matrix with assignment of the material properties. According to the connectivity, all these individual elemental stiffness matrices are then summed up in a proper way to form the global stiffness matrix. After the system matrices have been assembled, a numerical solver is then employed to calculate the unknown vector of nodal displacements under applied external loading. Thus the stress and strain can be derived from the nodal displacements calculated.
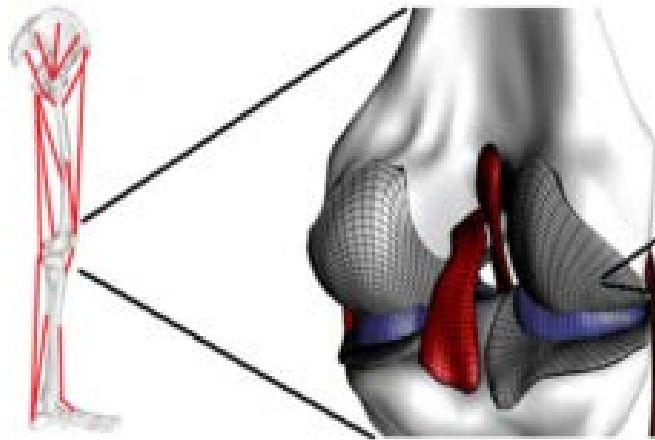
Figure 6. Finite element representations of biological structures can be used as a subsidiary model in different modeling modalities, e.g. musculoskeletal movement simulations coupled with finite element analysis of joint.[62]

Since its initial development for aerospace engineering in 1940s, FEM has been employed in a wide variety of industries. Advances in magnetic resonance imaging (MRI) techniques have enabled the development of sophisticated 3D FE models to precisely capture the patient-specific geometries of both hard and soft tissues in the region of interest (RoI) .Exponential improvement in computational power allows

generation of highly sophisticated models to more precisely simulate complicated tissue responses, thereby reflecting more realistic biomechanical behaviours. In the past decades, extensive FE models have been developed. Of those studies, coupling the FE model with *in-vivo* kinematic data is a common way to analyse true tissue deformation (Figure 6) [62]. This results in a more convincing simulation and prediction of the loading condition in FEA. The following section will review numerous studies published in literature that have used FE techniques to analyse the stress and strain distribution at the knee joint under different loading conditions for investigating the effects of ligament injury, meniscus injury, cartilage defect and normal knee joint contact mechanism [63].

2.4.2 Up-to-date FEA technique on knee biomechanics

The up-to-date studies have demonstrated validity and effectiveness of knee biomechanics under simulated realistic loading under either physiological or non-physiological conditions. Since there have been a large body of FEA studies on analysing the biomechanics of the knee joint, this review will focus only on those that used a complete 3D model of the human knee (including the femur, tibia, articular cartilage, meniscus and primary ligaments) for its relevance to this study.

Validation of the FE model of human knee was considered an important step for its critical role in understanding the biomechanical details. Li et al [17] presented a detailed three-dimensional finite element model of knee joint and validated it via the experimental data. At that time, the geometry of the knee joint was obtained from Magnetic Resonance (MR) images of a cadaveric knee specimen, in which both soft

and hard tissues were included. The same specimen was tested in a biomechanical testing system and the kinematics under anterior-posterior tibial loads was obtained. Such kinematic data was then compared with the results (tibia anterior-posterior translation) calculated from finite element solution. The agreement between the FEA and experimental results has proven the validity of the computational model. Therefore, the procedure and protocol of FE modelling in Li et al's study could be considered as a benchmark for future FE study concerning the knee biomechanics.

Since the articular cartilage is relatively thin in the knee joint, the variation of cartilage thickness was essential during either manual or automatic segmentation process of FE modelling. The effect of cartilage thickness variation on contact stress was quantified through five FE models of knee in Li et al's study [64]. One was the average FE model constructed from the mean values of the digitised contours of the cartilage and the other four were constructed by varying the mean value of thickness by ±5% and ±10%. Their results demonstrated that the 10% of variation in the cartilage thickness may result in a difference of approximately 10% of peak contact stress in the linear-elastic model where contact mechanics was involved. Therefore, the variation of cartilage thickness was considered to have significant influence on the FE results. Further investigation by Li et al[64] into the effect of variation in material properties of soft tissues on contact stress claimed that the stress distribution is also sensitive to the accuracy of material properties of the cartilage model, especially to the variation in the Poisson's ratio. As a result, the FE results are considered sensitive to both cartilage thickness and material properties of cartilage and other soft tissues. Therefore, selecting proper material model and accurate segmentation of knee joint soft tissues are critical in a FEA study.

Although the FE results are sensitive to material properties of soft tissue cartilage, the FE results are less sensitive to the materials properties of hard tissue bones. To avoid unnecessary computational expenses, bone was normally considered as rigid body attributable to its relatively high density and Young's modules comparing with other soft tissues in knee joint. In Donahue et al's study[16], a 3D FE knee joint model was generated based on CT images to determine whether assuming bone as rigid body could affect contact behaviour. Under the application of a 800 N compressive load, the maximum pressure, mean pressure, contact area, total contact force and coordinate of the centre of pressure were determined. The findings suggested that the contact responses within knee joint have no significant difference whether the bone is assumed rigid body or deformable body. This explains why bone has been considered either as rigid body or linearly elastic isotropic material in literature.

To define the boundary condition, rotation is an important consideration of knee joint loading, as reported by Bendjaballah[63]. Their study aimed to construct a detailed knee model included all major tissue structures (e.g. tibia, femur, cartilages, menisci and ligaments) for investigating the contact mechanism between menisci and cartilages with and without rotation constrained. Their knee model was reconstructed from CT images of a cadaveric knee joint. Only hard tissues can be clearly observed from the CT images, therefore a laser based three-dimensional coordinate digitising system was used to impose the geometry of soft tissues into the bone structure. The incremental response of the tibiofemoral joint in full extension was determined under axial forces of up to 1000N applied on femur. When the axial rotation was left

unconstrained, the load transferred through the joint was found to be greater for the lateral compartment (60%) than for the medial compartment. If the axial rotation is fixed, two compartments share the load nearly equally. Therefore, the constraint of the axial rotation had significant effects on the results of loading between the two compartments and should be considered when applying loading and boundary conditions in FEA.

Most of abovementioned FEA studies applied simple force condition without considering patient-specific physiological loading during functional activities, while it could represent a more realistic mechanical behaviour within the knee joint. In Yang et al's study [21], the soft tissue deformation in knee joint was analysed by post-processing of a subject-specific musculoskeletal loading state. The entire stance phase of the gait cycle of three healthy subjects with normal, varus and valgus alignment respectively was employed in the FEA for simulating soft tissue deformation. Either varus or valgus moment caused by varus and valgus alignment was respectively generated at different times of the stance phase of gait cycle, and a correlation between varus/valgus moments with the normal stress distribution of cartilages and menisci was indicated. Loading data varies between individuals, which imply that different functional patterns between individuals such as varus/valgus moments, internal and external rotational moments, have significant influence on the FEA results. In another study by Yang [65], the importance of considering the subject-specific loading data in FEA was again emphasised by simulating the tibiofemoral joint contact loading with different lower limb alignments, which resulted in different loading distributions across different compartments.

2.4.3 Current FEA applications in knee joint studies

With the validated FE models published in numerous FE studies, there has been considerable confidence of using FEA technique for such clinical problems as HTO treatment. A previous study [66] used FEM to study the three-dimensional stress and strain behaviour in the MCL (medial cottateral ligament), where the kinematic data from a musculoskeletal modelling study (motion analysis and force platform during gait analysis) was employed to the FE model to simulate patient-specific stress/strain distributions. They found that the strain distribution within the MCL was non-uniform and changed with flexion angle. The highest MCL strains occurred at full extension in the posterior region of the MCL, proximal to the joint line during valgus loading, which suggests that such a region may be most vulnerable to injury under such loading conditions.

Peña et al [20, 67, 68] conducted a series of FEA studies to investigate the stress and strain behaviours in the soft tissues of a healthy human knee joint, after meniscectomy and with an osteochondral defect. The same MRI-based model was used for all these studies. In the study of meniscectomy, the minimal principal stresses corresponding to a compressive load at full extension were obtained for the posterior region of the medial meniscus and the corresponding region of the cartilage. Under an axial compressive loading at the demur, the maximal contact stress in the articular cartilage after meniscectomy was about twice of that in a healthy joint. For a study on overall loading distribution of all soft tissues of the knee joint[67], the results reproduced complex, non-uniform stress and strain distribution occurred in such soft tissues (Figure 7) connecting to the human knee joint under an external physiological load. Their further FEA study [68]was conducted to explore the

influence of osteochondral defect size and location on the stress and strain concentration around the defect rim. From their results, it was found that no stress concentration observed around the rim of small defects, since the stress distribution was mainly borne by the meniscus. Nevertheless, significant stress concentration was found around the rim of large defects, which was considered to be of important clinical implications regarding the long-term integrity of the adjacent cartilage of osteochondral defects. Overall, all the results predicted from FEA have considerable clinical significance on investigating these common knee joint diseases.
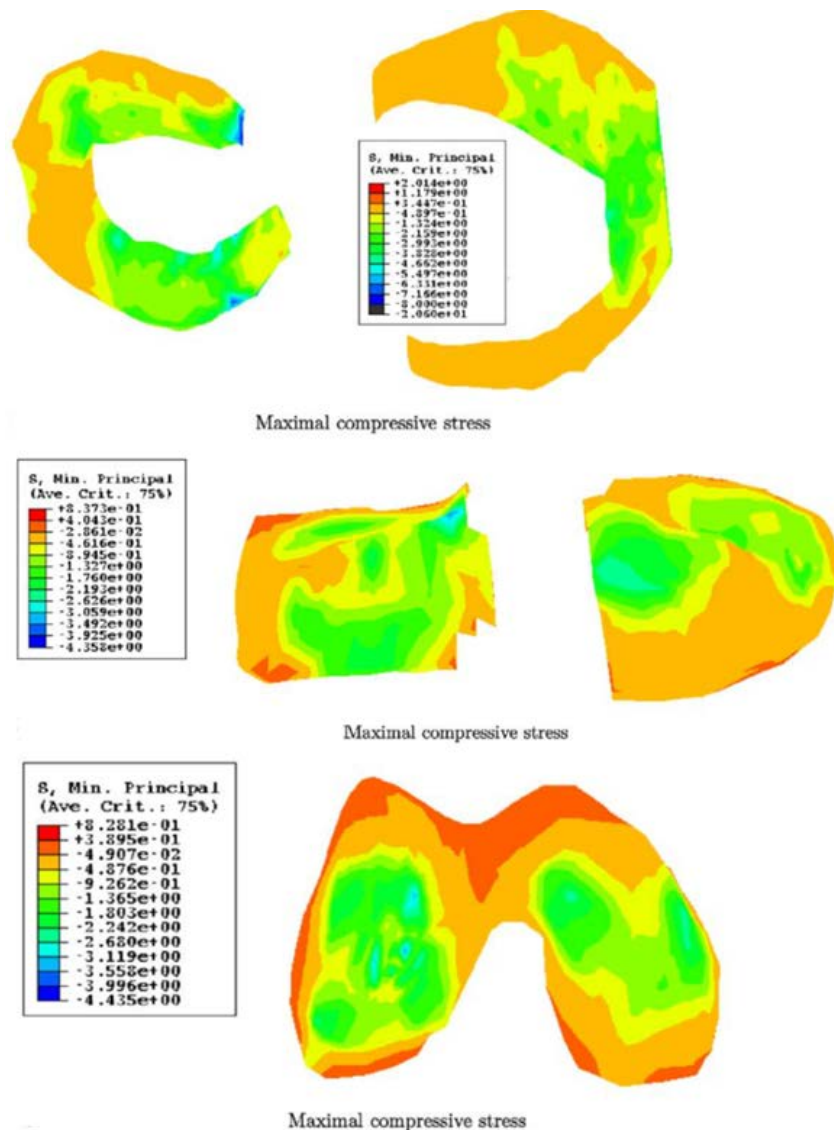
Figure7.Stress distribution on the menisci and cartilages. [67]

With its advantages over *in vivo* cadaveric studies and the potential in clinical utility in the orthopaedic area, FEA technique was used in a few studies on the HTO procedure. Izaham et al [69] used FEA to analyse two common types of fixing plate of HTO, while another study by Blecha et al [70] investigated two plate positioning systems to examine their effects on the overall loading distribution of knee joint. Although both studies proved the expelling success of FEA technique employing to contribute in such a clinical issue as HTO treatment, the surgical simulation of HTO was conducted by simply extruding a wedge out of proximal region of tibia rather than actually rotating the tibia to alter the alignment. This simplification eliminates the involvement of the rearrangement of compressive loading distribution due to an increased valgus moment after changing alignment. It was necessary to change the mechanical loading axis for reflecting a proper HTO surgery, which could be simulated by bending the distal portion of the tibia. Therefore, a precise HTO simulation involving bending of tibia to vary lower limb alignment would definitely provide more realistic and clinical relevant results.

In literature, Yang et al [65] investigated the effects of the frontal plane tibiofemoral angle on the stresses and strains distribution at the knee cartilage which was considered most relevant to the objective of this study. In their study, three patients with valgus, normal and varus knee alignment were studied to relate the variation of loading distribution from one compartment to another with the shifted loading axis. Although this study provided important insight into the understanding of the effect of HTO correction angle on stress distribution of the knee cartilage; it could be more persuasive to explore the loading distribution relative to the different loading axes

(e.g. WBL and relative frontal plane correction angle) in one specific subject, since different anatomical geometries of different patients may influence the loading distribution and magnitude to a considerable extent.

2.5 Knowledge gap and research aims of this study

As abovementioned, the current literature lacks of consensus with regard to the ideal correction angle to maximize osteotomy survival rate and post-operative knee function based on knee biomechanics. While some have examined this issue with survival studies *in vivo* and cadaveric experiments, none can predict the effect of correction on tibiofemoral load. Furthermore, FEA has been used to assess the local stress and strain distribution at the tibiofemoral joint for understanding soft tissue behaviour subject to different loading conditions. However, there have been no studies available on assessing the effect of variation of HTO correction angle through FE modelling.

To address such knowledge gaps in the current literature, the aim of this study was to introduce a patient-specific approach to determine the effect of simulated medial open-wedge HTO with varying correction angles on contact pressure and shear stress distributions within the tibiofemoral cartilages and menisci. The contact pressure represents the compressive loading on the soft tissues of knee joint; while the shear stress was believed to associate with increased catabolic factors and decreased cartilage biosynthetic activity and leads to cartilage damage[34]. It was hypothesised that: (1) the stresses at both cartilage and meniscus of the medial knee compartment would decrease as the valgus correction angle increased; and (2) stress between two compartments would be equally distributed when reaching a specific HKA angle. Thus this study is dedicated to understanding of these critical issues relevant to HTO treatments.

Chapter 3 Modelling and Surgical Simulation

An overview of the methodologies applied in this study is shown in Figure 8. Firstly, a subject was selected for MRI scanning; and then both a knee joint model and a whole lower limb model were developed based on the MRI images by segmentation. The lower limb alignment was measured two-dimensionally on the lower limb model and interoperates it onto the knee joint model for obtaining proper alignment in knee joint as a reference for simulating different HTO corrections. The loading and boundary conditions applied to the models were obtained via the specific gait test and analysis. The stress distributions across the cartilage and menisci predicted by the finite element method would then be quantified in each model with different degrees of corrections.
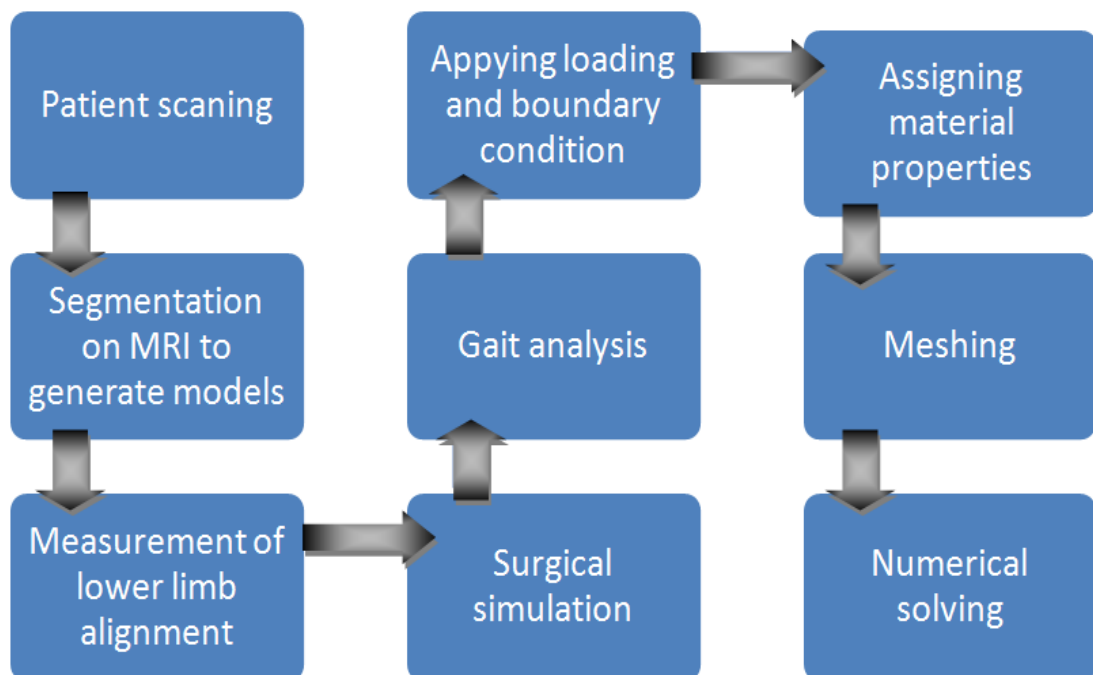
Figure 8. Overview of the methodology

The process of employing FEA technique to predict respective stress/strain results will be described in next Chapter. In this current Chapter, the involved modelling issues, such as subject selection and scanning, modelling of knee joint, measurement of lower limb alignment and surgical simulation of the medial opening wedge HTO, are discussed in detail.

3.1 Subject selection and MRI scan

The present study aimed to develop an *in-silico* procedure by using MRI based finite element analysis technique to quantify the stress distribution on soft tissues of knee joint under different degree corrections of HTO. Since the patients underwent HTO are normally suffering unicompartment OA, which suggests that the cartilage of this compartment is not intact (e.g. cartilage holes of defects), and the defected cartilage may induce considerable complications of the overall stress distribution at the cartilage to be investigated. To restrain our attention to the key issue of correction angle, therefore, a volunteer with normal lower limb alignment has been selected for this study. The height and weight of the subject was 179cm and 74kg, respectively.

As the most fundamental part of a biomechanical FEA, accurate anatomical model has become possible as the rapid development of high resolution medical CT or MR imaging techniques, in which the contour of region of interest based on the signal intensity (i.e. grey value) can be manually or automatically segmented [71]. Since the grey value can be directly associated with the mineral density of certain human tissues, the geometry and materials of the model are almost identical to the original anatomy. Despite the fact that MRI uses a magnetic field to do the same thing as CT does without known side effects due to radiation exposure, MRI provides much better details in the soft tissues (by stimulating the hydrogen contained molecular in soft tissues). Such advantages in MRI allow us to capture the geometry and some material properties of the soft tissue during segmentation, rather than using some complicated methods, e.g. using laser-based three-dimensional coordinate digitizing system to impose geometry of soft tissue into the bone geometry generated from the

CT images in literature[16]. Thus, the MRI scanning was performed in this soft tissue focused study.

Due to the limitation of Field of View (the size of the two dimensional spatial encoding area of the image) in MRI scanning, it is impossible to scan the whole lower limb in the sagittal plane, which is nevertheless the ideal plane for segmenting major soft tissues in the tibiofemoral joint. For this reason, two sets of MRI scanning were conducted in both axial and sagittal views (Figure 9a). The scan through the axial plane was able to obtain the whole leg from hip to ankle, through which a whole lower limb model can be generated for the alignment measurement. The other scan was performed in the sagittal plane to obtain the MRI data with tibia and femur bones and all soft tissues (cartilages, menisci and ligaments) involved, from which a detailed model of knee joint can be generated.

During the sagittal plane scan, the subject's left knee, positioned at full extension, was subjected to the MRI scanner with a proton density weighted SPACE sequence and 3.0 Tesla magnets. The MR scan was performed with a surface coil and spanned from the medial to the lateral extremes of the knee. The scan consisted of parallel digital images separated at 0.5 mm intervals (resulted in 163 slices in total) with a FOV of 150 ×150 mm with 256×256 pixel resolution (Figure 9b). During this MR scanning protocol, the contrast between hard and soft tissues in the knee joint was enhanced.

Although the use of axial plane scan is capable for obtaining the data of the whole low limb, it cannot process the whole leg in one cycle because the scanning space

can only cover part of the leg. Four cycles had been used to scan the whole leg separately, i.e. hip to femur, femur to knee joint, knee joint to tibia and tibia to ankle. During the entire process, fish oil capsules have been attached on the skin as anatomical landmarks that could be used for registration and assembly of the whole leg model which will be described in next section.

During the axial plane scanning, the subject remained in the same position as in sagittal plane scanning for maintaining the identical coordinate system for the both sets of data (the axial and sagittal planes). This is because the alignment of this leg measured on the whole leg model (generated from the axial plane) would be interoperated onto the knee model generated from the sagittal plane during the alignment measurement. Since the whole leg model would be used for measurement only, a thicker space between two slices (1mm which resulted in 81 slices in total) was used in this scanning for minimising time cost. Also, the soft tissues would not be included in this model, instead a sequence of IW (intermediate-weighted) TSE (turbo spin-echo) which is considered ideal for bone tissue observation was employed during the scan (Figure 9a).

Axial view
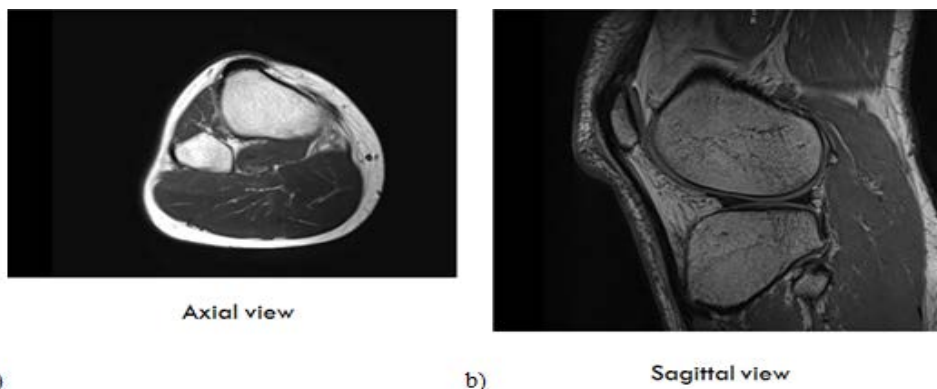
a)   b)   Sagittal view

Figure 9a) IW TSE sequence MRI of using axial view, b) PD weighted SPACE sequence MRI of usig sagittal view

3.2 Modelling of the knee joint

As mentioned in the previous section, image-based modelling has become a popular and effective procedure for the application of finite element methods to a wide range of biomechanical studies that were previously challenged by the difficulty of obtaining the realistic geometry of human anatomy. ScanIP (4.0, Simpleware, UK) is a commercial image processing software package that allows for the conversion of 3D anatomical data obtained from MRI/CT scans to a 3D solid and FE model.

During the importation of the DICOM (Digital Imaging and Communications in Medicine) data from MRI scans into ScanIP, the contrast between different "regions" of the knee joint in terms of grey value can be adjusted in order to help distinguish different tissues. Re-sampling is another important step prior to the modelling process, as it can reduce the overall size of the image while maintaining a good resolution for retaining small anatomical details. A resolution of 0.45×0.45×0.45mm resulted from a more visually defined image was adopted in this study.

Segmentation of the models was conducted manually through visual identification of the region boundaries. This is because the grey value intensities between different tissues (such as bone and muscle) was somewhat fairly similar to each other, which made the automatically segmentation sometimes lose control of region identification. As shown in Figure 10, the Paint Tool in ScanIP was first used to outline the region of interest and then the "Floodfill" tool was used to create the active mask within that region.
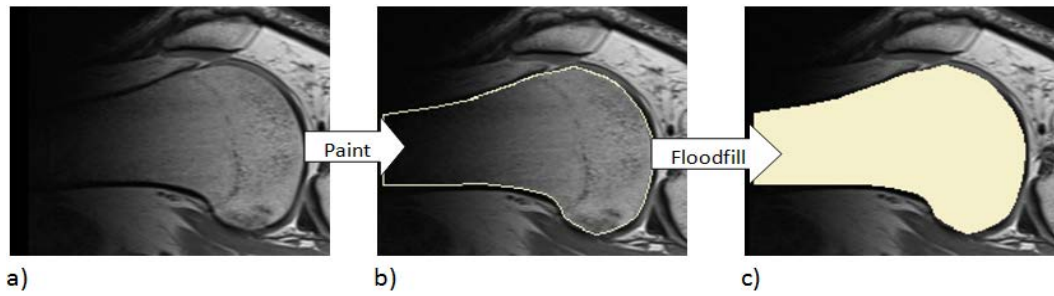
Figure 10. Demonstration of the process of useing segamenting tools

This process was repeated for all slices. In total, there were 11 masks generated representing eleven different tissues in the knee joint, which are respectively femur, femoral cartilage, tibia, tibial cartilage, fibula, fibula cartilage, menisci, MCL, LCL, ACL and PCL (Figure 11).
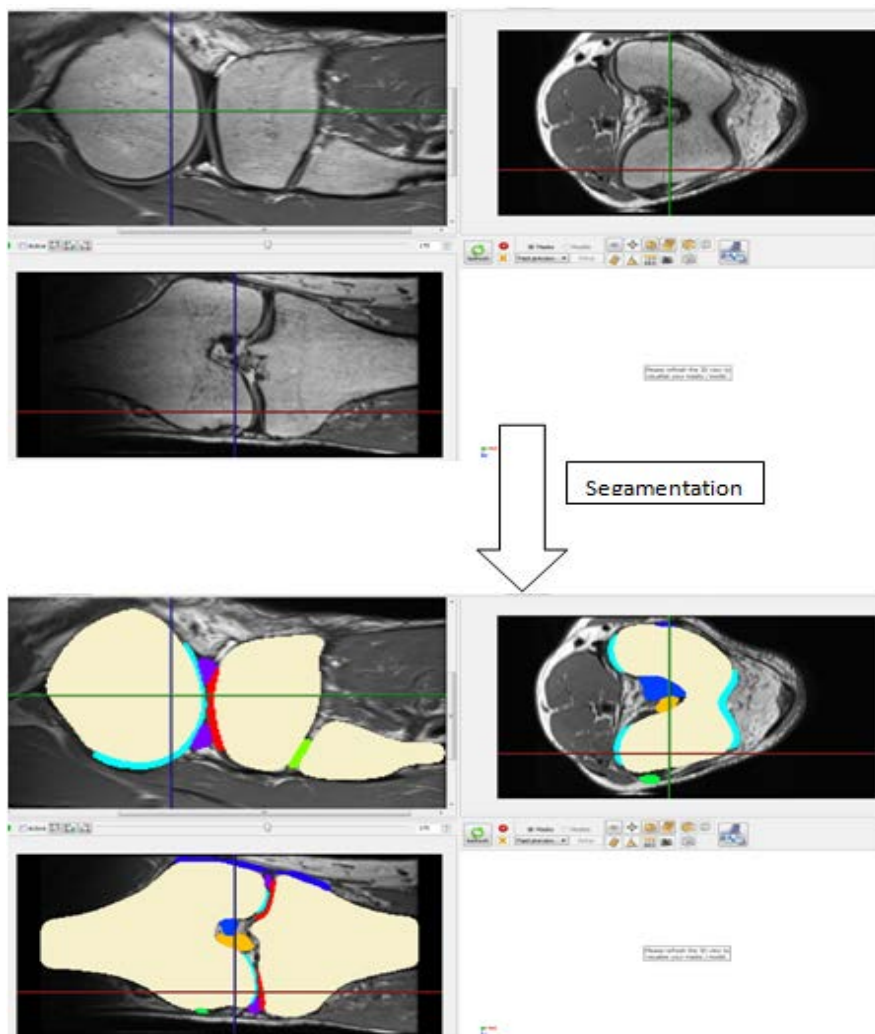
Figure 11. Demonstration of segmentation of all tissues

Once the segmentation of all slices were completed, all masks were stacked together to form a 3D model, which was visualised in ScanIP. However, the model was relatively rough at this stage due to lack of interpolation between masks of abjection slices (Figure 12a). A recursive Gaussian filter was then employed on each mask to smooth the model. Of the Gaussian filter, the Gaussian kernel sigma is a spatial parameter that control how many neighbouring pixels around each target pixel should contribute to the smoothing operation. Specifically, the bigger the Gaussian kernel sigma used, the more powerful the smooth effect, at the same time the more the original structure and anatomical feature might however be lost. Therefore, picking an appropriate Gaussian kernel value is critical to obtain an accurate and smooth model, i.e. properly balancing the smoothness and accuracy of the model. After a number of tests, a cubic Gaussian Kernel sigma of 1.2mm was selected to obtain a final model (Figure12b).
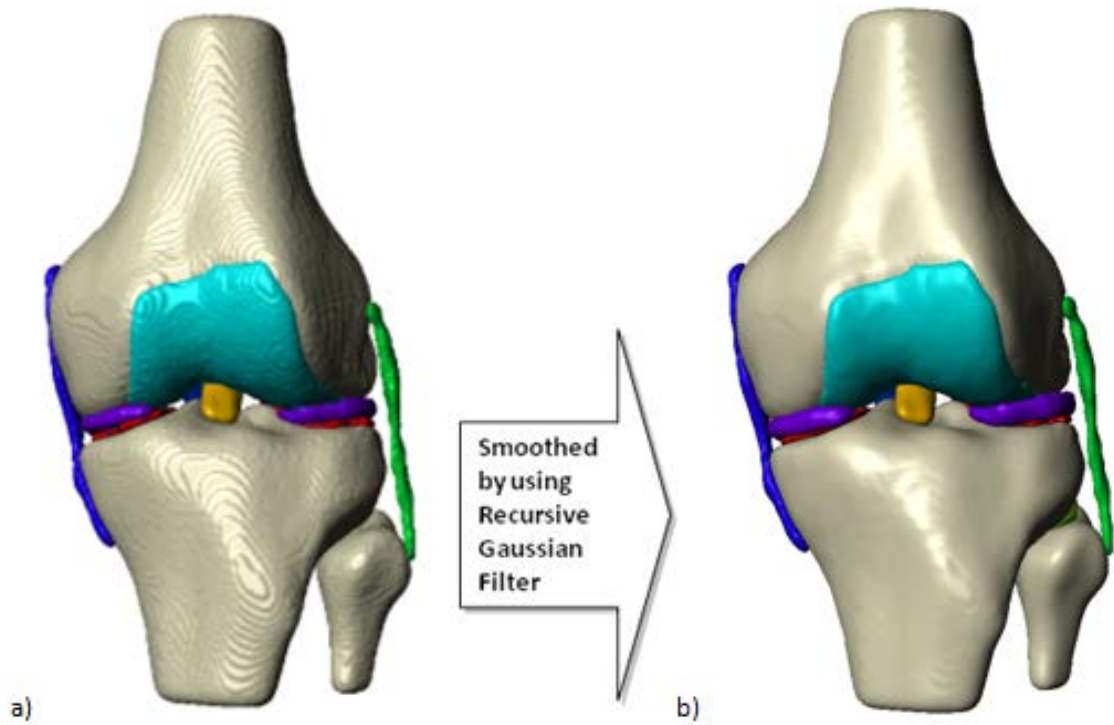
Figure 12. The construction of a) the surface model and b) the smoothed surface model

As mentioned in the previous section, there were four sets of axial MR images containing the entire lower limb. Therefore, these four parts of leg model, which include femoral head to mid femur region, mid femur region to knee, knee to mid region of tibia and mid region of tibia to ankle, were generated using the identical modelling parameters and procedure (Figure 13).
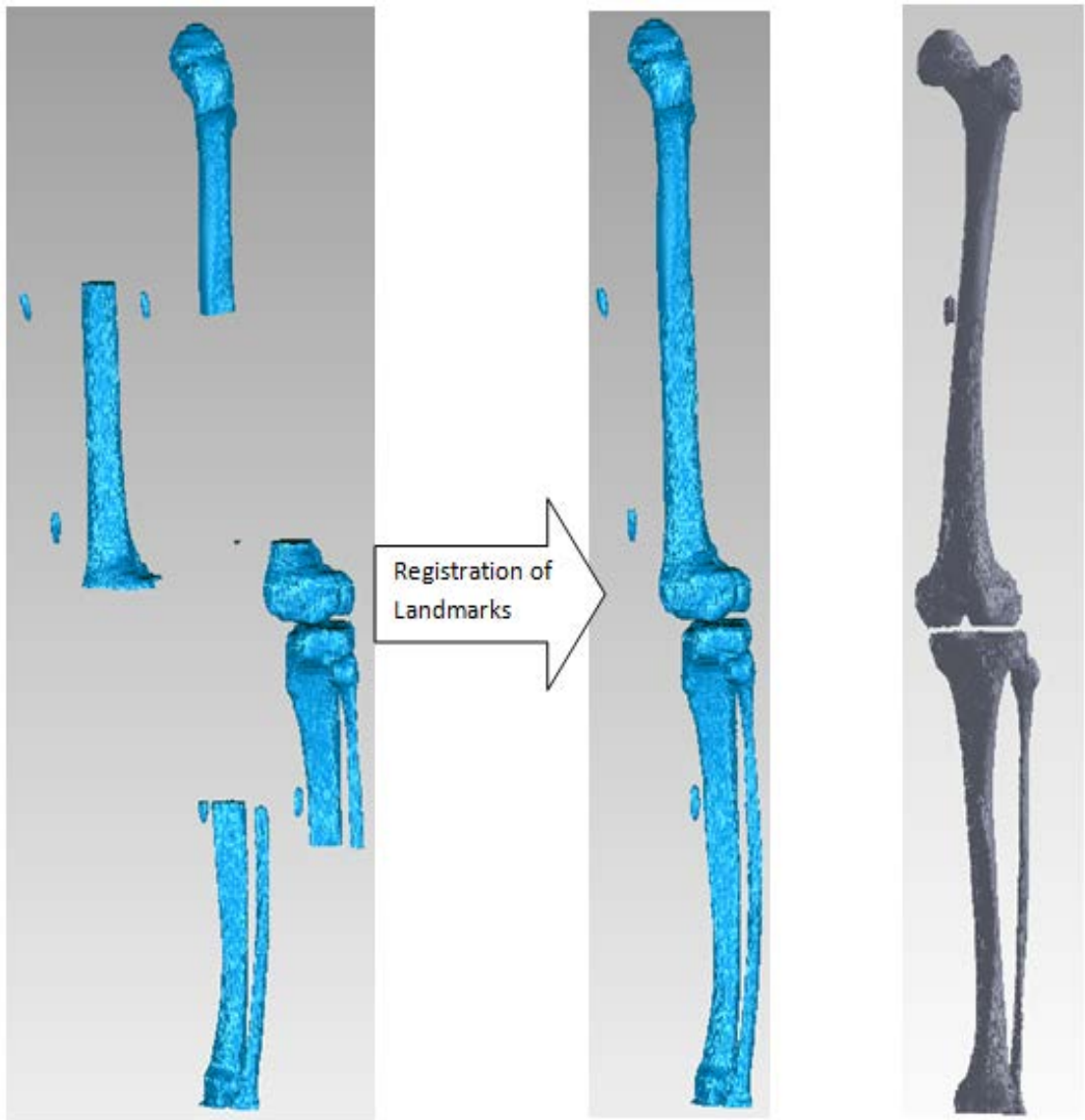
Figure 13. Process of constructing the whole lower limb model

3.3 Surgical simulation of HTO

Following the generation of the surface models of knee joint in ScanIP, all these surface models were imported into Rhinoceros (v 3.0, Rober McNeel & Associates, USA) to be converted into the solid models. For constructing knee models with different degree of medial opening wedge HTO correction, the CAD software packages Solidworks (v2012, DassaultSystemes, UK) and Rhinoceros were used to play a part together to accurately simulate the operated knee with the help from experienced orthopaedic surgeons.

Before introducing the modelling process, it would be helpful to have an overview of the actual HTO surgical procedure. After exploring the proximal-medial tibia region, a guide wire will be inserted obliquely and directed towards the tips of the fibula under fluoroscopic guidance (Figure 14a). The entrance point should be set on the medial side of the tibia, with approximately 35 mm underneath the tibial plateau and equidistant from anterior and posterior tibial cortices. While the guide wire should be stopped by the point positioned approximately 18 mm beneath the lateral edge of tibial plateau. Once the guide wire has been positioned, an oscillating saw was used to create an incomplete osteotomy, starting distally along the guide wire until a 10 mm continuous lateral hinge remained (Figure 14b). A combination of stacked osteotomies and laminar spreaders will then be used to perform tibial opening until the pre-operatively planned correction angle has been achieved. Femoral head allograft will then be used to fill the gap and stable fixation can be realised using an osteotomy plate (Figure 14c).
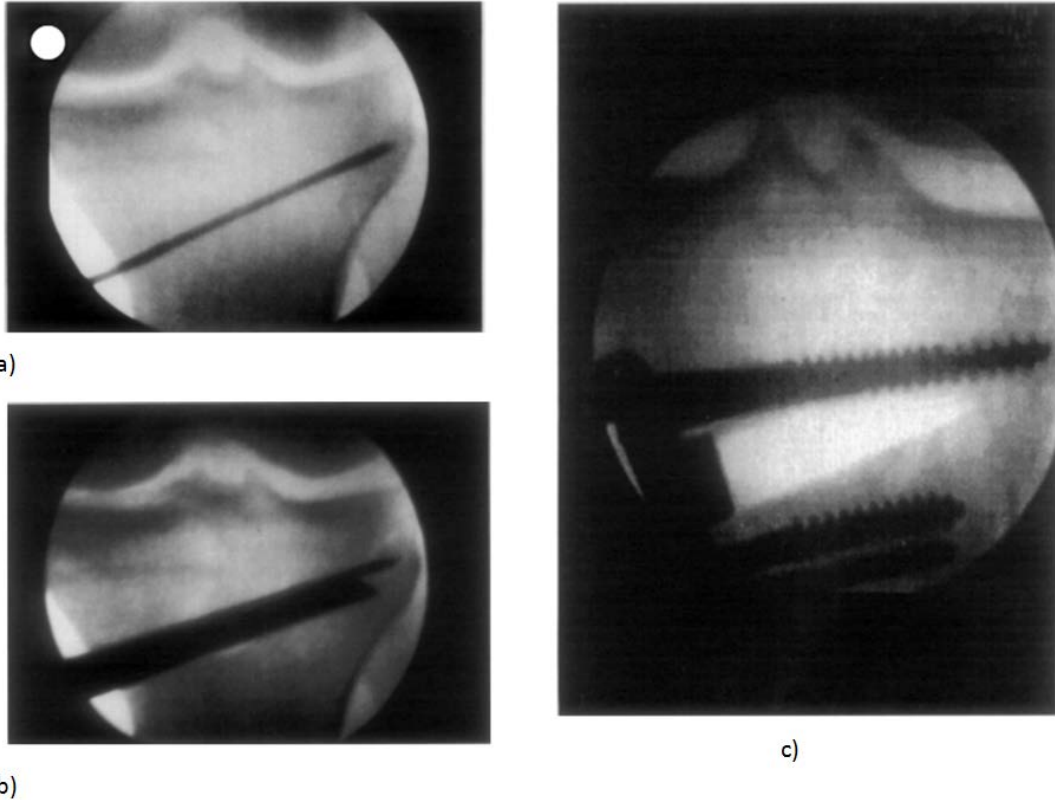
Figure 14. Surgical procedure of HTO: a) a guide pin has been placed; b) the osteotomy has been inserted just below the guide pin and 10 mm of lateral tibial cortex has been left intact; c) the plate and screws in place [72]

However, it is difficult to directly simulate this process in a real surgery. In this study, Rhinoceros was used to bend the tibia to a specific degree, and the modified tibia was then imported into Solidworks to cut a wedge area of the tibia. To bend the tibia for achieving a specific amount of angular degree, a hinge axis was defined at the position of 18mm distal from tibial surface and 10mm medial from the lateral tibial plateau for rotation (Figure 14 b).

The detailed process of bending the tibia laterally to a specific angle is illustrated in Figure 15. A more detailed sketch of calculating the specific translations to simulate the HTO can be found in Appendix A.
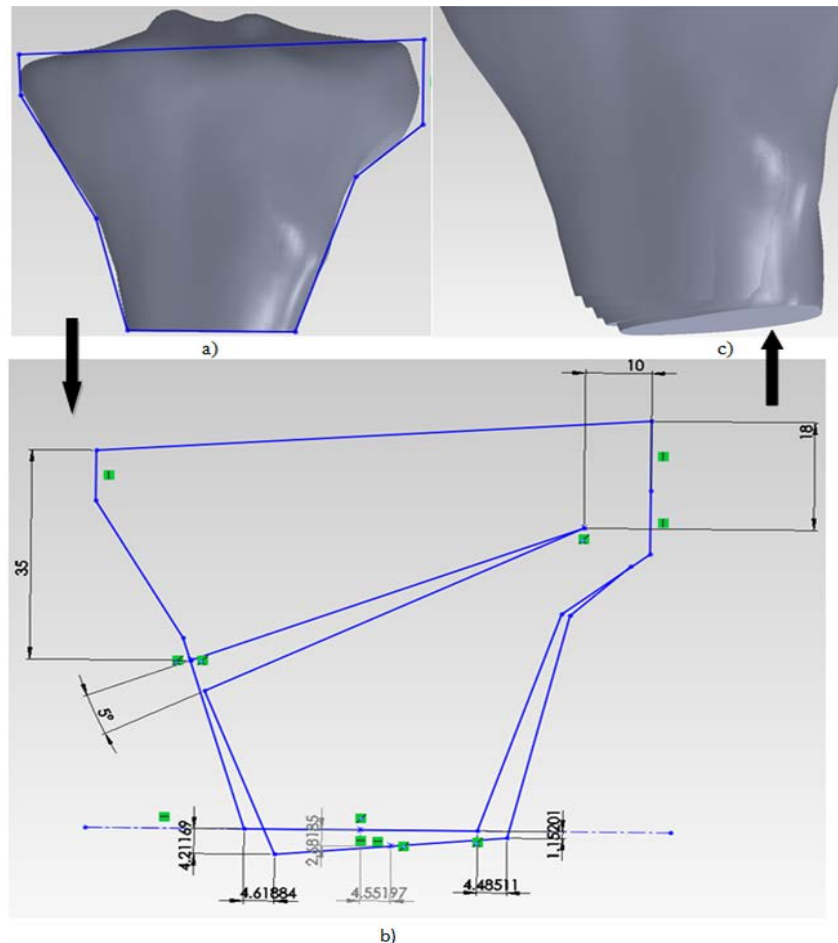
Figure 15.Demonstration of correcting tibia laterally: a) sketch of the contour best fits the tibia; b) calculation of the translation of the votex and midpoint of the distal surface of tibia and c) deformation of the original tibia to the corrected tibia by matching the distal region

The tibia shape was approximately outlined in Solidworks (Figure 15a) and a simulation of the HTO surgery was performed based on such a profile. The position of the insertion to cut the tibia for opening a wedge was based on the procedure described earlier in this section. After bending the distal region of the tibia to a certain angle, the new positions of two vortex combined with the middle point of the bottom surface were recorded. By using the "Deform" function in Solidworks, which allows solid body to either extend or contract, the distal region of the tibia could be extended and rotated (i.e. deform) in order to match the bottom surface to the new position. The new position of bottom surface was recorded in Solidworks. As a result, the bending of tibia to simulate the opening wedge in HTO could be achieved (as

shown in Figure 15 c). In this study, the tibia was bent to obtain a wedge angle from 0° to valgus 10° with an increment of 2.5°, which generated five knee models with different HTO correction angles of 0°, 2.5°, 5°, 7.5° and 10°, respectively.

At this stage, the models were actually representing the knee joints of different alignments. However, to finally realise the HTO treatment, the wedge region should be cut out in Solidworks (as shown in Figure 16 a and b) to simulate the "wedge opening in HTO.
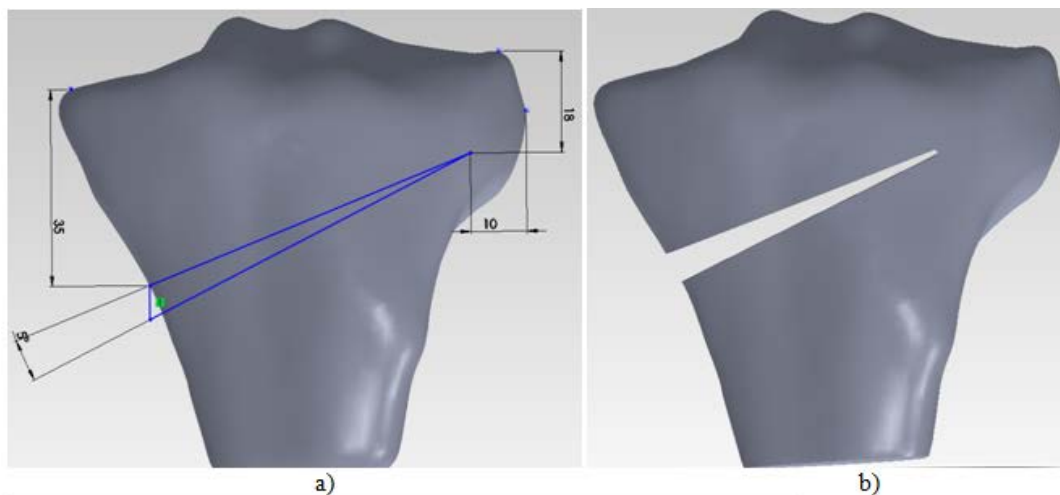
Figure 16. Demonstration of wedge openning: a) calculate and sketch the cutting position on the tibia, b) remode the wedge region to simulate the wedge openning osteotomy.

Last step was to place the plate, screws and the wedge to the cut tibia for simulating the fixation of HTO (Figure 17). Both screw and fixing plate were created in Solidworks based on the Tomofix HTO plate (DePuy Synthes, USA).
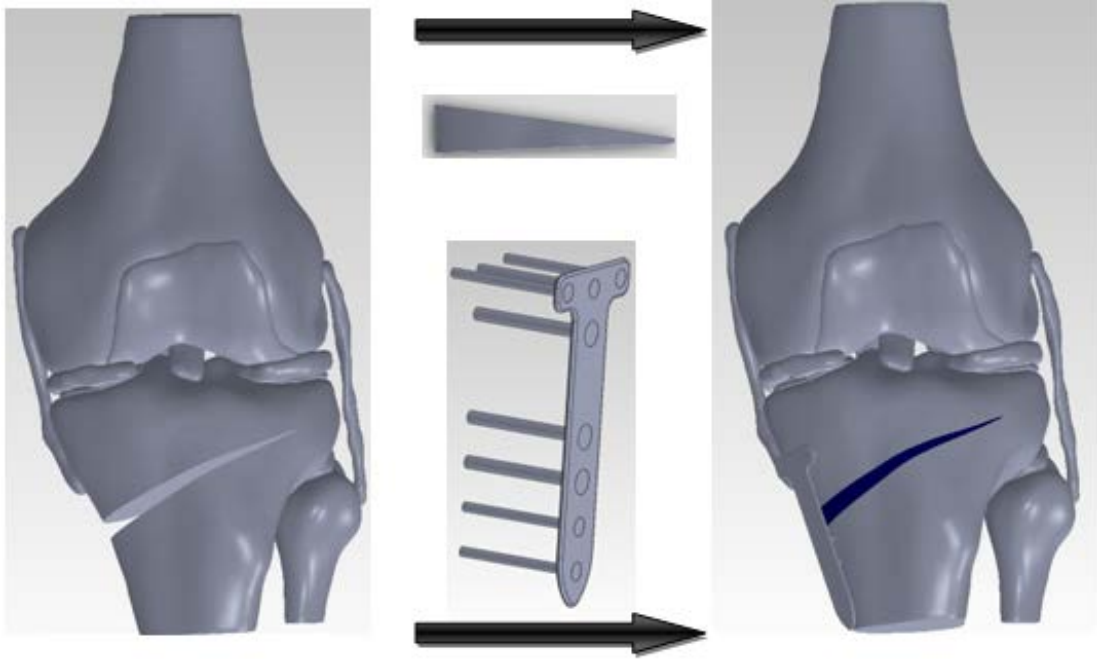
Figure 17. Insertion of the plate, screws and bone-graft substitute

In summary, all the solid models with specific opening wedge angles are shown in Figure 18.
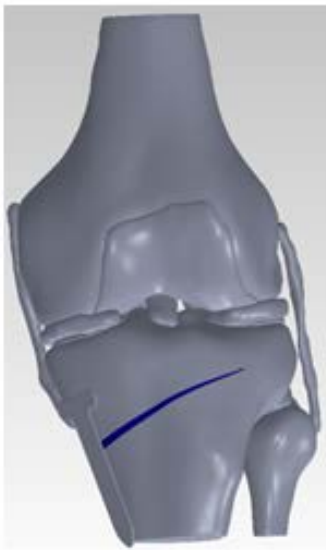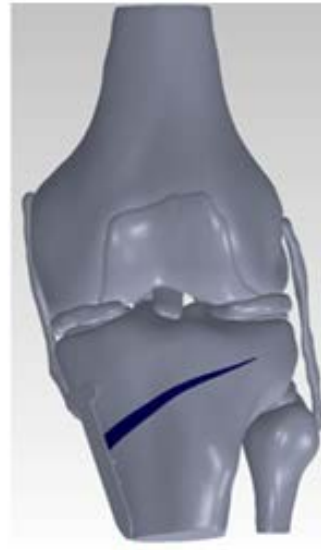
Figure 18. The original knee model and four corrected knee models

3.4 Measurement of lower limb alignment

Following creation of these five models to represent one normal and four abnormal knees with different HTO correction angles, the measurement of the lower limb alignment had been performed to verify the accuracy of the frontal plane correction. As described in Chapter 2, the lower limb alignment can be referred to the HKA angle. But in this study, it is hard to measure the HKA angle in the knee joint model as it does not include the hip and ankle. Therefore the alignment measurement was performed in the whole lower limb model and the knee joint model separately.

Recalling that the measurement of the HKA angle of the lower limb was based on three points: 1) centre of the femur head, 2) midpoint between tibial spines; and 3) centre of the talus, therefore the only available point is the midpoint between tibial spines in the knee joint model. For this reason, in the original knee joint model, we started from the midpoint between tibial spines to draw a line to the midpoint of the distal surface of the tibia, at the same time, draw a line from the midpoint between tibial spines to a random point of the proximal surface in the femur (Figure 19). The angle between these two lines can be referred to as the tibiofemoral angle (Figure 19 a). By assuming that the original knee model has a frontal plane tibiofemoral angle of 0°, the frontal plane tibiofemoral angles of the other four models could be then obtained. After measuring the actual HKA angle of original knee based on the whole lower limb model, the actual HKA angle of the other corrected knee models can be interoperated by adding the correcting angle to the actual HKA angle of the original knee.

Interestingly, the actual correction angle on the frontal plane used in clinical practice was smaller than the opening wedge angle (i.e. correction angle on the frontal plane of tibia). A wedge angle of 5° will be equivalent to an actual frontal plane correction angle of 3.97° (Figure 19). The reason of this difference is due to the fact that the correction degree used in this study was based on the degree bended on the frontal plane of tibia, which would be slightly smaller than the actual degree of the correction angle in the HTO clinical procedure. Note that the frontal plane of the tibia was different from the actual frontal plane which is based on femur. This internal rotation of the tibia would result in the decrease of the correction angle based on the frontal plane of tibia when such an angle was measured on the frontal plane of femur. As a result, the amount of stress decrease at the medial compartment might be somewhat smaller compared to the published HTO studies for the same degree correction. The 2.5°, 5°, 7.5° and 10° valgus is thus equivalent to the 1.49°, 3.97°, 5.21° and 7.94°valgus, respectively. The figures of the measurement of the frontal plane HKA angle can be referred to Appendix B.
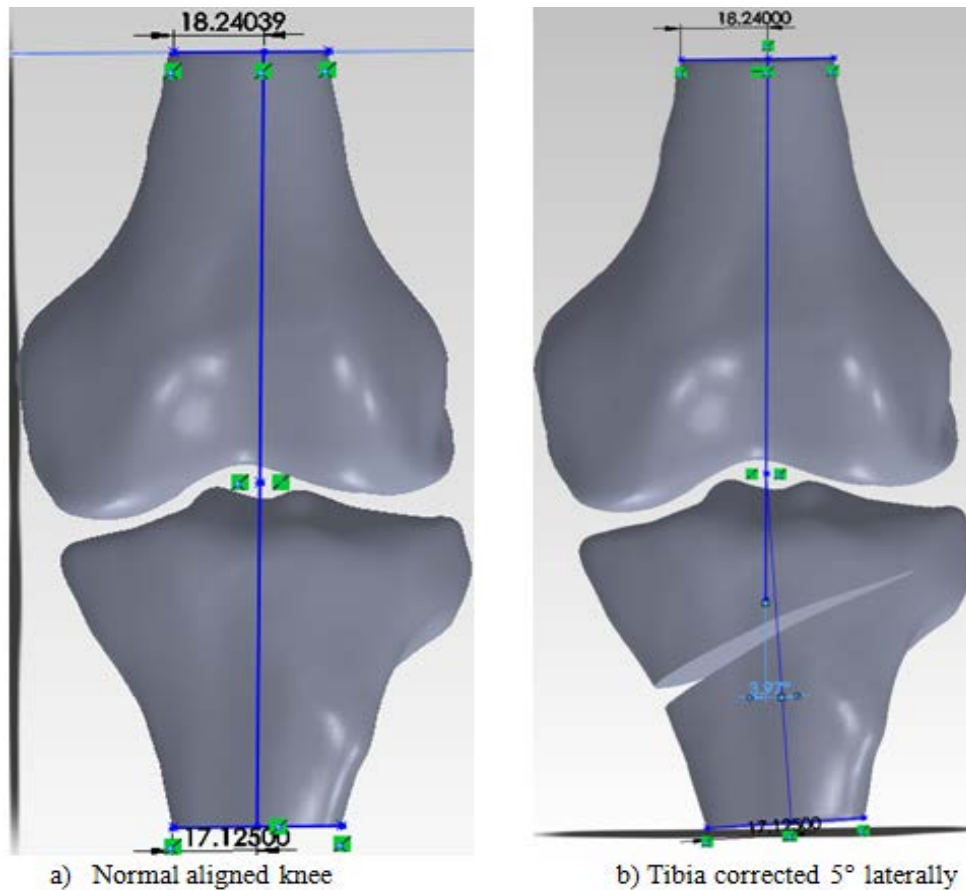
Figure 19. Correction angle of a) normal aligned knee and b) the knee with 5° valgus correction

Moreover, by considering the actual frontal plane, HKA angle of the original knee model was 1.3° varus, which was measured from the whole lower limb model (Figure 20). The actual frontal plane HKA angle of all models referred to 2.5°, 5°, 7.5° and 10° valgus is thus equivalent to the 0.19°, 2.67°, 3.91° and 6.64°valgus, respectively. In this study, nevertheless, the objective was to investigate the effect of shifting loading axis laterally on the trend of the variation of the stress distribution between two compartments; it is more convenient to use the opening wedge angle rather than the actual frontal plane HKA angle. Therefore, for comparing the results of the previously published clinical studies of HTO in the Chapter of discussion, the effect of this unmatched situation will be added up for consideration.
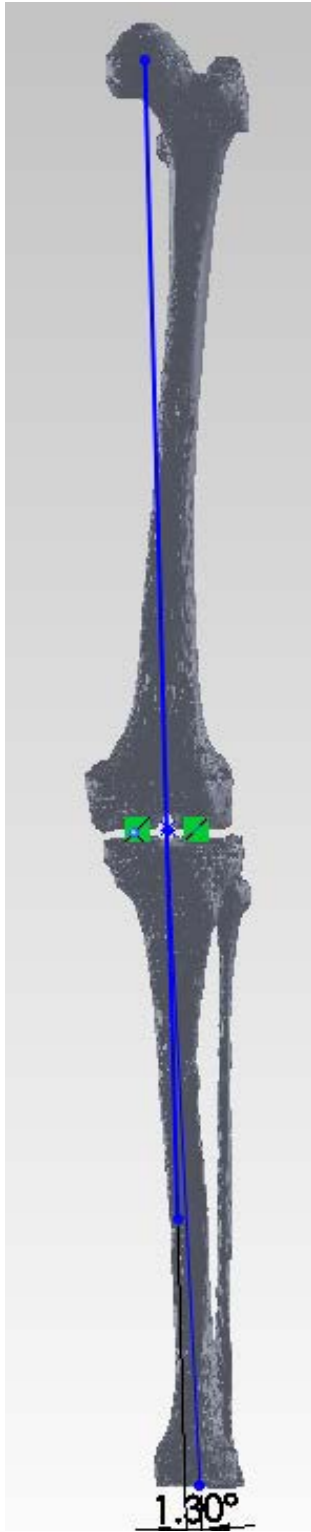
Figure 20. HKA angle of the whole lower limb

Chapter 4 Finite Element Analysis

FEA is based on the solution to a complex system of discretised model with elements (which consist of nodes). The element is programmed to contain the material properties which determine how the structure will react to specific boundary and loading conditions. In FE solution, the displacements of each node are calculated and used to obtain the stress and strain through the generalised Hooke's Law. In general, four important components comprise the overall FEA process, which are:

- Meshing

- Assigning material properties

- Defining loading and boundary conditions

- Solving linear equation sets

The following sections will describe the entire FEA process (including pre-processing and solution) through these four components. Specifically, the surface models were firstly exported from ScanIP and converted to solid model in Solidworks. Once the solid models were generated, meshing was performed to divide the models into finite number of elements in ABAQUS. Prior to numerical solution of displacement, material properties of respective tissues and certain loading and boundary conditions were assigned to the model, which is known as pre-processing of FEA. ABAQUS had been used to perform all the analyses in this study.

4.1 Meshing

A proper selection of type and size of elements for generating mesh could directly contribute to the accuracy of FEA, which is required to precisely mirror the anatomical details of the subject concerned. Although the meshing algorithm embedded in ScanIP can generate tetrahedral meshes, it is not able to generate smooth mesh at some surfaces, such as edge of the thin layer structures (i.e. menisci and cartilages). As shown in Figure21a, failing to achieve smoothness in the surface edge and two parts in contact would result in some sparkle elements, which might cause drastic stress concentration in FEA. Moreover, the solid model generated in ScanIP was based on the meshed elements. In other words, only a dense meshing (Figure 21b) could capture a smooth model which will however significantly raise the computational cost in FEA solution process. In Figure 22b, a less dense mesh was generated in ScanIP, but clearly, the model has lost some smoothness on the surfaces (Figure 22 a).

a)   b)
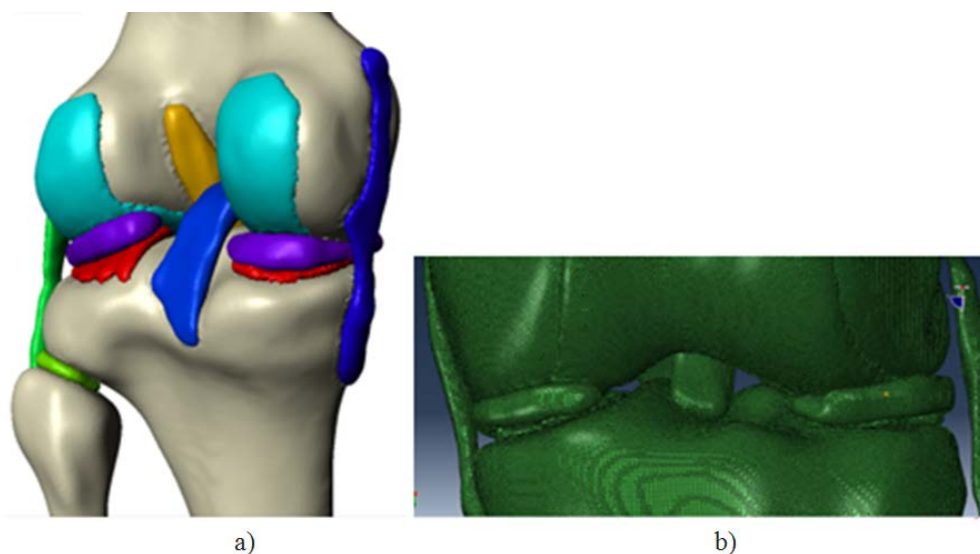
Figure 21.Fine mesh resulted by using the meshing algorithm embedded in ScanIP: a) the surface model based on fine mesh, b) the mesh of the model
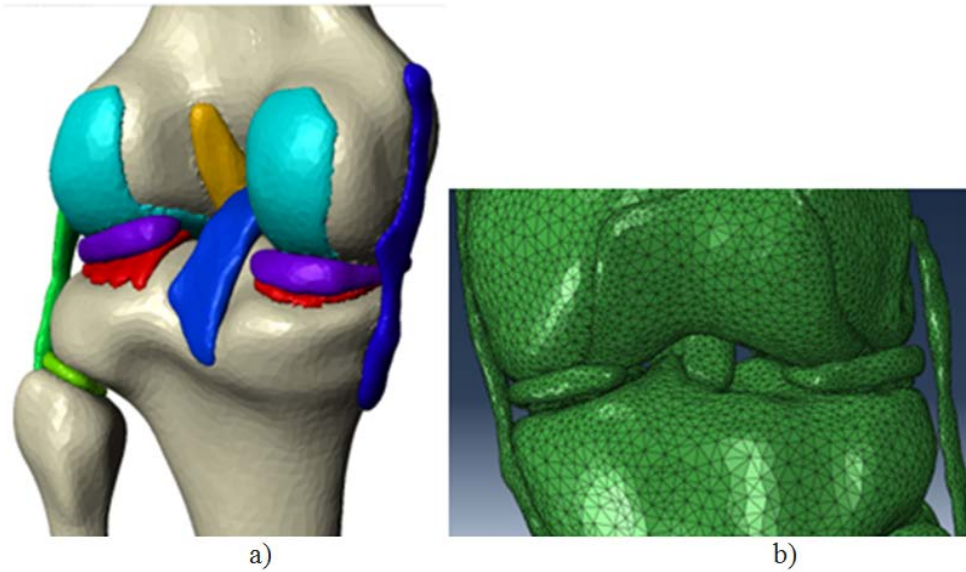
Figure 22. Coarse mesh by using the meshing algorithm embedded in ScanIP: the surface model based on coarse mesh, b) the mesh of the model.

For this above reason, only the surface models were constructed in ScanIP and exported into Rhinoceros to generate solid models. Since the surface model obtained from ScanIP was generated based on the pixels of the MR images, it is necessary to construct new surface on the model, otherwise the surface model with a large amount of tiny surfaces would make it very difficult to process and limit the meshing capacity in ABAQUS. The meshing algorithm in ABAQUS was controlled by the edge of each subsurface on the whole surface of the model. In Rhinoceros, new patches were manually constructed on the surface model and each patch was developed into one subsurface by merging the original pixel-based subsurface. The re-constructed surface model was shown in Figure 23. In this figure, the smoothness of the edge of cartilages and meniscus were retained well. The meshing quality in the new surface model can be freely controlled in ABAQUS, such as defining elemental sizes and element types, and more importantly, different meshing density can be defined at different regions.
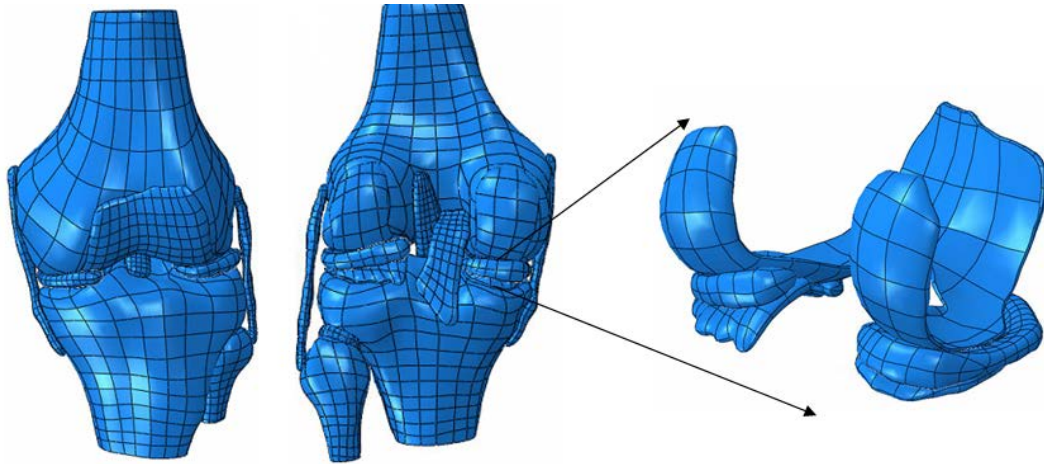
Figure 23.Re-constructed surface models with patches

Once the solid models were constructed in Rhinoceros, they were imported into ABAQUS for mesh generation (Figure 24). The bone, articular cartilage, meniscus and ligaments were discretised into 10-node tri-linear tetrahedral elements. Tetrahedral elements were chosen over hexahedral elements attributable to its great flexibility in meshing complex curved geometry.
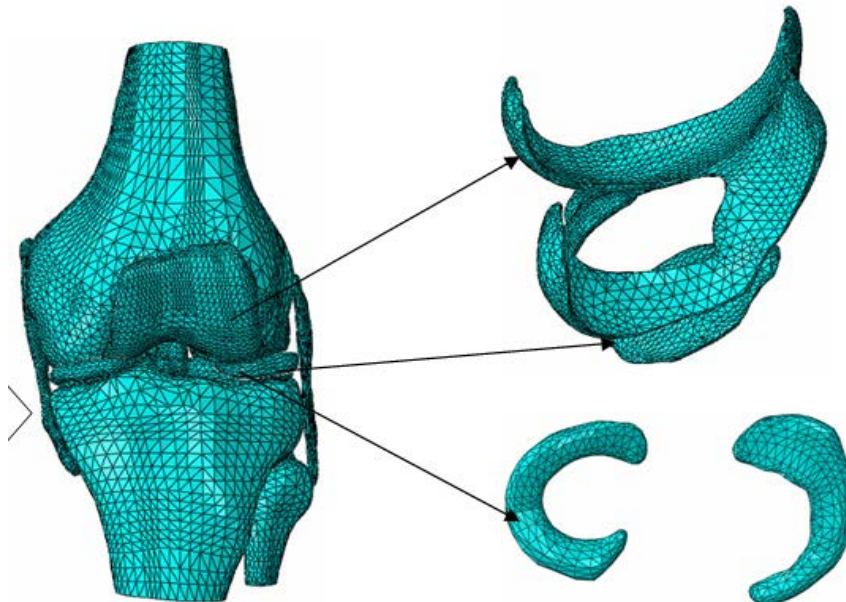
Figure 24. Mesh result of the use of meshing algorithm in ABAQUS

4.2 Loading Condition

In this section, two loading conditions adopted in this study were described. The first (load case 1) is the single axial loading and the second (load case 2) is the subject-specific forces and moments obtained from the gait analysis.

4.2.1 Loading case 1

In order to validate the knee models available in literature, a single axial force was applied on the femur to obtain the stress distribution at menisci and cartilages, which can be compared with those stress values obtained in other studies. Most of the FEA studies on knee joint only concerned the stress distribution at both cartilages and menisci under pure axial loading. Since the subject selected in this study had a weight of 74 Kg, an axial force of 740 kN (approximate body weight) was applied at the centre point of the cross section of femur (Figure 25).
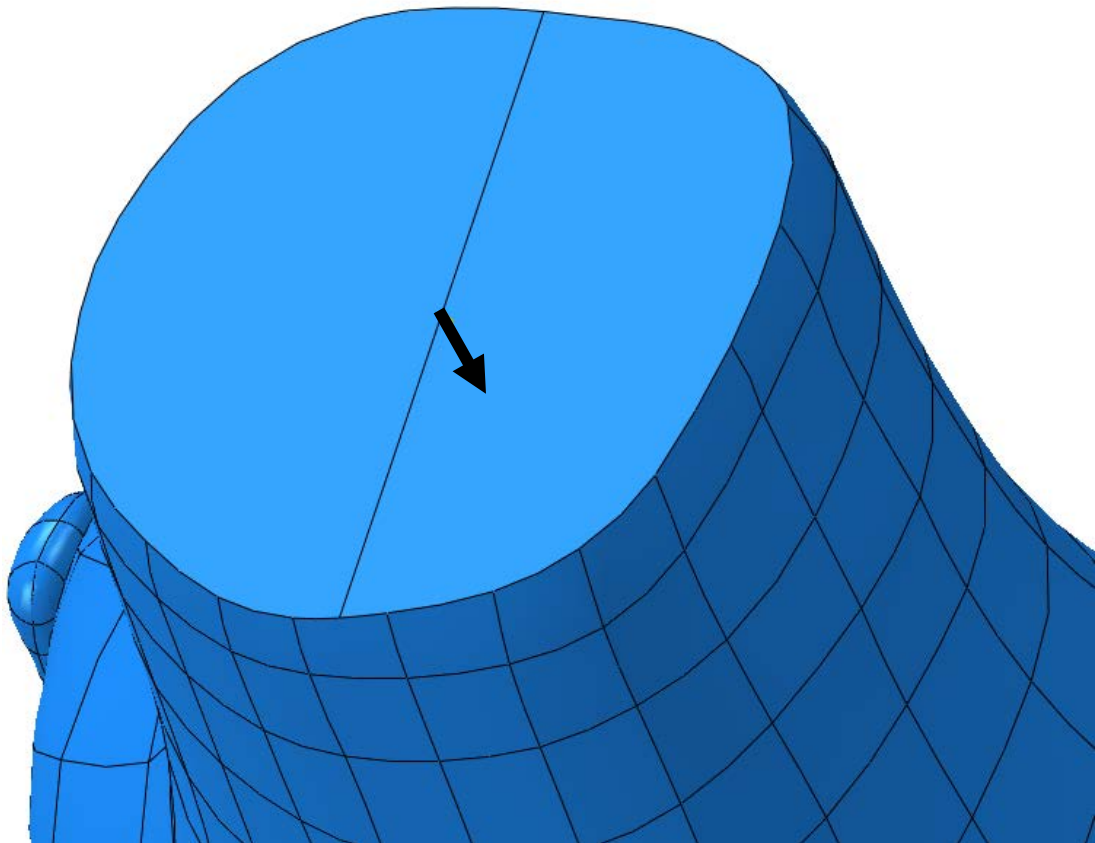
Figure 25. Single axial force applied on the mid-point of the proximal surface of the femur

4.2.2 Analysis of the gait data

During the gait analysis, a twelve-camera motion analysis system combined with two force-platforms was used to collect the subject-specific kinematic and kinetic data. Retro-reflective makers were placed at bony landmarks to define the different segments of the leg. The motion analysis cameras recorded the data at a frequency of 1200 Hz and were time synchronized with the motion analysis system. The ground reaction forces and centre of pressure were measured by the force platforms. Ten trials of walking at a self-selected speed were conducted while monitoring the ground reaction forces and the kinematics of one leg. The over ground walking with the self-selected speed was preferred to screen natural function of the knee. In this case, treadmills and timing techniques to control speed would not be required. An

inverse dynamics analysis was then performed to calculate the knee-joint reactions forces and moments. Although 10 individual trials are conducted during the gait analysis, the data input into the finite element model was provided by taking the average of these ten trials as plotted in Figures 26-28.

Before interoperating the gait data, it is useful to define the coordinate system in the gait analysis. Flexion is defined as positive, while extension is defined as negative in the sagittal plane. Adduction of the tibia with respect to the femur is defined as positive, while abduction of the tibia with respect to the femur is defined as negative on the frontal plane. Internal rotation of the tibia with respect to the femur is defined as positive, while external rotation of the tibia with respect to the femur is defined as negative in the transverse plane.

According to Figure 26, the primary points of the interest are at 0%, 100% of the gait cycle, since a full extension (0° for flexion angle) was considered in the model.
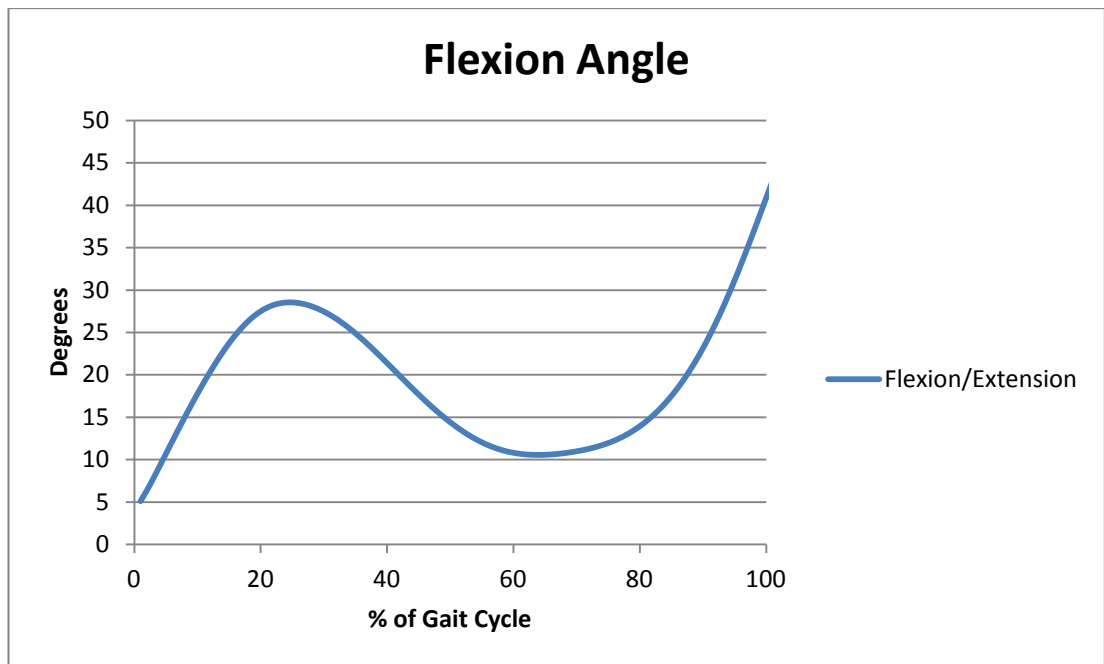
Figure 26. Knee joint angles
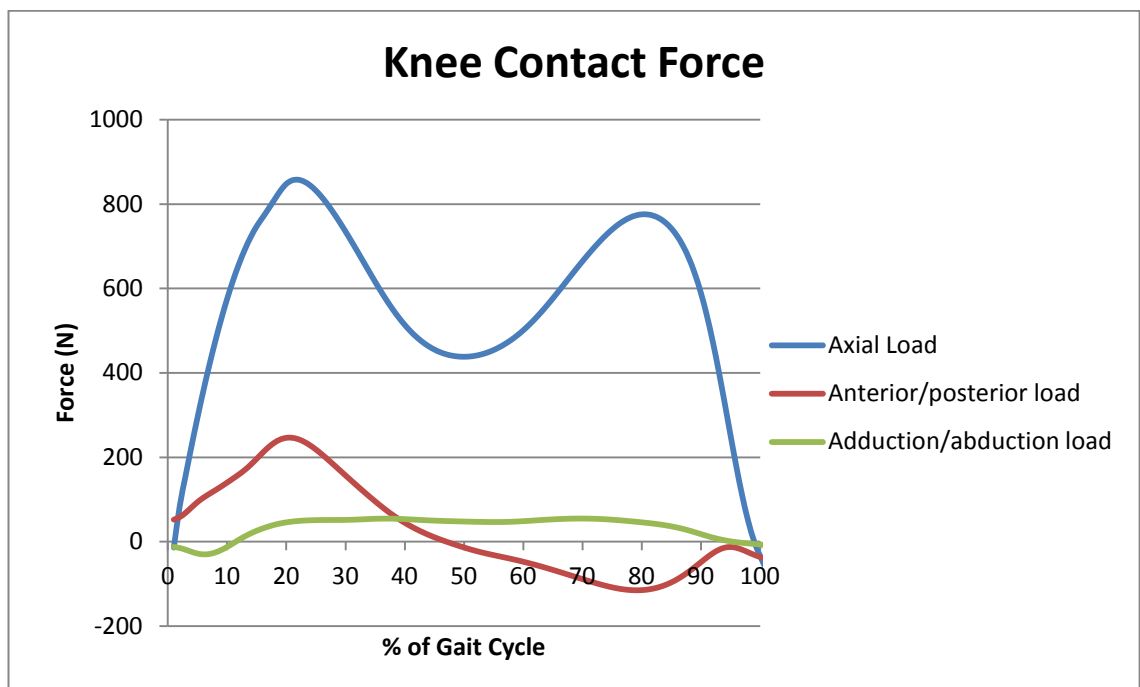
Figure 27. Knee contact forces

When the knee contact force are examined at 0%, it is noted however that only a small force is being generated since at this stage the foot only just hit the ground. A more realistic representation of the peak loading that occurs post heel strike is

consequently located at 5% of the gait cycle, which corresponds to a flexion angle of approximately 10°. Although this does not completely agree with the fully extended models, a flexion angle of 10° was considered a sufficiently small deviation from full extension. It was therefore decided that the best loading point of interest to be taken was that at 5% of the gait cycle.
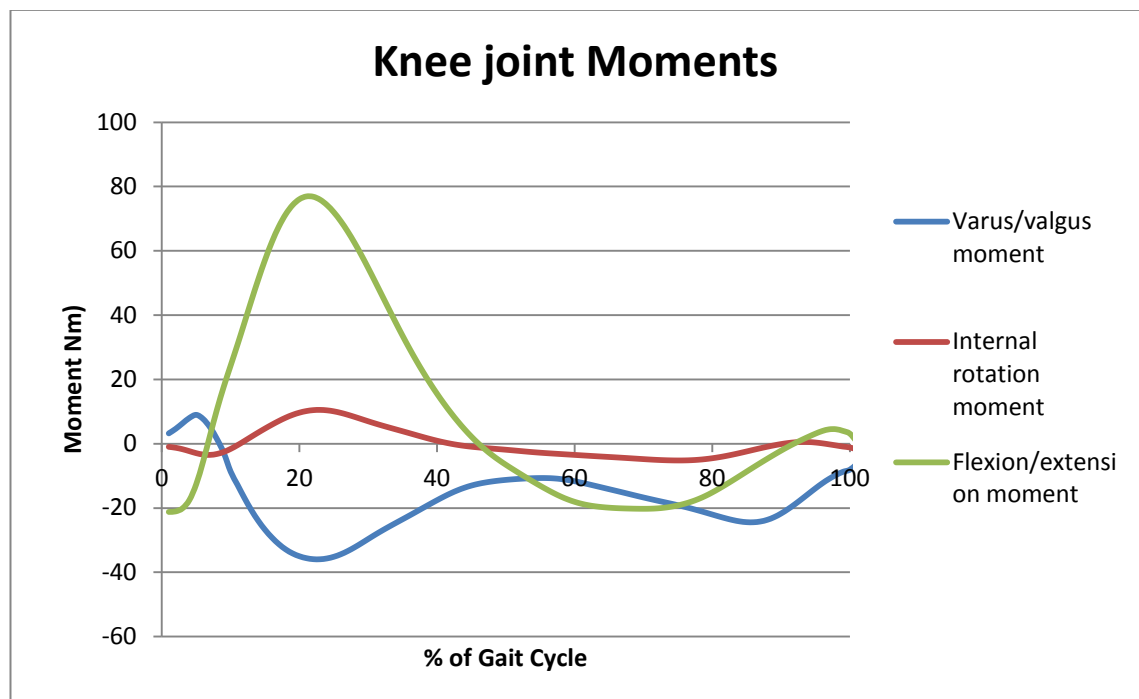
Figure 28. Knee joint moments

Similarly, the averages of the internal moments for both knees are provided in the three planes as shown in Figure 28. At 5% of the gait cycle, there is flexion of the femur with respect to the tibia in the sagittal plane (flexion moment), adduction of the femur with respect to the tibia on the frontal plane (varus moment), and external rotation of the femur with respect to the tibia in the transverse plane (external rotation moment).

61

4.2.3 Loading case 2

In the second loading case, the tibia and fibula were fixed in all translations and rotations. At the heel strike, the femur is in 0° flexion and all other translation and rotation of the femur were unconstrained. The loading applied to the FE model was obtained using motion analysis and force platform data as explained in Section 2.1 and was applied to the midpoint of femur.

The loading condition that were applied to the model included the axial forces F_z, the anterior/posterior force F_y, and the varus/valgus moment M_y and the internal/external rotation moment M_z. All forces and moments were illustrated in Figure 29. The flexion/extension moment was not directly applied as an input of the loading condition because the knee functions as a hinge joint (i.e. pin joint motion in the sagittal plane), meaning that there is no external moment in the sagittal plane generated in the knee joint. The effect of the internal flexion/extension moment is balanced out by the flexion angle. However, the knee is relatively fixed in the transverse and frontal plane, which means that the knee joint generated external moments to balance the effect of internal/external rotation and valgus/varus motion. For this reason, the varus/valgus moment M_y and the internal/external rotation moment M_z need to be considered when applying the loading condition.

In this loading case, the flexion/extension moment was not applied to the model since the femur was assumed to be fully extended while the leg was perpendicular to the ground, which means that the flexion moment was cancelled out at this stage.
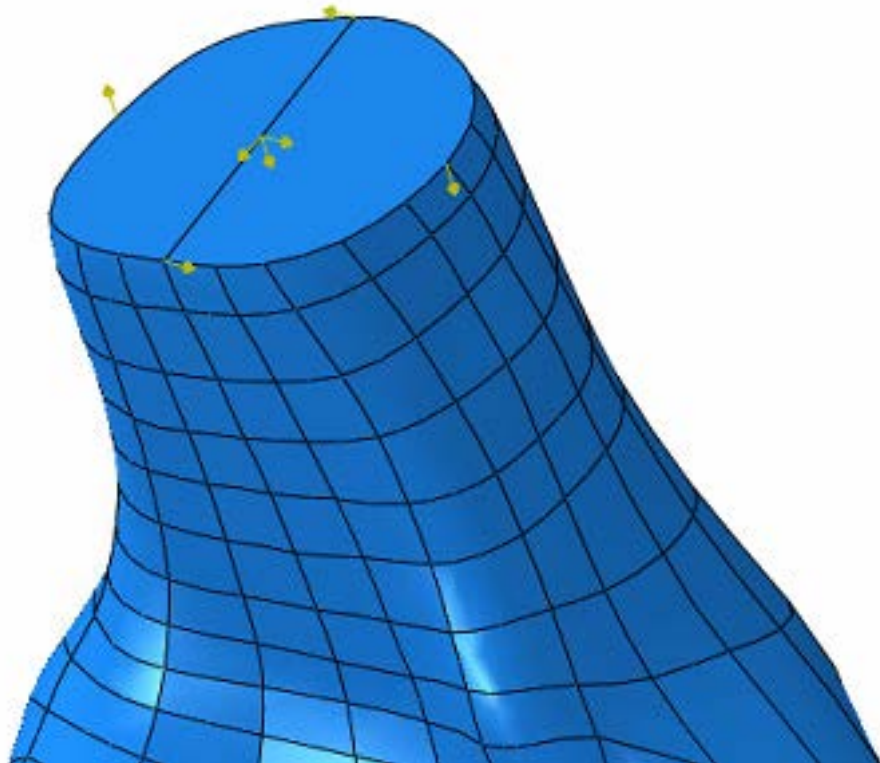
Figure 29. Combination of forces and moments applied on the mid-point of the proximal surface of the femur

4.3 Material Properties

Selection of material constitutive models to best reflect the tissue behaviour is one of the most critical yet challenging steps in the biomechanical FEA studies, since the material properties of tissues, especially soft tissues, remain rather controversial. Despite the non-linear behaviours of many soft tissues, the material properties of the tissue might vary between *in vivo* and *in vitro* [73]. The difficulty of testing the material properties of soft tissues *in vivo* is one of the reasons that lead to such controversy in assigning appropriate material properties in FEA.

According to the previous FEA studies on knee joint, the Young's Modulus of the bone is much higher than those of the soft tissues; therefore variation of bone material properties has nearly no effect on the mechanical behaviours of the soft tissues. As this study had a focus on the biomechanics of soft tissues, so the difference between cancellous bone and cortical bone was negligible. Although some studies in literature considered the tibia and femur as rigid body, my study have implant attached to the bone which might be reasonable to consider the bone as deformable body. Also as mentioned in the previous Chapter, the stress distribution on the soft tissues within knee joint is less sensitive to the material property variation of the bone. Therefore, femur, tibial and fibula were assumed to be a linear elastic and isotropic material with a Young's Modulus of 8 GPa and a Possion's ratio of 0.3 [16] here.

Generally speaking, cartilage is viscoelastic tissue in nature. In this study, however, articular cartilage was assumed to behave as single-phase linear elastic and isotropic

material because the loading time of interest corresponding to that of a fully extended

leg touching the ground is far less than the viscoelastic time constant of cartilage

(1500sec) [74]. This is considered sufficiently accurate to predict instantaneous

cartilage response, as demonstrated by Donzelli et al [75], who proved that there

were no significant changes in the cartilage contact responses shortly after loading.

In summary, the material properties of bone, cartilage, plate, screws and wedge are

shown in Table 3.

Table 3 Material properties of linear elastic isotropic tissues

Component	Young's modulus (MPa)	Poisson ratio	References
Bone	8,000	0.3	[16]
Cartilage	5	0.46	[67]
Plate + Screws	114,000	0.3	[69]
Wedge	2100	0.35	[69]

For meniscus, two material models were developed to simulate its mechanical

behaviours. The first one was isotropic and linearly elastic, and single-phased

material with Young's Modulus of 59MPa and Poisson's Ratio of 0.49[67]. The

second model was hyperelastic derived from *in vivo* measurements[76]. Based on *in

vivo* indentation, the meniscus constitutive model can be derived from the stress-

strain relationship [64], to illustrate the variance of the compressive moduli at

different loading stages. In this case, the 3rd order Ogden strain energy density

equation provided the best fitted response to the *in vivo* data by using the least-square

method as shown in Figure 30.
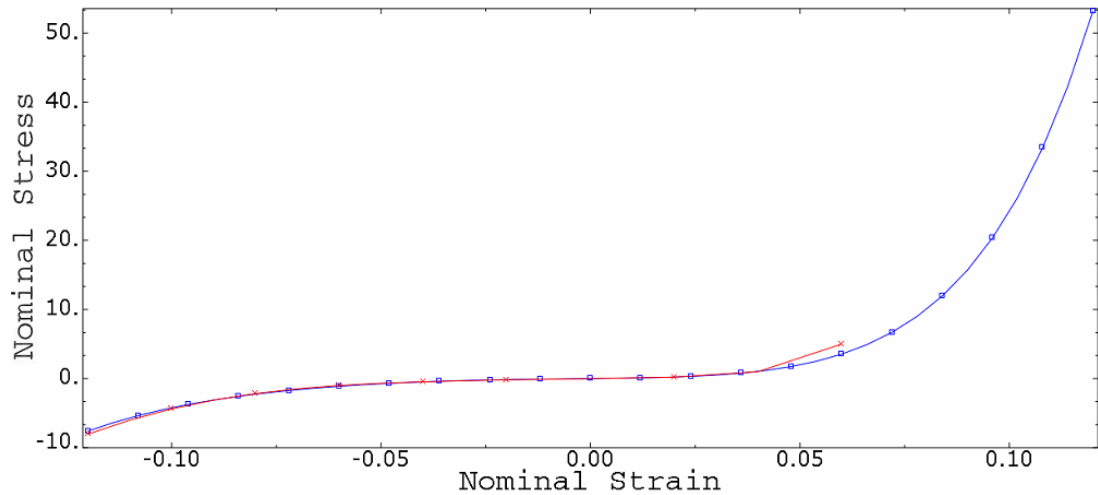
Figure 30.Comparison between in-vivo and calculated stress-strain data of menical material properties: experimental data from an identation test (red curve) compared to calculated Ogden strain energy density (blue curve), stresses are in MPa.

From the literature, the linear elastic material model of meniscus adopted an "average" modulus of 59MPa [67], and the stress concentration was more likely to occur with such a stiff material when the contact was not fully established. Moreover, according to the experimental data of meniscus material testing, the linear behaviour of the stress and strain curve was only observed in the low and extremely high loading region (as shown in Figure 30). The hyperelastic material model has the capability of providing more accurate prediction of stress under the moderate loading, which is often a more realistic case in clinic. Therefore, the hyperelastic material model was used in this study to describe meniscus behaviour.

For the same reason, ligaments were assumed to be isotropic and hyperelastic. Different to menisci, hyperelasticity for ligament was represented by an incompressible Neo-Hookean model with parameters of C_{10} and D_1 for ligaments [77], in which the C_{10} refers to the stiffness of the Neo-Hooken strain energy function and D_1 denotes the inverse of bulk modulus. The relative Neo-Hookean constants of

specific ligaments were calculated from the experimental data from Arnoux et al.'s study [78].All the constants of ligaments calculated are summarised in Table 4.

Table 4. Material parameters for the ligaments (MPa)

Ligaments	C_{10}	D_1
ACL	1.95	0.00683
PCL	3.24	0.0042
MCL	1.45	0.00127
LCL	1.45	0.00127

4.4 Numerical solutions

ABAQUS was used to obtain approximate solutions to all static simulations in the present study. Contact interfaces were modelled between femur, tibia cartilage surfaces and menisci surfaces. Finite sliding of pairs of curved, deformable surfaces was involved in the contact condition of all the models. All of the surfaces were modelled as frictionless [17]. The "hard' contact model was used to define the surface interaction, implying that no penetration was allowed of the nodes from one surface into the other surface. Slave and master surfaces were defined for each contact pair. An augmented Lagrangian algorithm was adopted to simulate the contacts between femur cartilage, tibia cartilage and menisci with frictionless behaviour assumed to mimic the lubrication in the joint. The boundary condition remains consistent with literature, in which the tibial is fixed in all translations and rotations while the femur remains unconstrained.

Chapter 5 Results

FE analysis was carried out to obtain the distribution of the stresses on the knee joint cartilages using the subject specific loading data and knee joint model. In this Chapter, von Mise equivalent stress was obtained to see the overall stress distribution while the compressive stresses were used to investigate the actual loading on the cartilage caused by different degrees of HTO correction. Shear stress in cartilages was also obtained here since it was considered a major cause of OA progression[4]. Contact pressure was calculated for comparing the results with the published FEA studies in order to validate the FE knee model.

Firstly, the stress distributions in the original knee joint model under axially compressive loading was obtained, which allows the comparison between stress results of the model used in this study and those obtained in other FEA studies in literature. After that, the stress distributions at the knee joint of each scenario under combined loading condition (i.e. loading case 2) was also obtained in order to investigate the effect of correction degree of HTO on the more realistic stress distributions at the soft tissues of the knee joint.

5.1 Stress distribution at knee joint under sole axial loading and multi-loading

Although only the contact stresses on the surface of cartilages and menisci, rather than the internal stresses, were concerned, both stresses may be important to the degeneration of cartilage [79]. Since most published FEA studies on knee joint investigated the contact pressure on the menisci and cartilages under axial loading, the FE model of the original knee were applied with a single axial load to calculate the contact pressure on the menisci and cartilages.

Before starting to investigate the results obtained from FEA, it should be noticed that for all stress contours plotted in this Chapter, the medial compartment was placed on the left hand side whilst the lateral compartment was on the right hand side. For the menisci and femoral cartilages, the anterior side was facing upward whilst the posterior side was facing downward. However, the anterior/posterior orientation was opposite in tibia cartilage to the menisci and femoral cartilage. For clarification, the orientations of these different soft tissues in knee joint were illustrated in Figure 31.
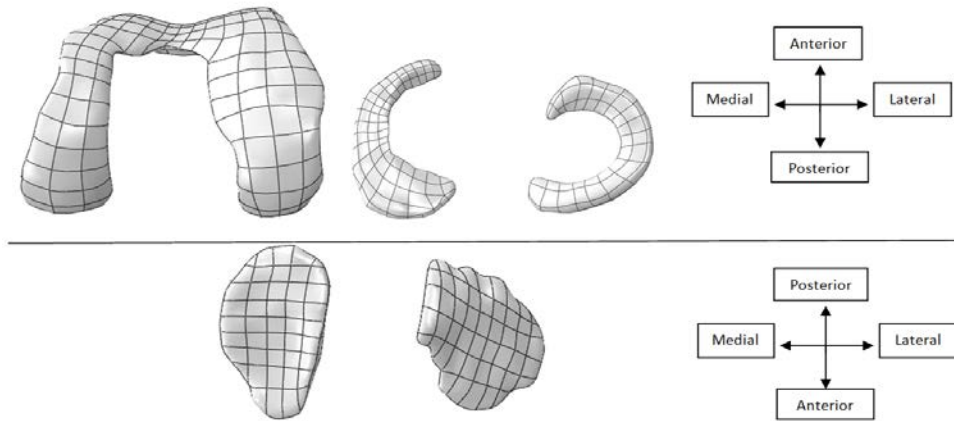
Figure 31. The orientations of femoral cartilage, menisci and tibia cartilages

The maximal contact pressure was found to be 3.2MPa in the anterior horn in the lateral meniscus and 1.8 MPa in the middle region medial meniscus. The maximal contact pressures in the femoral cartilage and tibia cartilage were found to be 1.88MPa and 3.06MPa, respectively. All these contact pressures obtained here strongly agreed with the results of the previously published FEA studies of knee joint in literature [19, 21, 66, 67].

As shown in Figure 32, the contact pressure contours of menisci and cartilages under the loading case 1, in which the model was subjected to a single compressive load, were compared with the contact pressure contour of same tissues in loading case 2 where the subject-specific loading data was employed. Overall, the maximum contact pressure and major pressure concentration were found in the lateral compartment under loading case 1, whereas the maximum contact pressure and major pressure concentration appeared in the medial compartment under loading case 2. Also the pressure distributions were found to be shifted posteriorly when compared the contact pressure distributions in loading case 1 with those in loading case 2.
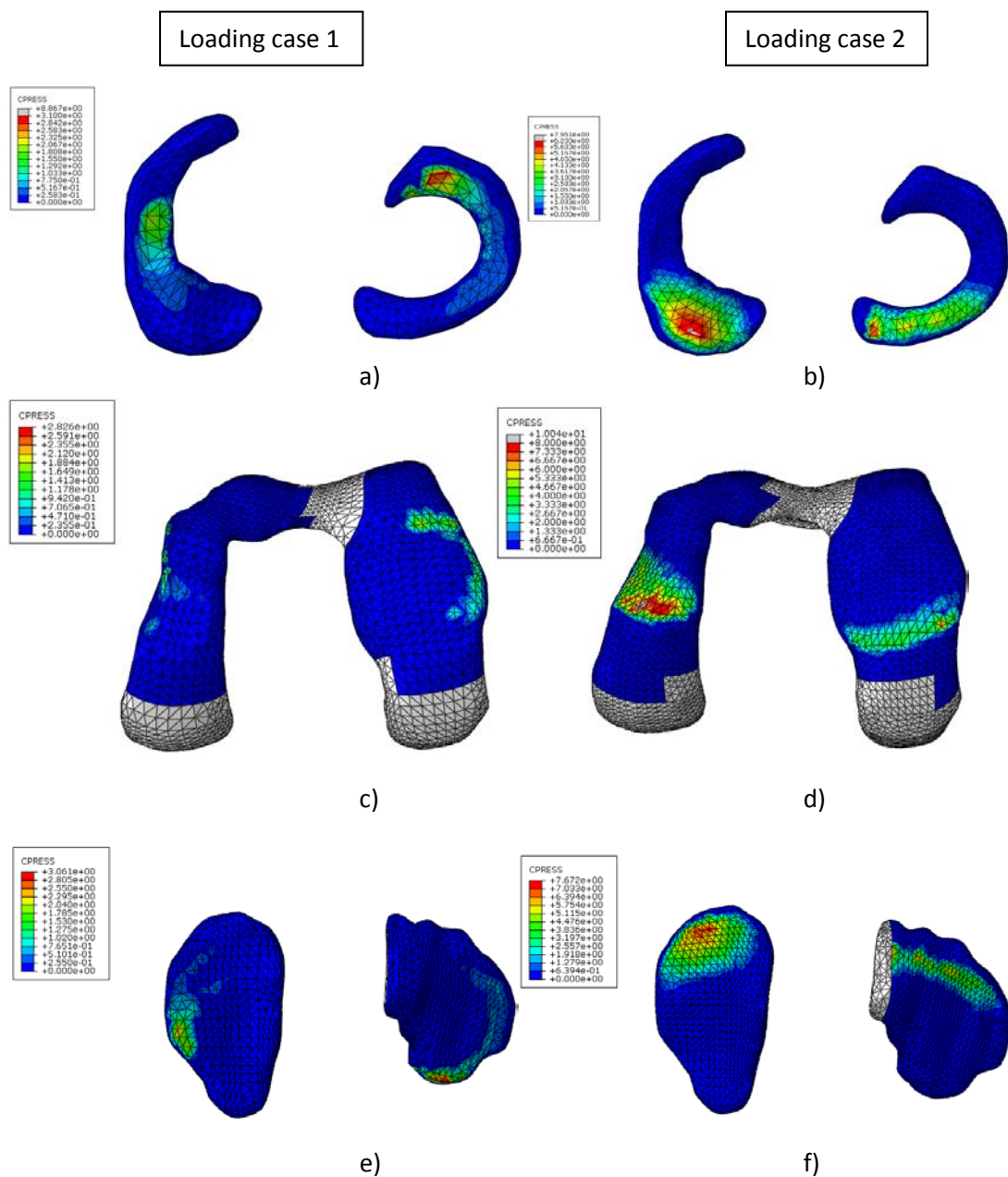
Figure 32. Contact pressure in the menisci, femoral cartilage and tibial cartilag under two loading cases

These above results were considered reasonable since such pressure distribution can properly reflect the forces and moment application in loading case 2. In addition to the axial force F_z, the anterior-to-posterior force F_y would change the loading point from the middle region of the knee posteriorly while the varus moment M_y combined with the internal rotation moment M_z would result in an increase in the loading

through the medial compartment. This explains the pressure distribution across two compartments in loading case 2. According to Yang et al's study [21], the maximal contact pressure on the medial meniscus could be increased up to three times in the case of applying subject-specific loading data compared to that by applying an axial compressive force only. Therefore, the results obtained from the current FE knee joint model is fairly consistent with the literature data, indicating that this knee model should be capable for further investigating into other stress distributions.

5.2 Overall von Mises stress of the knee joint after shifting loading axis

Upon validating the knee model, the von Mises equivalent stresses were obtained to observe the overall stress distribution of the knee joint after shifting the loading axis from medial to lateral. The equivalent stress variation was exhibited in Figure 33 and the same range of stress legend was used for all the models for comparison.
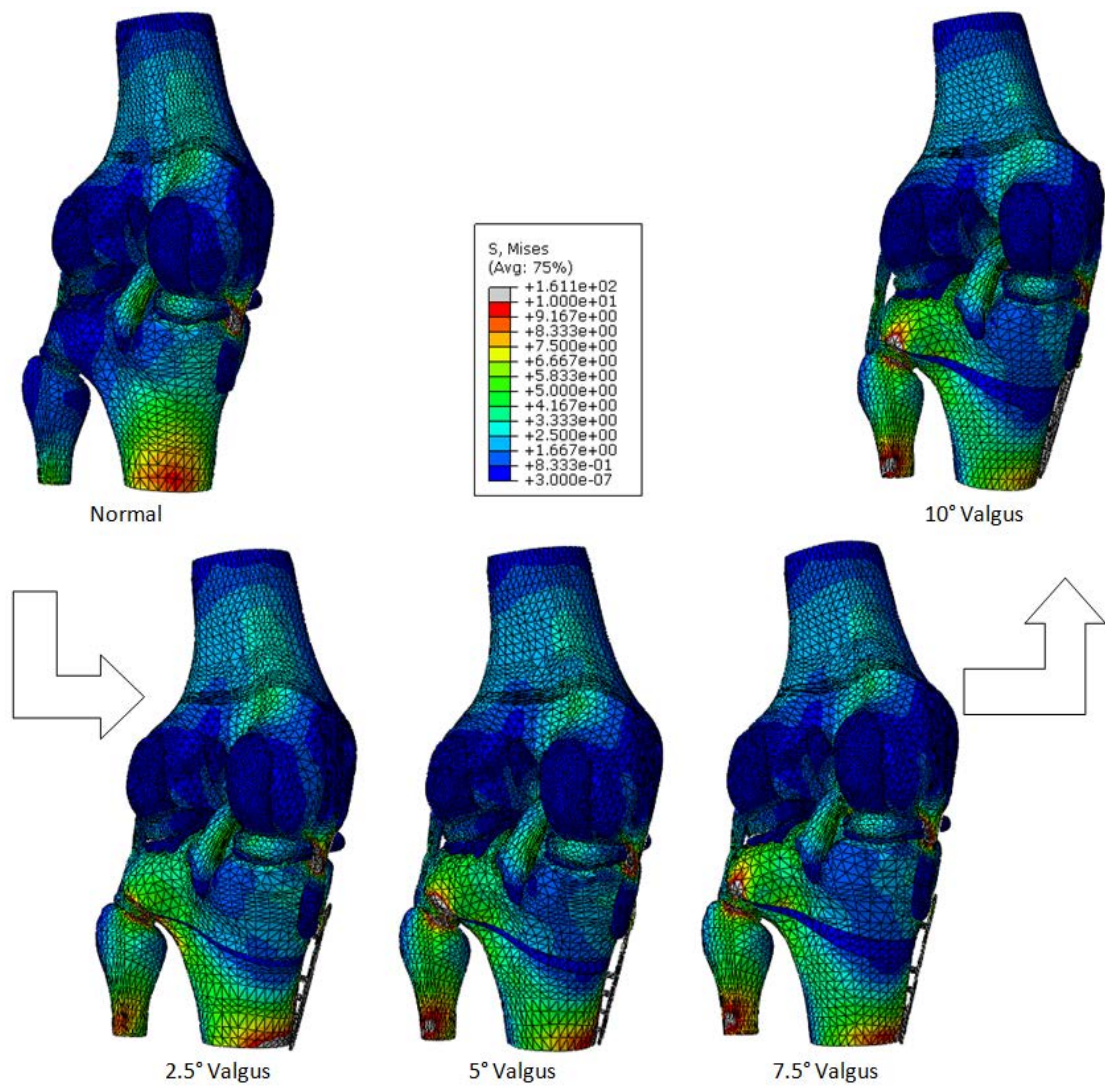
Figure 33. The overal von Mise stress distribtion of the knee joint models

For the first (initial) model, the maximum stress appeared in the medial side due to loading axis through the medial compartment combined with the varus moment. When the tibia was bended 2.5° laterally, the maximum stress shifted to the lateral side. However, stress concentrations were observed in the medial side of the tibial bottom area. This may be caused by the effect of placing the fixation plate, since the stress concentration around the screw area was fairly close to the fixed boundary (distal surface of the tibia). Beside this, the equivalent stress results had confirmed the hypothesis of this study, i.e. stress increases laterally as the alignment shifted from varus to valgus.

5.3 Effect of correction angle on compressive stress at cartilages and menisci

Both cartilages and menisci are largely in compression with its minimal principal stresses (or maximal compression) oriented approximately normal to the articular surface. In order to better investigate the effect of the changing loading axis laterally on the stress distributions across both the compartments, the range of the maximum stress to minimum stress had been set to be a constant for all five models. Therefore, the stress distribution pattern between different models becomes comparable.

The compressive stress in the menisci was shown in Figure 34. The blue region indicated the higher compressive stress whilst the red region indicated the lower compressive stress. A clear trend of decreasing compressive stress on the medial meniscus was demonstrated as the blue region accumulated in the posterior region of the medial meniscus was fading as the correction angle increased from 0° to 10° valgus. At the same time, the stress distribution started to increase in the lateral meniscus due to the loading axis shifting laterally by correcting the tibia from 0° to 10° valgus.
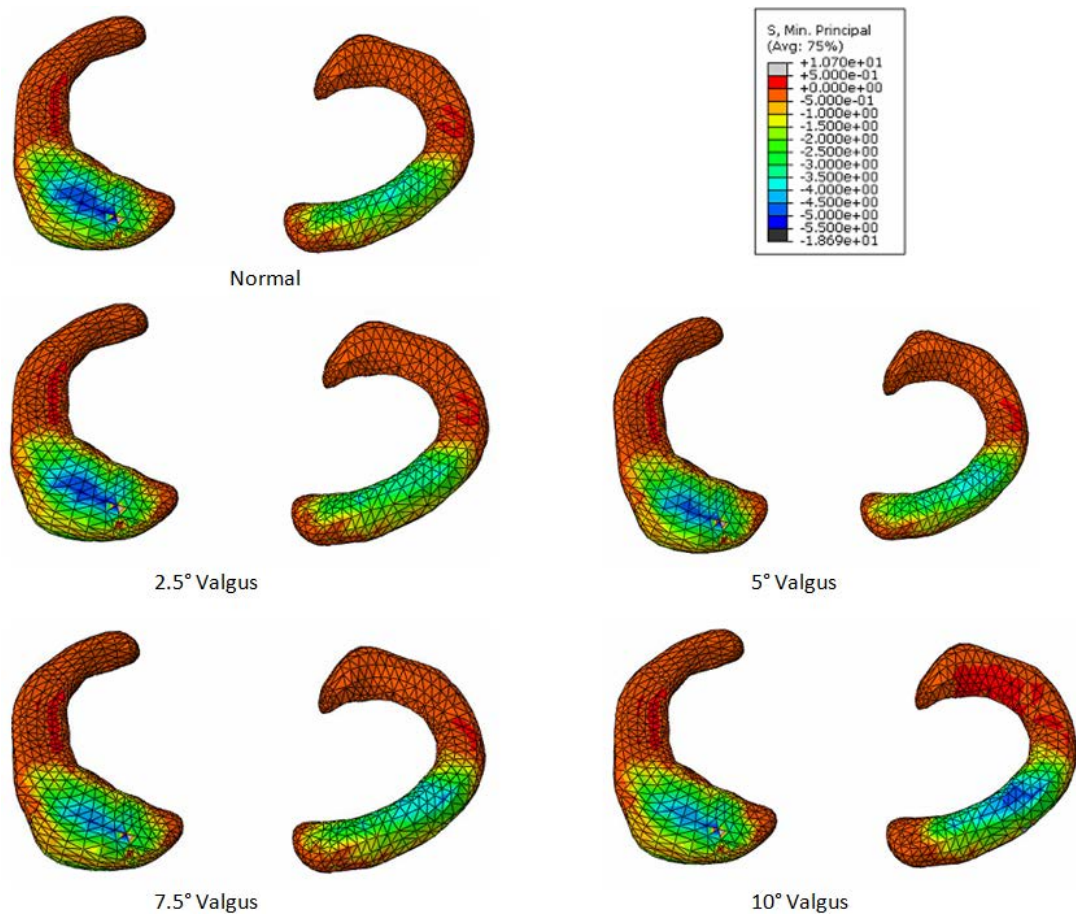
Figure 34. Maximal compression stress distribution in the menisci of all models

In Figure 35, however, the decrease in compressive stress on the medial side of femoral cartilage was not so obvious compared to the variation in stress distribution on the medial side of meniscus. On the other hand, the increase of stress on the lateral side of the femoral cartilage could be observed as there was a spot of blue region, indicating that a higher compressive stress appeared in the model with 7.5° and 10° valgus, respectively. The bigger region of the blue spot in the model with 10° valgus compared to the model with 7.5°valgus clearly indicates that a higher compressive stress was accumulated on the lateral side of femoral cartilage for such an angle.
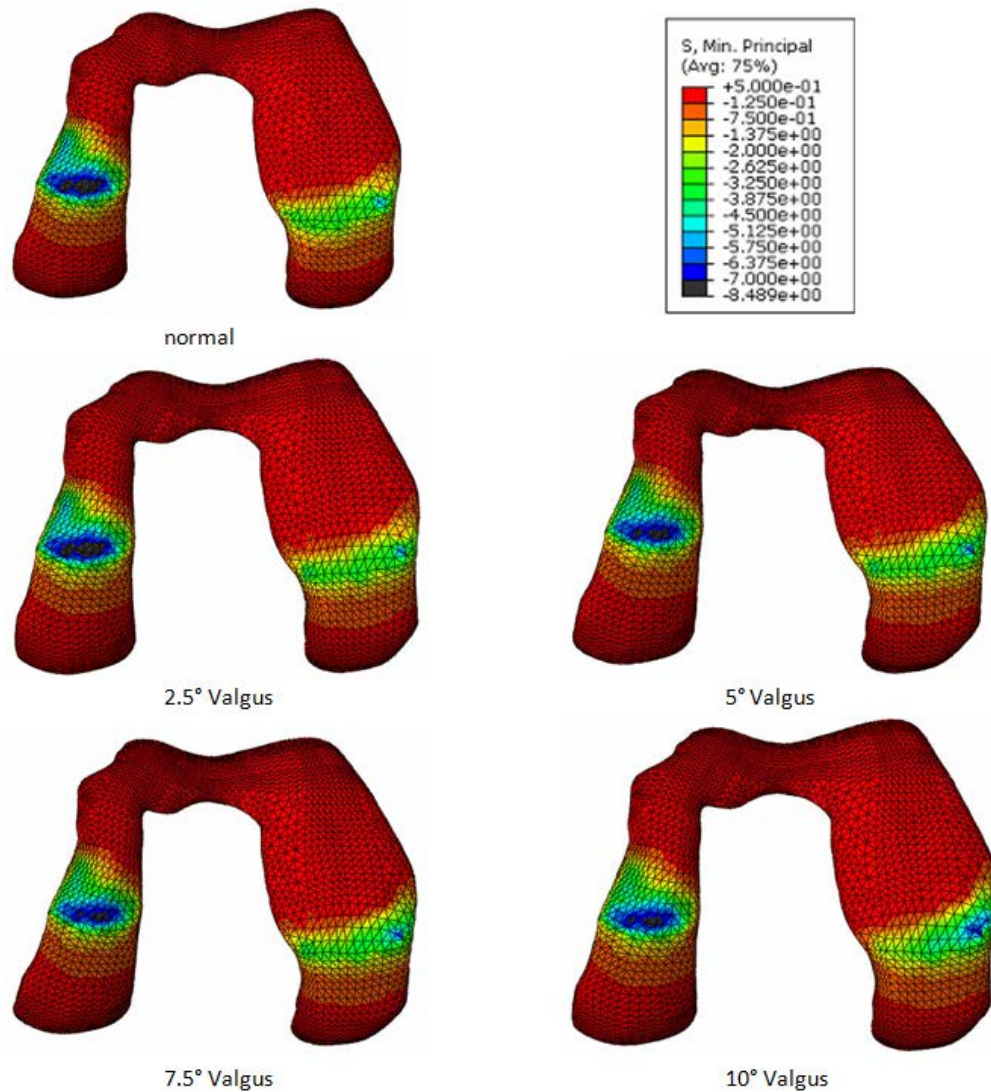
Figure 35. Maximal compression stress distribution in the femoral cartilages of all models

As shown in Figure 36, a similar trend of the variation of stress distribution can be observed for the tibial cartilage. The compressive stress decreased in the medial tibia cartilage as the valgus angle increased. Overall, the results of such HTO correction indicated that the decrease of loading in the medial compartment could be achieved by increasing the valgus angle, in other words, shifting the loading axis laterally.
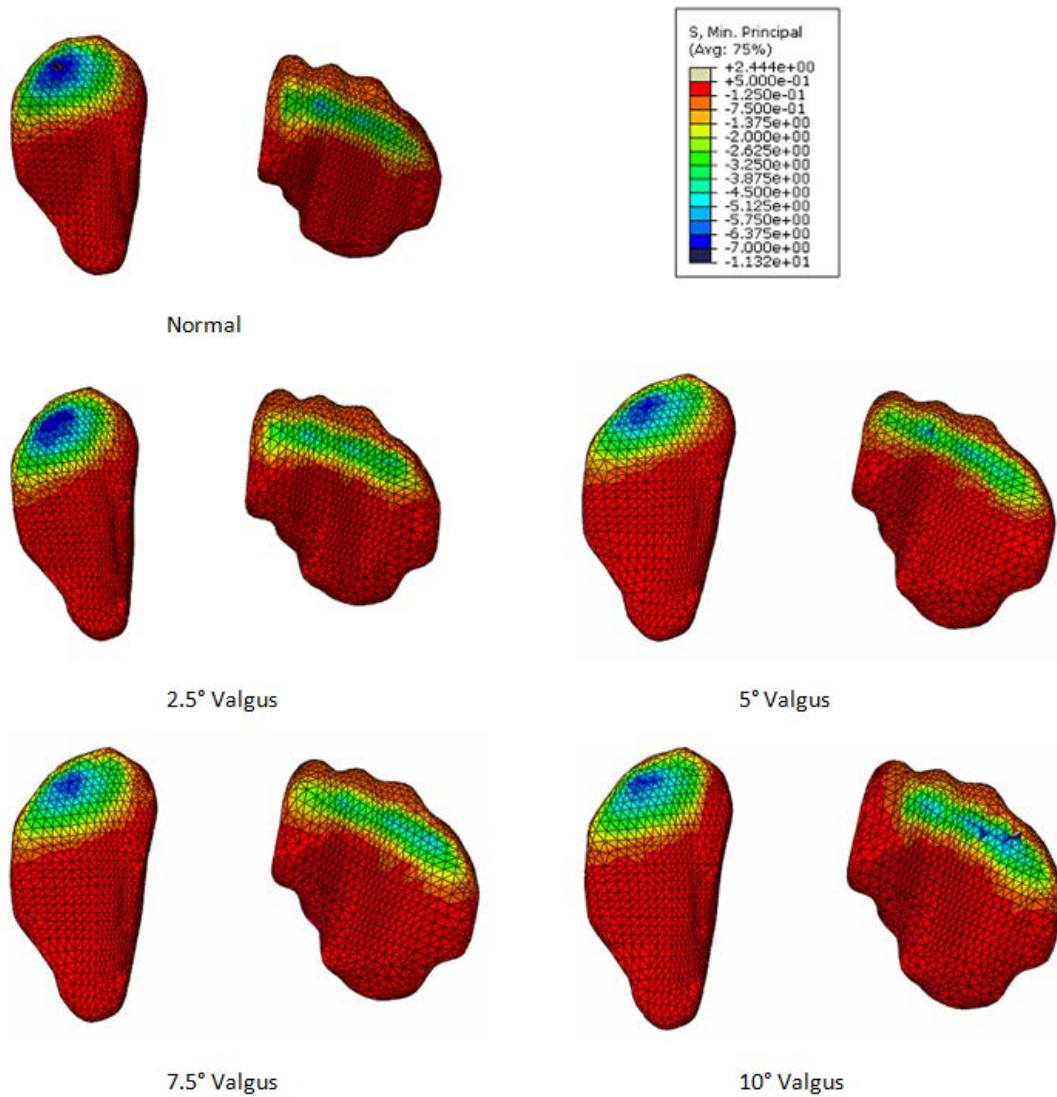
Figure 36. Maximal compression stress distribution in the tibial cartilages of all models

The maximal compressive stress calculated for both compartments of three soft tissues have been summarized in Table 6 (refered to Appendix C), which also been plotted in Figures 37-39 below. When the correction angle changed from 0° to 10° valgus, the maximum compressive stress for medial meniscus, medial femoral cartilage and medial tibia cartilage was observed to decrease from 6.4MPa to 4.9MPa (23% reduction), 7.7MPa to 6.9MPa (10% reduction) and 5.8MPa to 4.9MPa (16% reduction) respectively. Meanwhile, the maximum compressive stress for the lateral

meniscus, lateral femoral car taiga and lateral tibia cartilage was increased from 2.4MPa to 3.9MPa (63% increase), 3.3MPa to 5.6MPa (70% increase) and 3.3MPa to 5.8MPa (76% increase) respectively, when the correction angle changed from 0° to 10° valgus. Since the increase of stress in the lateral compartment was much smaller than that in the medial compartment, this huge difference of stress variation between two compartments required a larger valgus correction (6.6 HKA) to achieve a balance of stress distribution between two compartments.
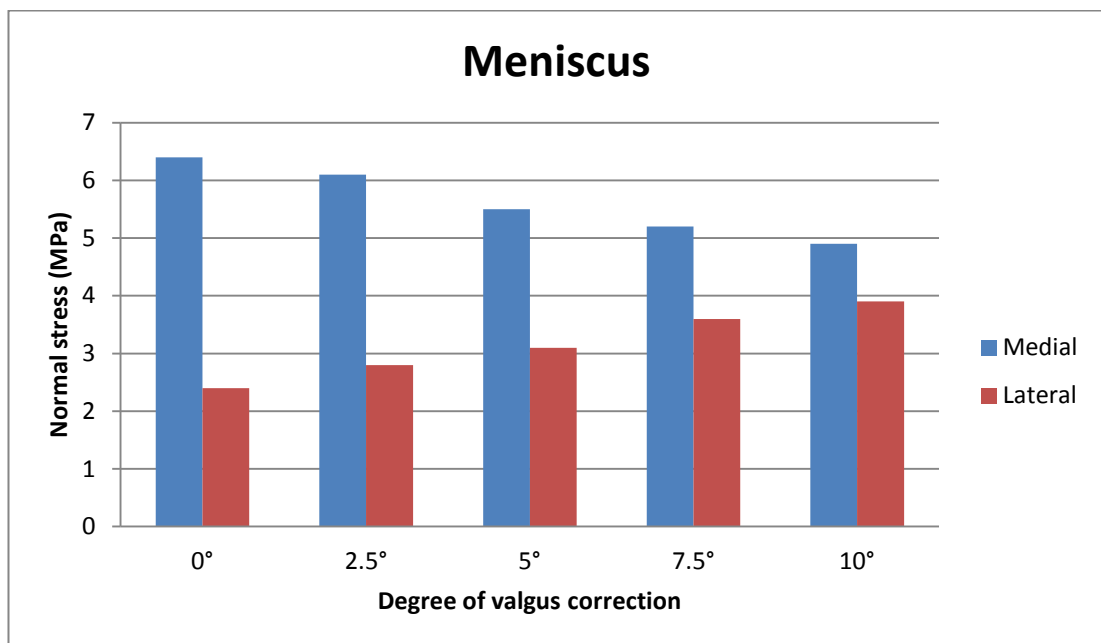
Figure 37.Variation of maximum compressive stresses in menisci of both compartments across the change of valgus correction
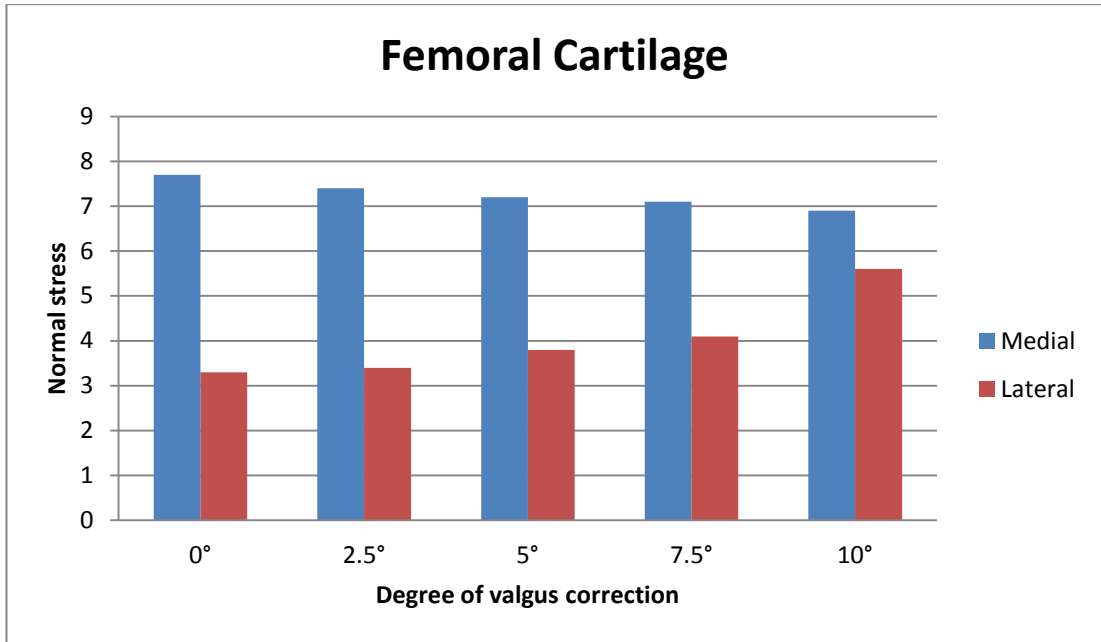
Figure 38. Variation of maximum compressive stresses in femoral cartilages of both compartments across the change of valgus correction
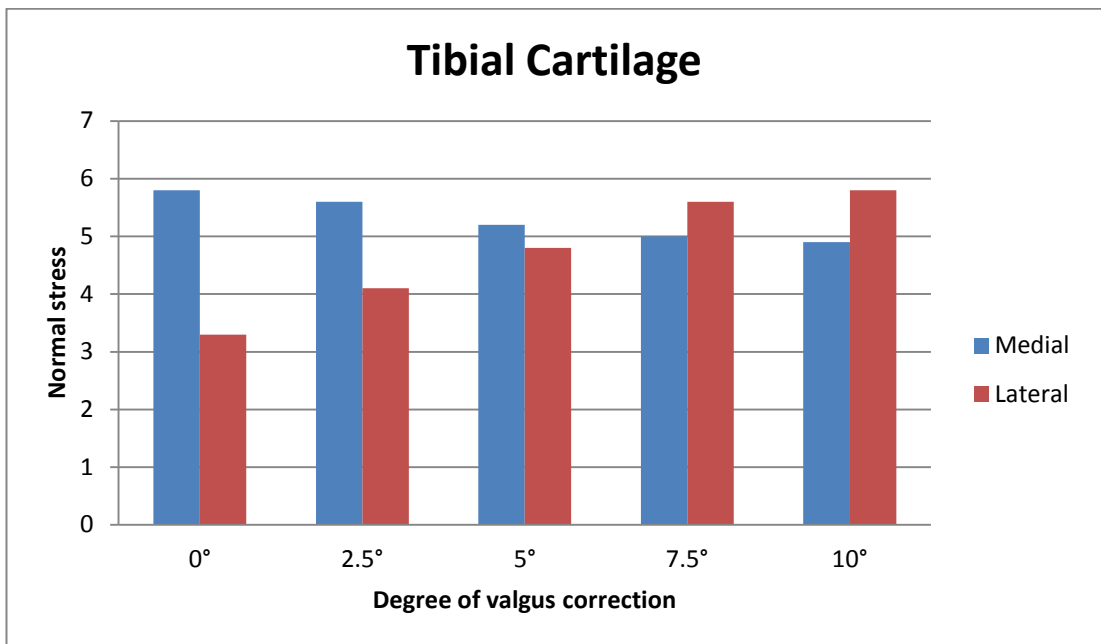
Figure 39. Variation of maximum compressive stresses in tibial cartilages of both compartments across the change of valgus correction

5.4 Effect of correction angle on shear stress distribution at cartilages and menisci

The shear stress, as mentioned earlier, was considered one of the major risks of accelerating the degeneration of cartilage. Therefore, the peak overall shear stresses (Tresca equivalent stress) of each model were calculated to see if the shifted loading axis has some effect on decrease in shear stress in the medial compartment in this section. As shown in Figure 40, some similar results were observed for the shear stress distributions between the menisci in these two compartments. The results clearly showed that shifting the loading axis (by increasing the valgus correction angle) has effectively decreased the medial compartment shear stress and increased the lateral compartment shear stress. As shown in the same Figure, the red region indicated the maximum shear stress and the blue region represented the minimum shear stress at this case.
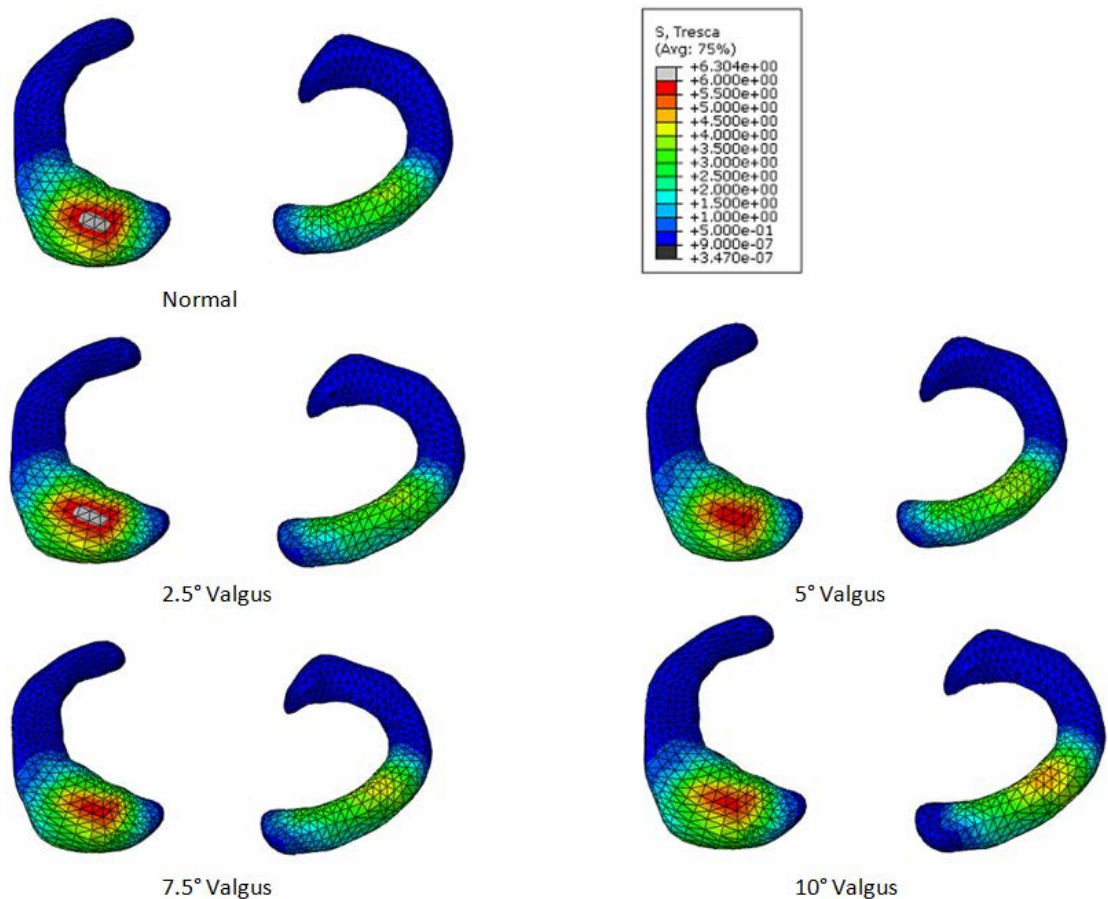
Figure 40. Shear stress distribution in the menisci of all models

As shown in Figure 41, a clearer decrease in the shear stress distribution can be observed on the medial side of the femoral cartilage. The shear stress concentration on the medial side of the cartilage observed in the normal knee model was spread out and clearly the stress distribution became more uniform after 10° valgus correction. However, there was an increased stress concentration on the lateral side of the cartilage in both models for the 10° valgus. This implies that when the lower limb was aligned in the situation of 10° valgus, there would be a certain risk of initiating the degeneration of cartilage in the lateral compartment.
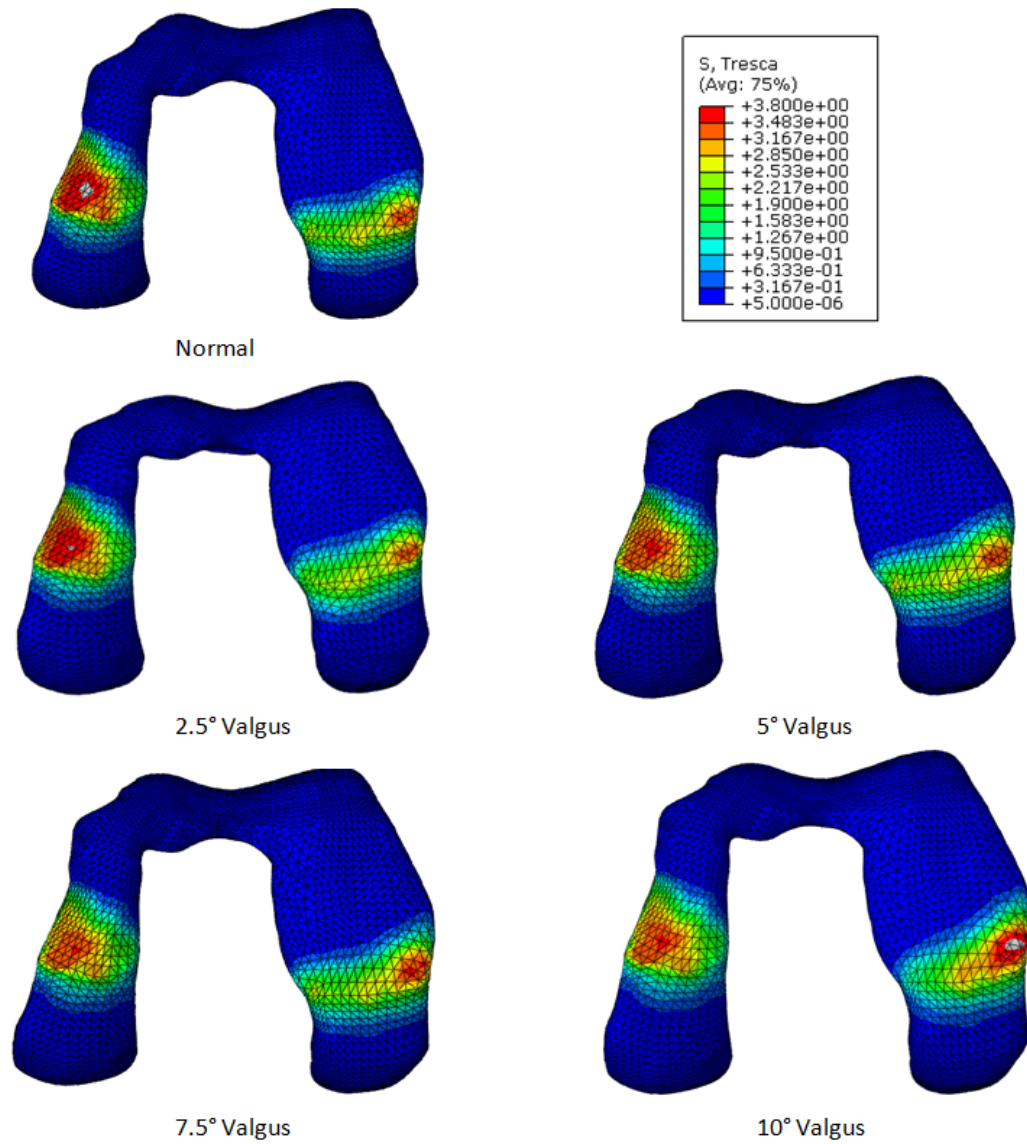
Figure 41. Shear stress distribution in the femoral cartilages of all models

The shear stress distributions on the tibia cartilages were shown in Figure 42. Although the trend of decrease in the shear stress concentration on the medial side and subsequent increase in the stress concentration on the lateral side cannot be observed clearly, the marginal variation in the shear stress distribution is still consistent with shifting of loading axis laterally.
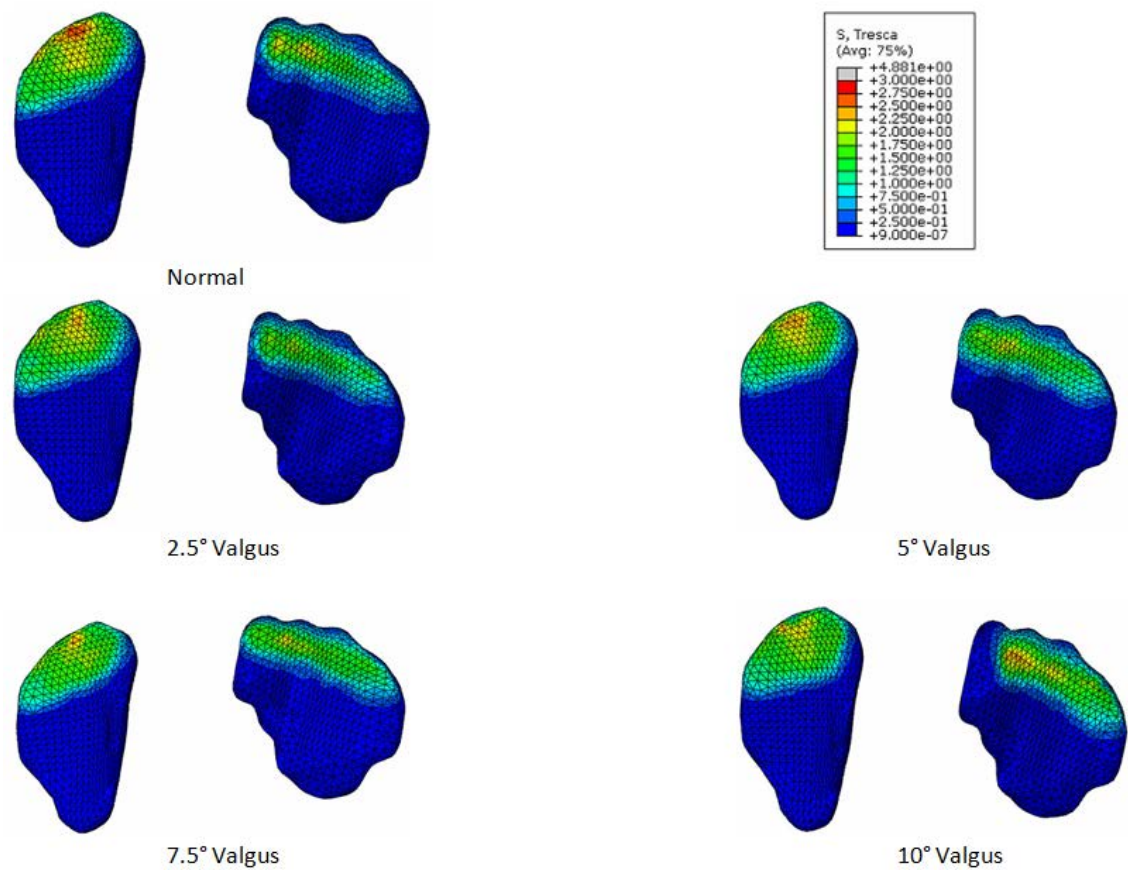
Figure 42. Shear stress distribution in the tibial cartilages of all models

Looking at the Table 7 (referred to Appendix C) and the Figures 43-45, when the correction angle changed from 0° to 10° valgus, the maximal shear stress was calculated decreasing in medial dimensions of meniscus, femoral cartilage and tibia cartilage, that is a reduction from 6.325MPa to 5.76MPa (9% reduction), 4.7MPa to 3.4MPa (28% reduction), and 4.0MPa to 2.0MPa (a reduction of 50%) respectively. At the same time, the maximum shear stress for the lateral meniscus, femoral cartilage and the lateral tibia cartilage have been observed to increase from 3.2MPa to 5.3MPa (66% increase), 2.7MPa to 4.1MPa (52% increase) and 2MPa to 2.5MPa (25% increase) respectively when the knee alignment changed from 0° to 10° valgus. Different to compressive, the larger reduction of shear stress in the medial compartment resulted in a smaller amplitude difference

between medial stress decrease and lateral stress increase. Therefore a balanced stress distribution between two compartments was achieved in a smaller valgus correction (5°) compared to that in compressive stress.
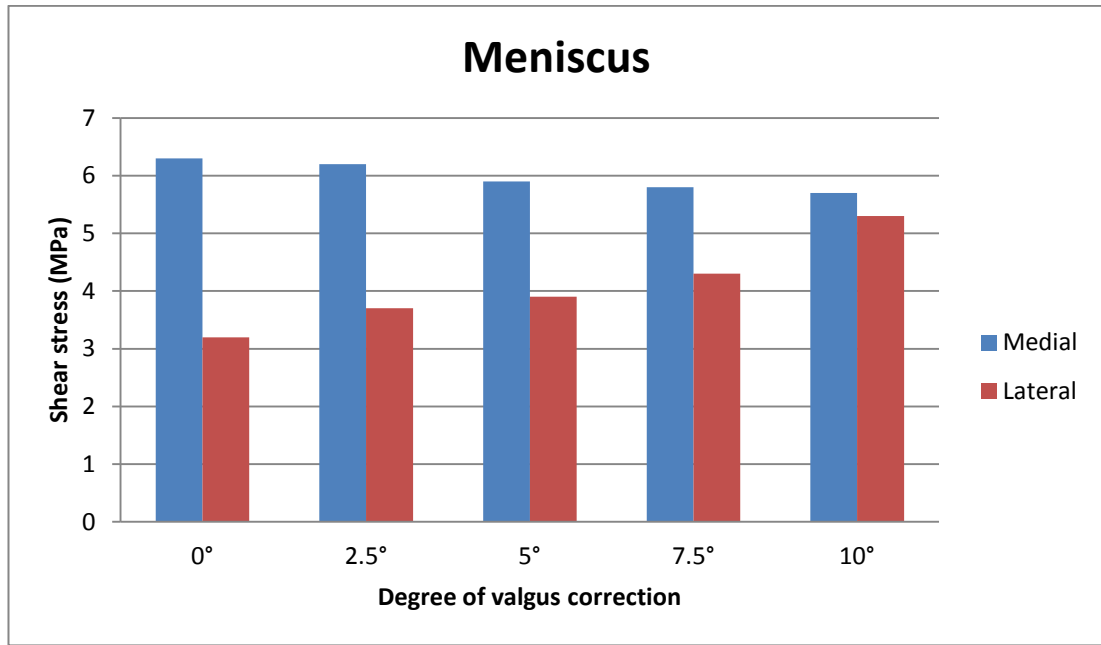
Figure 43. Variation of maximum shear stresses in menisci of both compartments across the change of valgus correction
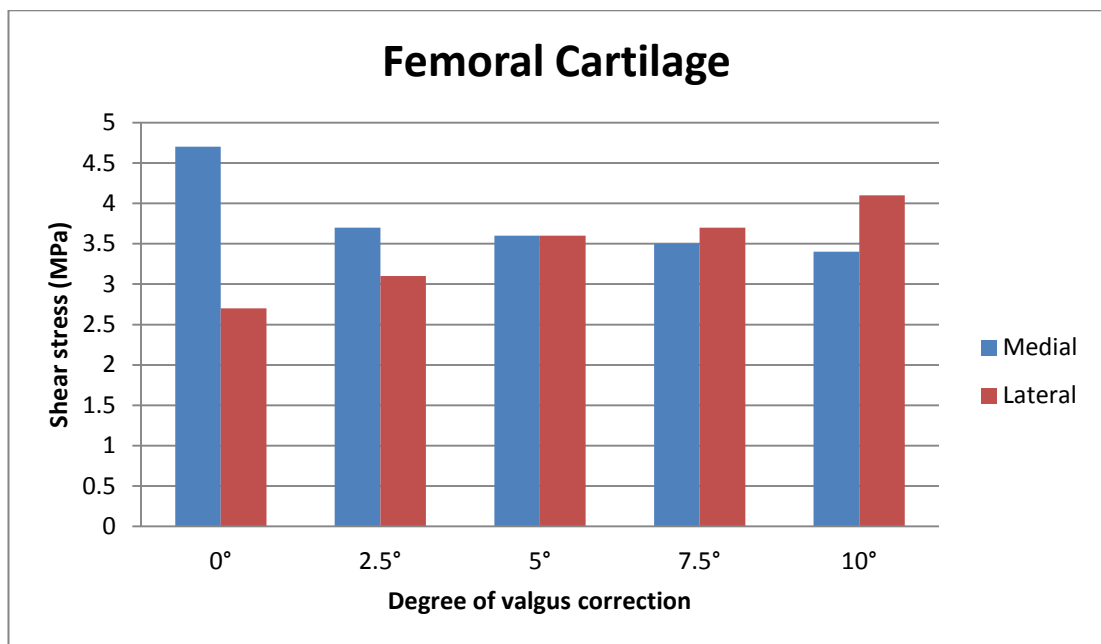
Figure 44. Variation of maximum shear stresses in femoral cartilages of both compartments across the change of valgus correction
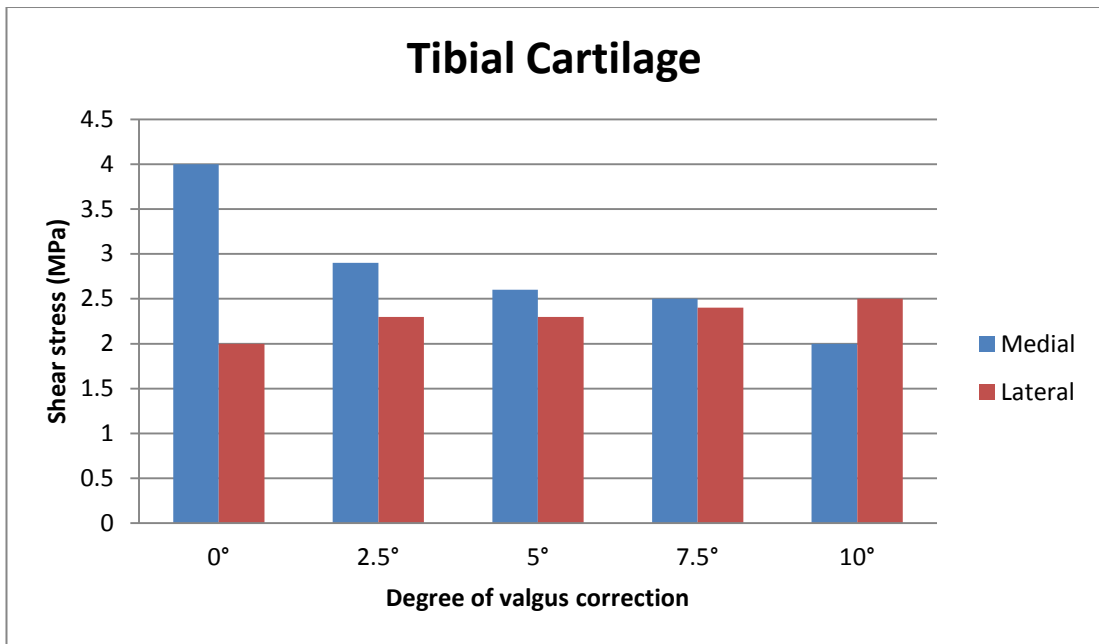
Figure 45. Variation of maximum shear stresses in tibial cartilages of both compartments across the change of valgus correction

Chapter 6 Discussion

In this Chapter, the validation of the model and investigation of the effect of subject-specific loading on stress distribution at knee joint were firstly discussed. Then, the effects of changing frontal correction angle of HTO on the stress distribution at the knee joint were explored by comparing our findings with other HTO studies based on the clinical outcome and experimental biomechanics. Finally, the limitation of this study will be outlined.

6.1 Validation of the model with literature

The underlying motivation for this study was to develop a computational procedure to explore the biomechanical implications and effects induced by the correction degree of HTO treatment. For this purpose, subject-based FEA has been adopted to simulate the loading condition at knee joint because FE models have been extensively used for representing complex biological structures [80]. To obtain an acceptable FE prediction, it is essential to validate the model. It is however rather difficult and challenging to validate the computational results with the *in vitro* or *in vivo* experimental results in this study as the knee model was generated based on a volunteer rather than cadaveric knee specimen. Therefore, the original knee model (normal aligned) was applied under a single compressive load (body weight) to obtain the contact pressure for comparing with published FEA studies [16, 57, 65, 67, 81, 82].

The maximum contact pressure of 3.1 MPa was observed on the surface of meniscus which was fairly close to the contact pressure obtained by Pena et al [67]'s study (data), in which an axial compression of 1150N was applied on a FE model of knee joint while the bone was considered as rigid body, cartilages and menisci behaved as linear elastic and isotropic, and ligaments was modelled as hyperelastic and isotropic. In their study, the maximal contact pressure appeared in the posterior region of the medial meniscus with average value of 2.9 MPa and in the anterior horn of the lateral meniscus with 1.45 MPa. Although the contact pressure was slightly higher in this study, it is within an acceptable range considering the difference between the subjects modelled. In other words, the difference in the geometry (e.g. thickness of

cartilage, thickness of meniscus) might be an important factor towards the stress deviation. In another study by Donahue et al [16], a FE model of knee joint was subjected to a compression of 800N. The maximum contact pressure obtained was 2.6 MPa, which is lower than that predicted in this study due to the reduced axial loading. Therefore, the consistence between the result of contact pressures in this study and the literature data demonstrated that my FE model is able to generate reasonable results.

Refer to literature, it is common to use subject-specific knee model in FE biomechanical studies since the different geometrical structures among people's knee joints, especially cartilage thickness, may affect the stress and strain distribution [16, 17, 19, 67, 79, 83, 84]. However, few of those studies have attempted to incorporate subject-specific joint geometry with loading and boundary conditions based on subject-specific gait data[21, 62].

In this study, the subject-specific gait data was used as an input in the FE model (loading case 2) and a comparison of the results between these two loading cases was established in the previous Chapter. Under loading case 1, the maximal contact pressure was observed in the lateral meniscus whilst the maximal contact pressure was shifted to the medial meniscus in loading case 2. This is because the varus moment at the beginning increased the loading in the medial compartment. This result is consistent with the findings of the previous studies indicating that approximately 70-75% of the load is transferred to the medial compartment of the knee joint due to the varus moment [57, 82].

The maximum normal stress of 3.11 MPa was found on the lateral femoral cartilage and 2.68MPa on the medial cartilage. The magnitude of the normal stresses on the medial knee cartilage doubled with the application of the varus knee moment in the current model. This comparison further indicated the importance of including the varus knee moment when studying knee biomechanics and may explain why knee OA occurs more frequently on the medial compartment of the knee than the lateral compartment [24], since alignment within 2° varus is still considered as normal aligned knee.

It is no doubt that the varus knee moments are the primary factor in the loading distribution to the medial compartment of the knee joint during normal gait. However, at the single leg support phase of the gait cycle, a varus-aligned knee will have a moment that increases the loading on the medial compartment of the knee, while a valgus-aligned knee will have a moment that increases the loading on the lateral compartment. In other words, the subject-specific loading condition would be different from individual to individual. For an individual with valgus-aligned knee, the valgus moment is most likely generated at the single leg support phase, while the varus moment occurs at the single leg support phase for the individual with varus-aligned knee [85]. This again indicated the importance of assigning the subject-specific functional data to the subject-specific knee structure.

In summary, calculating and comparing the magnitude of the contact pressure with literature combined with interpreting the effect of applying patient specific loading pattern in FEA on the stress distributions, were used to validate the subject-specific

FE knee model in this study. The consistence between my results and the published

data allows the FE model in this study to obtain persuasive results.

6.2 Effect of varying correction angle on stress distribution

Prior to the investigation of varying correction angle into the stress distribution, it is important to clarify that the correction angle is different to the HKA angle used in the clinical world. The correction angle referred to the amount of valgus correction degree, while the HKA angle referred to the Hip-Knee-Ankle alignment. In the conventional HTO surgery, the final goal of alignment is referred to the HKA angle since the amount of correction varies from patient to patient. But in this section the correction angle was used for biomechanical analysis to solely investigate the effect of varying correction angle (changing alignment) on the stress distribution of knee joint. Their difference merely resides in the angle definition but not in the biomechanical trend.

According to the limited HTO studies in literature, the effect of changing correction angle during HTO on the stress distribution at the soft tissues of knee joint has been investigated herein. The results from this subject-specific FE model quantified the role of the correction angle on the stress distribution in the knee joint. The knee alignment influenced load distribution at the knee; varus and valgus alignment increased medial and lateral load, respectively.

As abovementioned, the underlying motivation of this study was to establish an *in-silico* method to investigate how the change in knee alignment could influence the stress distribution at the soft tissues of knee joint; and subsequently obtain an optimal position of loading axis (i.e. the respective correction angle of HTO). The finite

element analysis was carried out here to quantify the stress distribution with the subject-specific data. The shifting of the loading axis laterally was achieved by bending the tibial to a certain valgus angle in this direction. In this study, four valgus angles of tibia were simulated at 2.5°, 5°, 7.5° and 10°.The decreases in both compressive stress and shear stress in the medial compartment were successfully achieved by changing the knee alignment from normal (slightly varus of 1.29°) to valgus. At the same time, the stress distribution increased in the lateral compartment as a result of increasing amount of valgus degree. These findings well supported the hypothesis proposed in this study.

As mentioned in the precious section, the varus moment contributes on a large portion of loading in the medial compartment. This explained the incidence of the major stress distribution in the medial compartment (cartilages and menisci) in the original knee model. The loading condition was identically applied on the femur to all the cases; therefore the results were used to essentially investigate the effect of shifting loading axis on the stress distribution in the knee joint. Although the results of this study could not directly relate to the clinical outcomes of the actual HTO and the gait data might change after surgery (which is one of the limitations of this study), the results did provide certain biomechanical insights into the evaluation of an optimal correction angle during HTO treatment in terms of stress redistribution.

The results also showed that the increased valgus alignment led to a smaller difference in the maximum values of both compressive and shear stresses between the medial and lateral cartilages. A more uniform stress distribution and a smaller difference between the maximum values on either side of the knee could explain why

Harman et al [86] observed that the valgus knee on the tibial plateau showed to wear out in a more uniform fashion. Although my result was based on the premise of applying the varus moment at that stage of interest during the gait cycle, this uniformly-distributed stress pattern might explain the overall performance during this functional activity. In addition, this finding might contribute to the decision of choosing optimal correction angle during HTO surgery.

It is surprising that limited studies were focused on the actual intra-articular effect of an osteotomy, which was intended to shift the loading axis from varus to valgus. The only related study, by Yang et al [65], was to investigate the effect of the frontal plane HKA angle on the stress and strain distributions at the knee cartilage, which constructed the knee joint FE models for three individuals. They found a lower stress in the medial compartment of the varus-aligned knee joint compared with that calculated in the same compartment of both valgus- and normal-aligned knee joint. More interestingly, at the heel strike of the gait cycle, varus-aligned subject and valgus-aligned subjects initiate the varus and valgus moment, respectively. Compared with Yang et al's study [21], the results obtained from my current model restricted the investigation only into the effect of changing HKA angle on the stress distribution in knee joint, which appeared a more accurate and effective way for the simulation of HTO treatment. Although the gait data of post-HTO patient may change due to the changing alignment of lower limb, it is reasonable to quantify the variation of stress distribution under the sole effect of changing HKA angle. Moreover, the simulation of different valgus angles on a single subject might avoid the issues in Yang et al's study on anatomical difference of individuals that may influence the loading distribution substantially.

6.3 Optimization of correction angle

Note that, the correction angle used in this study was based on the angular measurement bended on the frontal plane of tibia, which would be slightly larger than the actual degree of the correction angle used in clinical HTO procedure. This is because the frontal plane of the tibia was different to the frontal plane of the femur. The internal rotation of the tibia would result in some decrease in the correction angle measured from the frontal plane of tibia. Therefore, as mentioned before, a 5° correction will be equivalent to a 3.97° correction, which was described in Section 3.4. As a result, the amount of stress decrease in the medial compartment might be smaller in this study compared to the previous published HTO studies for the same degree correction. The 2.5°, 5°, 7.5° and 10° valgus correction were equivalent to the 1.49°, 3.97°, 5.21° and 7.94° valgus correction angles, respectively. By considering the offset of the actual frontal plane HKA angle of the original knee model, the 2.5°, 5°, 7.5° and 10° valgus correction were equilibrium to the 0.19°, 2.67°, 3.91° and 6.64° valgus alignment in terms of HKA angle, respectively (Table 5). It must be emphasized again that the offset does not affect the biomechanical analysis and trends of stress distributions obtained in this study.

Table 5 Summary of the correction angles (positive degree indicated valgus and negative degree indicated varus)

Correction angle	Actual correction angle (Frontal Plane)	HKA angle (Frontal Plane)
0°	0°	-1.29°
2.5°	1.49°	0.2°
5°	3.97°	2.7°
7.5°	5.27°	3.9°
10°	7.94°	6.6°

6.3.1 How to determine optimal alignment

As mentioned in Chapter 2, it is surprising after several decades of osteotomy that there is little agreement between studies on the ideal alignment. Although the "Fujisawa point" which targeted a lateral shift of the weight bearing line to a maximum of 62.5% of the medial to lateral width of the tibia plateau (equivalent to 3.5° of valgus) [54] has gained the most recognitions in literature [11], large amount of clinical studies recommended different HKA alignment varying from 2° valgus up to 8° valgus [6, 7, 10, 38, 46, 87]. The possible reason caused such debatable issues may be due to different surgical techniques, population and statistical analysis used in these separate studies. More importantly, the patient's variability rises as another possible reason to this controversial HKA alignment recommendation. Does an individualised HKA angle provide better outcome for HTO patient?

Since there remains lack of biomechanical evidence to rigorously define the optimal correction angle in an individual patient, a more direct way to investigate the alignment optimisation by analysing the knee joint loading *in vivo* has been carried out in this study. The desired alignment will determine the angle to which the medial compartment is unloaded and the lateral compartment loaded, with an implication for potential chondral regeneration medially and degeneration laterally [88]. The balance of loading between two compartments could be critical to the success of HTO. Presumably the appropriate correction is the minimum over-correction (i.e. slightly valgus) necessary to achieve unloading in medial compartment and prevent recurrence of varus deformity, thereby avoiding overloading on lateral compartment cartilage by excessive valgus.

Although the FE method should be able to quantify the internal loading in both compartments for determining a possible alignment by avoiding an overloading on lateral cartilage to achieve sufficient unload in medial cartilage for pain revival, the *in vivo* tolerance of human cartilage to contact stress and the direct correlation between pain and contact stress are unavailable. Therefore, it might be reasonable to assume the achievement of equal stress distributions between two compartments as a standard. Also this uniform loading situation most closely approximates physiological loading in neutral aligned lower limb and therefore represents an ideal outcome for patients [13].

In this study, the recommended HKA angle is 6.6° of valgus when considering compressive stress and 3.9° of valgus when considering shear stress. The compressive stress is directly related to the pain while the shear stress is believed as an important factor of OA progression. Different recommendations based on considering peak shear stress and peak compressive stress is because the shear stress considered the tearing force resulted from internal moments compared to that compressive stress only considered the "pushing" force by functional loading, which implies that the change in shear stress is more sensitive to the variation in the correction angle (i.e. Smaller correction allows shear stress to have uniformly-distribution between the two compartments comparing to compressive stress). Although the shear stress is believed to potentially affect the OA progression, compressive stress which directly relates to pain has been so far commonly accepted as a more critical factor in clinical HTO. Prior to adapting shear stress for optimising the HTO alignment in our approach more research is required on investigating how significantly the shear stress influences OA and HTO.

6.3.2 Comparison with biomechanical studies of HTO in literature

To validate the feasibility of the method used in this study, the recommended alignment from the outcome of this study was compared with the published cadaver studies that have investigated the effect of the medial opening wedge HTO on the intra-articular cartilage pressure of the knee. One literature study performed osteotomy proximal to the distal attachment of the MCL on cadaveric specimens and observed an increased medial compartment pressure at a correction of 8°valgus [12], which is contradict to ours. The reason for the discrepancy between their study and this study may be related to the differences in the location of the osteotomy. The present study simulated an osteotomy distal to the MCL attachment and detected a reduction in medial compartment loading. This finding is consistent with Mina et al's cadaver study [13] that also performed an osteotomy distal to the attachment. However, Mina et al recommended the alignments of 0° to 4° of valgus to achieve equally stress distribution between the two compartments which is somewhat lower than the present study.

Such differences lead to a possible limitation of the current experiment, which is the use of a healthy knee to simulate clinical HTO. It may overestimate the required HKA in a clinical situation, because normally, the HTO patients may have had degeneration of medial meniscus and possible cartilage defects. In those cases, medial compartment unloading can be achieved with a smaller valgus correction angle. This may explain why the HKA of 6.6° valgus in this study is slight larger than the HKA angle recommended (2-5° valgus) in some recent publications [24, 25, 89]. Although employing the standard healthy model in this study on real patients will be another crucial step, at the first stage of development, selection of health

subject is considered necessary and applicable to avoid the possible stress concentration causing confusion in the biomechanical interpretation of most critical results.

6.4 Implications and limitations

The results from current study confirmed the hypothesis that the stress distribution in the medial compartment decreases as the loading axis shifted laterally; and also agrees with the previous research that observed medial opening wedge HTO was able to reduce the load in the medial compartment and disentangle the patient from OA in that compartment. Considering the importance of the cartilages and menisci in load dissipation that was established before, any excessive loading to both soft tissues can impose a greater risk of degeneration in the underlying bones; and thus contribute to the mechanical pathway leading to new onset and progression of OA. According to the FEA results obtained, the stress distribution, especially the shear stress which was considered a critical factor for accelerating the cartilage worn and progression of OA, on the lateral compartment increased as loading axis shifted laterally. This might indicate the initiation of the subsequent OA on the lateral cartilages. Therefore, a uniformly-distributed stress in both the compartments would be more ideal for preventing OA. This may be another consideration for deciding the optimal correction angle.

Although a uniformly-distributed stress in both compartments might be ideal for preventing OA in terms of mechanical concept, the recognised guideline of optimal HTO correction is still unavailable in literature. Therefore the present study focused on providing a new procedure to explore this debatable issue in a way of pre-operatively mechanical loading evaluation rather than providing an answer to this issue. This subject-specific non-invasive analysis of stress distribution that provided a quantitative insight into evaluation of the mechanical responses in the soft tissues

within knee joint as a result of adjusting the loading axis, may be used as a preoperative assessment tool to predict the consequential mechanical loading information for surgeon to decide the patient specific optimal angle. A feasible way could be to use computer navigation system for helping surgeon to achieve greater precision in implementing the exact correction angle that is considered most appropriate.

The key biomechanical limitation of this study is that the non-linear behaviours of the material properties of cartilage were not considered here. Although the cartilage were taken into account as linearly homogenous isotropic material in most of the previously studies published in literature, the real cartilage can behave nonlinearly, e.g. in a viscoelastic fashion. There are no studies actually investigated the influence of the viscoelastic behaviour of the femoral and tibia cartilage on the FEA results due to the short time span considered in those studies. Nevertheless, considering such non-linearity in FEA will generate more realistic results and definitely be a valuable motivation for future study.

Another limitation resides in neglecting muscle forces. The contribution of the muscle forces increases the total compressive forces at the knee three to six times the body weight during the gait cycle [90, 91]. However, the subject-specific muscle forces cannot be calculated using the inverse dynamic method discussed above. "Muscle force reduction method" introduced by Morrison [21] has been commonly used in biomechanics studies on knee joint to calculate the muscle forces. But the calculation of the muscle forces was based on the substantial assumption of generalising the position of the major muscle attachment and the line of action of

each muscle group. This limits the way to applying subject specific loading data more accurately. The use of EMG-driven models may provide improved data for individual muscle forces when applied to the FE model [92]. However, it is fairly challenge to use the EMG-driven models at this stage of studies due to limited resources available. In summary, the current FE studies did not consider the muscle forces and may underestimate the cartilage stresses. Nevertheless, the symmetric muscle force would mainly affect the stress magnitude rather than the distribution.

Chapter 7 Conclusion and future work

In this study, the 3D subject-specific finite element analysis was carried out to investigate the effect of post-operative alignment of the medial opening wedge HTO on the stress distribution at the cartilage and meniscus in knee joint. The finite element models involved in the present study were constructed based on the subject-specific MR images and had been validated with the literature data by comparing the contact pressures at the cartilage and meniscus under identical loading condition.

Our results showed that both the compressive and shear stresses at the cartilage of the medial compartment decrease as the valgus correction angle of the medial opening wedge HTO increases. In addition, the stress distribution at the medial cartilage became more uniform as the loading axis shifting to the lateral compartment. These results strongly support the hypothesis in this study.

Considering the lack of a standardised HTO alignment and no FEA studies have investigated the effect of correction angle of HTO on the stress distribution on the soft tissues in literature, the present study focused on establishing a new systematic method to explore this debated issues in a way of pre-operatively mechanical loading evaluation rather than providing an answer to this tissue.

After comparing with those published studies that investigated the effects of correction angle of HTO on either the clinical outcome or the biomechanical

outcome (e.g. stress distribution), results in this study are well correlated to the clinical data and recommendation in literature. More importantly, this patient-specific non-invasive analysis of stress distribution that provided a quantitative insight to evaluate the mechanical responses of the soft tissue within knee joint as a result of adjusting the loading axis, may be used as a preoperative assessment tool to predict the consequential mechanical loading information for surgeon to decide the patient specific optimal angle.

In order to obtain more reliable and persuasive results for deciding the optimal HTO correction angle, improvements in this study are required. Firstly, the muscle force could play an important role in the biomechanics of the knee joint during functional activities and therefore considering both magnitude of the net knee joint loading (muscle force combined with total reaction forces) and the location of applying the muscle forces would increase the overall stress magnitudes on the cartilage and meniscus, and possibly change the patterns of the stress distribution. Secondly, assigning the non-linearly behaved material properties to other soft tissues could be another potential area of improvement for the future work. It will surely increase the modelling accuracy. Therefore, the effort to overcome the challenges of these two limitations would be worthy in future study on this topic.

Furthermore, repeating the investigation on a number of real patients operated with clinical HTO procedures will allow for a better comparison of results. Gaining greater biomechanical and clinical insights will be expected by determining whether similar stress distributions are obtained across different patients, and whether the same patterns of stress distribution would exist in different patients.

Despite its limited generalisability and the need for further validation, the concept introduced here may develop into a useful procedural technique for patient-specific preoperative planning of HTO for medial compartment knee OA.

Appendix A

Detail sketch of calculating the specific translations to simulate the HTO, including all dimensions.
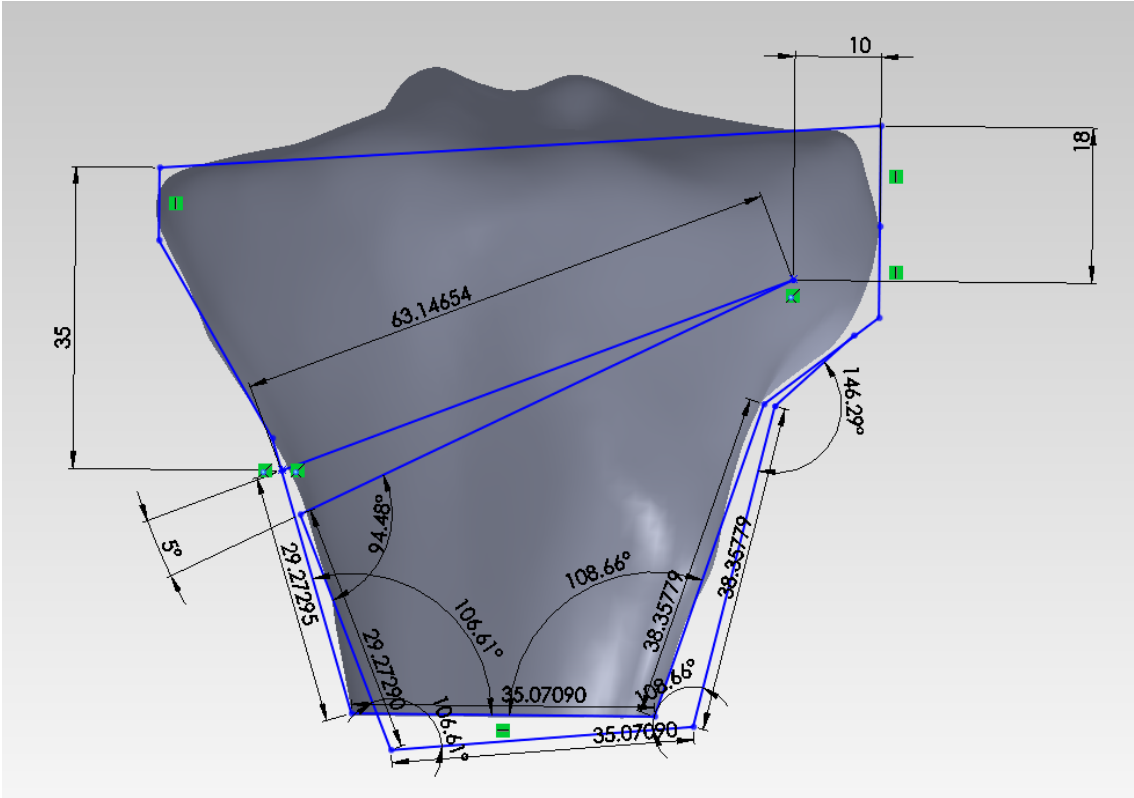
Appendix B

Actual correction angles on the frontal plane

0° correction
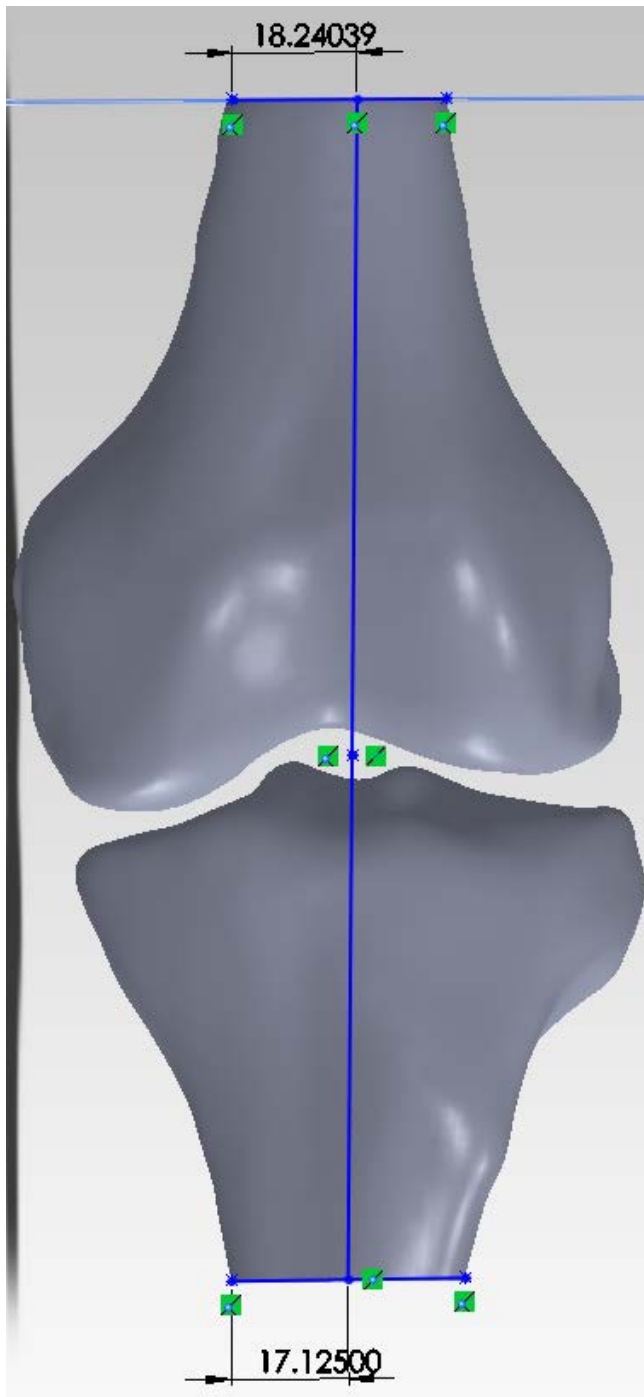
2.5° correction
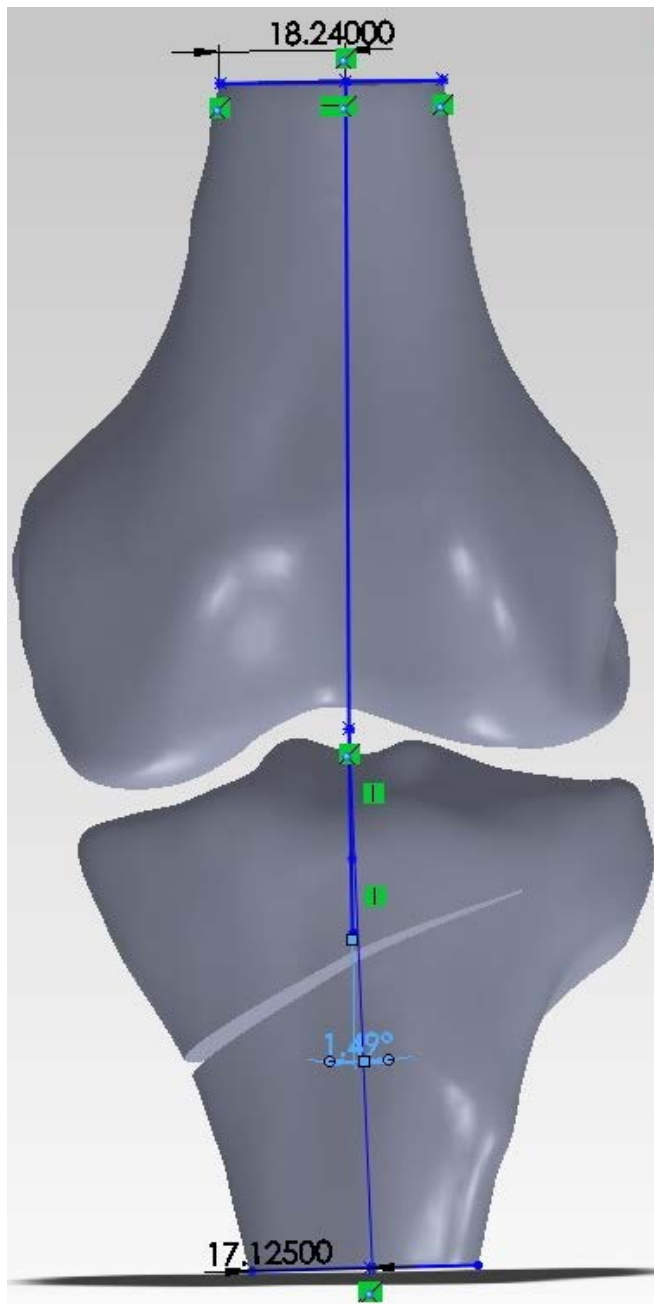
5° correction
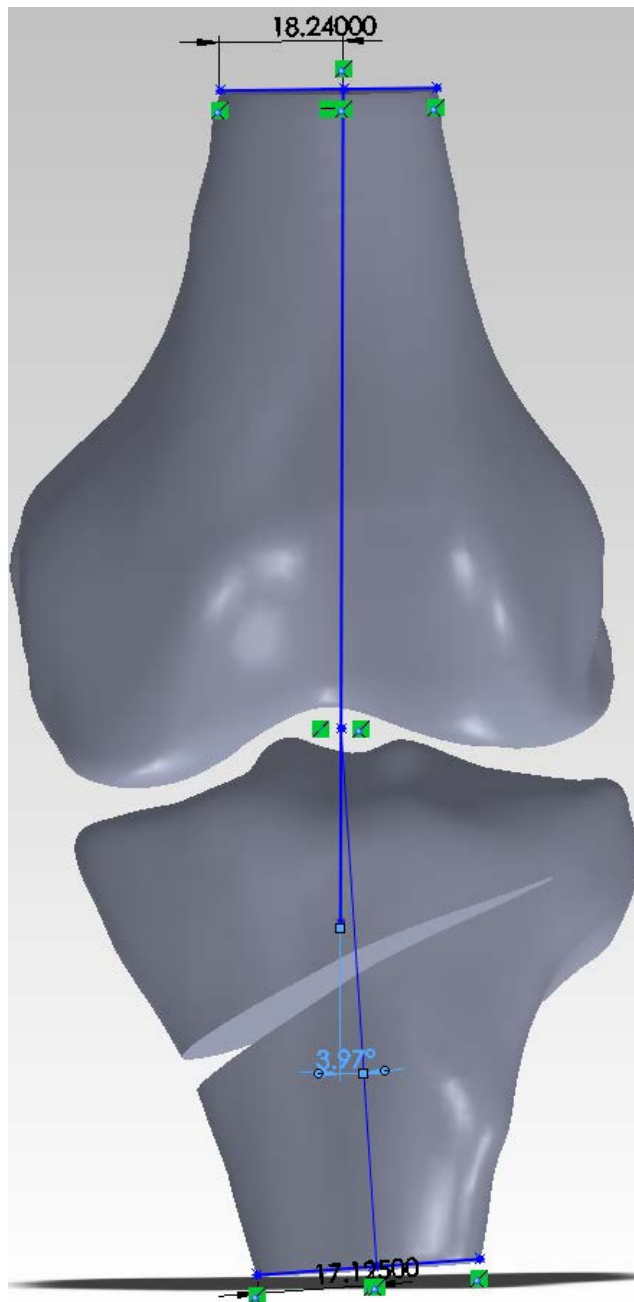
7.5° correction
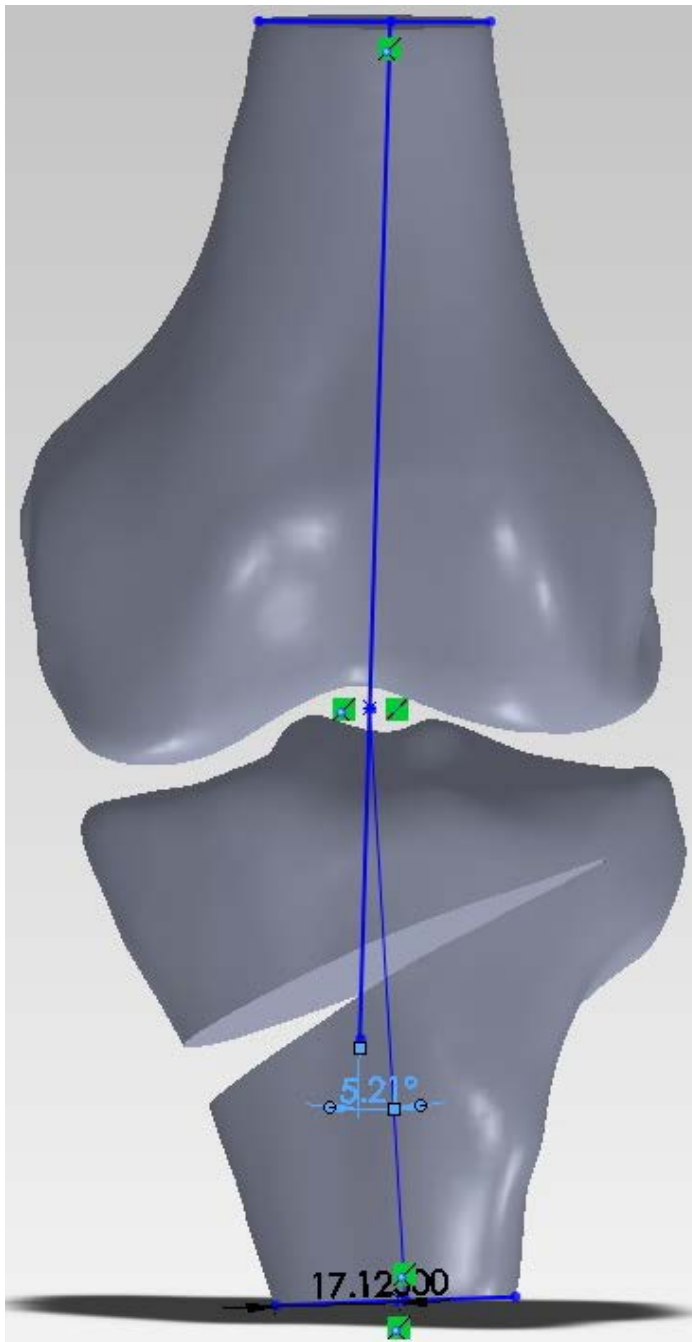
10° correction
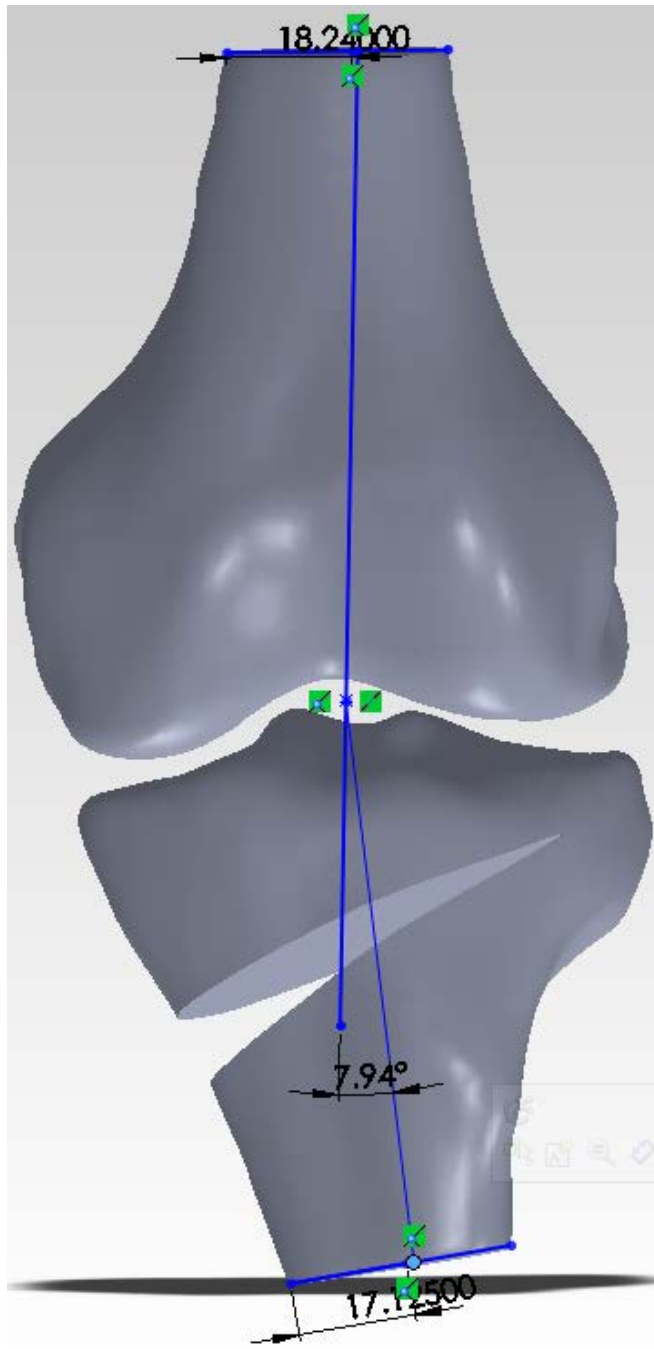
Appendix C

Table 6. Maximum Compressive stresses (MPa) on menisci and cartilages

Tissues	Maximum Normal Stress 0°	Maximum Normal Stress 2.5° Valgus	Maximum Normal Stress 5° Valgus	Maximum Normal Stress 7.5° Valgus	Maximum Normal Stress 10° Valgus
Medial Meniscus	6.4	6.1	5.5	5.2	4.9
Lateral Meniscus	2.4	2.8	3.1	3.6	3.9
Medial Femoral Cartilage	7.7	7.4	7.2	7.1	6.9
Lateral Femoral Cartilage	3.3	3.4	3.8	4.1	5.6
Medial Tibia Cartilage	5.8	5.6	5.2	5.0	4.9
Lateral Tibia Cartilage	3.3	4.1	4.8	5.6	5.8

Table 7. Maximum shear stresses (MPa) on menisci and cartilages

Tissues	Maximum Shear Stress 0°	Maximum Shear Stress 2.5° Valgus	Maximum Shear Stress 5° Valgus	Maximum Shear Stress 7.5° Valgus	Maximum Shear Stress 10° Valgus
Medial Meniscus	6.3	6.2	5.9	5.8	5.7
Lateral Meniscus	3.2	3.7	3.9	4.3	5.3
Medial Femoral Cartilage	4.7	3.7	3.6	3.5	3.4
Lateral Femoral Cartilage	2.7	3.1	3.6	3.7	4.1
Medial Tibia Cartilage	4.0	2.9	2.6	2.5	2.0
Lateral Tibia Cartilage	2.0	2.3	2.3	2.4	2.5

References

1.	Brouwer, R.W., et al., *Osteotomy for treating knee osteoarthritis (Withdrawn Paper. 2007, art. no. CD004019).* Cochrane Database of Systematic Reviews, 2007(3).
2.	March, L.M. and H. Bagga, *Epidemiology of osteoarthritis in Australia.* Medical Journal of Australia, 2004. **180**(5): p. S6-S10.
3.	Heijink, A., et al., *Biomechanical considerations in the pathogenesis of osteoarthritis of the knee.* Knee Surgery Sports Traumatology Arthroscopy, 2012. **20**(3): p. 423-435.
4.	Riegger-Krugh, C., et al., *Tibiofemoral contact pressures in degenerative joint disease.* Clinical Orthopaedics and Related Research, 1998(348): p. 233-245.
5.	Akizuki, S., et al., *The long-term outcome of high tibial osteotomy - A ten- to 20-year follow-up.* Journal of Bone and Joint Surgery-British Volume, 2008. **90B**(5): p. 592-596.
6.	Esenkaya, I. and N. Elmali, *Proximal tibia medial open-wedge osteotomy using plates with wedges: early results in 58 cases.* Knee Surgery Sports Traumatology Arthroscopy, 2006. **14**(10): p. 955-961.
7.	Schallberger, A., et al., *High tibial valgus osteotomy in unicompartmental medial osteoarthritis of the knee: a retrospective follow-up study over 13-21 years.* Knee Surgery Sports Traumatology Arthroscopy, 2011. **19**(1): p. 122-127.
8.	Tang, W.C. and I.J.P. Henderson, *High tibial osteotomy: Long term survival analysis and patients' perspective.* Knee, 2005. **12**(6): p. 410-413.
9.	Valenti, J.R., et al., *Long term evaluation of high tibial valgus osteotomy.* International Orthopaedics, 1990. **14**(4): p. 347-349.
10.	Sprenger and J.F. Doerzbacher, *Tibial osteotomy for the treatment of varus gonarthrosis. Survival and failure analysis to twenty-two years (vol 85, pg 469, 2003).* Journal of Bone and Joint Surgery-American Volume, 2003. **85A**(5): p. 912-912.
11.	Rudan, J., M. Harrison, and M.A. Simurda, *Optimizing femorotibial alignment in high tibial osteotomy.* Canadian Journal of Surgery, 1999. **42**(5): p. 366-370.
12.	Agneskirchner, J.D., et al., *The effects of valgus medial opening wedge high tibial osteotomy on articular cartilage pressure of the knee: A biomechanical study.* Arthroscopy-the Journal of Arthroscopic and Related Surgery, 2007. **23**(8): p. 852-861.
13.	Mina, C., et al., *High tibial osteotomy for unloading osteochondral defects in the medial compartment of the knee.* American Journal of Sports Medicine, 2008. **36**(5): p. 949-955.
14.	Bae, J.Y., et al., *Biomechanical analysis of the effects of medial meniscectomy on degenerative osteoarthritis.* Medical & Biological Engineering & Computing, 2012. **50**(1): p. 53-60.
15.	Beillas, P., et al., *A new method to investigate in vivo knee behavior using a finite element model of the lower limb.* Journal of Biomechanics, 2004. **37**(7): p. 1019-1030.

16. Donahue, T.L.H., et al., *A finite element model of the human knee joint for the study of tibio-femoral contact.* Journal of Biomechanical Engineering-Transactions of the Asme, 2002. **124**(3): p. 273-280.

17. Li, G., et al., *A validated three-dimensional computational model of a human knee joint.* Journal of Biomechanical Engineering-Transactions of the Asme, 1999. **121**(6): p. 657-662.

18. Mononen, M.E., et al., *Effect of superficial collagen patterns and fibrillation of femoral articular cartilage on knee joint mechanics-A 3D finite element analysis.* Journal of Biomechanics, 2012. **45**(3): p. 579-587.

19. Papaioannou, G., C.K. Demetropoulos, and Y.H. King, *Predicting the effects of knee focal articular surface injury with a patient-specific finite element model.* Knee, 2010. **17**(1): p. 61-68.

20. Pena, E., et al., *Effect of the size and location of osteochondral defects in degenerative arthritis. A finite element simulation.* Computers in Biology and Medicine, 2007. **37**(3): p. 376-387.

21. Yang, N.H., et al., *Protocol for constructing subject-specific biomechanical models of knee joint.* Computer Methods in Biomechanics and Biomedical Engineering, 2010. **13**(5): p. 589-603.

22. Zhang, X.S., et al., *3-D Finite Element Method Modeling and Contact Pressure Analysis of the Total Knee Joint in Flexion.* 2009 3rd International Conference on Bioinformatics and Biomedical Engineering, Vols 1-112009, New York: Ieee. 2867-2869.

23. Loeser, R.F., *Age-Related Changes in the Musculoskeletal System and the Development of Osteoarthritis.* Clinics in Geriatric Medicine, 2010. **26**(3): p. 371-+.

24. Sharma, L., et al., *The role of knee alignment in disease progression and functional decline in knee osteoarthritis.* Jama-Journal of the American Medical Association, 2001. **286**(2): p. 188-195.

25. Amendola, A. and D.E. Bonasia, *Results of high tibial osteotomy: review of the literature.* International Orthopaedics, 2010. **34**(2): p. 155-160.

26. Takeuchi, R., T. Saito, and T. Koshino, *Clinical results of a valgus high tibial osteotomy for the treatment of osteoarthritis of the knee and the ipsilateral ankle.* Knee, 2008. **15**(3): p. 196-200.

27. Smith, T.O., et al., *Opening- or closing-wedged high tibial osteotomy: A meta-analysis of clinical and radiological outcomes.* Knee, 2011. **18**(6): p. 361-368.

28. Coventry, M.B., *UPPER TIBIAL OSTEOTOMY.* Clinical Orthopaedics and Related Research, 1984(182): p. 46-52.

29. Karachalios, T., P. Sarangi, and J. Newman, *Severe varus and valgus deformities treated by total knee arthroplasty.* Journal of Bone & Joint Surgery, British Volume, 1994. **76**(6): p. 938-942.

30. Noyes, *Opening wedge tibial osteotomy: The 3-triangle method to correct axial alignment and tibial slope (vol 33, pg 378, 2005).* American Journal of Sports Medicine, 2006. **34**(9): p. 1537-1537.

31. Brown, G.A. and A. Amendola, *Radiographic Evaluation and Preoperative Planning for High Tibial Osteotomies.* Operative Techniques in Sports Medicine, 2012. **20**(1): p. 93-102.

32. Haddad, F.S., et al., *The PROSTALAC functional spacer in two-stage revision for infected knee replacements.* Journal of Bone and Joint Surgery-British Volume, 2000. **82B**(6): p. 807-812.

33.   Buckwalter, J.A. and J.A. Martin, *Osteoarthritis.* Advanced Drug Delivery Reviews, 2006. **58**(2): p. 150-167.

34.   Jackson, B.D., et al., *The effect of the knee adduction moment on tibial cartilage volume and bone size in healthy women.* Rheumatology, 2004. **43**(3): p. 311-314.

35.   Koshino, T., T. Murase, and T. Saito, *Medial opening-wedge high tibial osteotomy with use of porous hydroxyapatite to treat medial compartment osteoarthritis of the knee.* Journal of Bone and Joint Surgery-American Volume, 2003. **85A**(1): p. 78-85.

36.   Benzakour, T., et al., *High tibial osteotomy for medial osteoarthritis of the knee: 15 years follow-up.* International Orthopaedics, 2010. **34**(2): p. 209-215.

37.   Gouin, F., et al., *Open wedge high tibial osteotomies: Calcium-phosphate ceramic spacer versus autologous bonegraft.* Orthopaedics & Traumatology-Surgery & Research, 2010. **96**(6): p. 637-645.

38.   Koshino, T., et al., *Fifteen to twenty-eight years' follow-up results of high tibial valgus osteotomy for osteoarthritic knee.* Knee, 2004. **11**(6): p. 439-444.

39.   Naudie, D., et al., *Survivorship of the high tibial valgus osteotomy A 10-to 22-year followup study.* Clinical Orthopaedics and Related Research, 1999. **367**: p. 18-27.

40.   Billings, A., et al., *High Tibial Osteotomy with a Calibrated Osteotomy Guide, Rigid Internal Fixation, and Early Motion. Long-Term Follow-up*.* The Journal of Bone & Joint Surgery, 2000. **82**(1): p. 70-9.

41.   Flecher, X., et al., *A 12-28-year followup study of closing wedge high tibial osteotomy.* Clinical Orthopaedics and Related Research, 2006. **452**: p. 91-96.

42.   Gstöttner, M., et al., *Long-term outcome after high tibial osteotomy.* Archives of Orthopaedic and Trauma Surgery, 2008. **128**(3): p. 345-345.

43.   Hui, C., et al., *Long-Term Survival of High Tibial Osteotomy for Medial Compartment Osteoarthritis of the Knee.* American Journal of Sports Medicine, 2011. **39**(1): p. 64-70.

44.   Efe, T., et al., *TKA following high tibial osteotomy versus primary TKA - a matched pair analysis.* Bmc Musculoskeletal Disorders, 2010. **11**.

45.   Rinonapoli, E., et al., *Tibial osteotomy for varus gonarthrosis - A 10- to 21-year followup study.* Clinical Orthopaedics and Related Research, 1998(353): p. 185-193.

46.   Korovessis, P.M.D., et al., *Medium- and long-term results of high tibial osteotomy for varus gonathrosis in an agricultural population.* Orthopedics, 1999. **22**(8): p. 729-735.

47.   Nakhostine, M., et al., *A SPECIAL HIGH TIBIAL OSTEOTOMY TECHNIQUE FOR TREATMENT OF UNICOMPARTMENTAL OSTEOARTHRITIS OF THE KNEE.* Orthopedics, 1993. **16**(11): p. 1255-1258.

48.   Rudan, J.F. and M.A. Simurda, *HIGH TIBIAL OSTEOTOMY - A PROSPECTIVE CLINICAL AND ROENTGENOGRAPHIC REVIEW.* Clinical Orthopaedics and Related Research, 1990(255): p. 251-256.

49.   Yasuda, K., et al., *LONG-TERM EVALUATION OF HIGH TIBIAL OSTEOTOMY FOR MEDIAL OSTEOARTHRITIS OF THE KNEE.* Bulletin of the Hospital for Joint Diseases Orthopaedic Institute, 1991. **51**(2): p. 236-248.

50.   Hernigou, P., et al., *PROXIMAL TIBIAL OSTEOTOMY FOR OSTEOARTHRITIS WITH VARUS DEFORMITY - A 10 TO 13-YEAR*

FOLLOW-UP-STUDY. Journal of Bone and Joint Surgery-American Volume, 1987. **69A**(3): p. 332-354.

51. Briem, K., et al., *Effects of the amount of valgus correction for medial compartment knee osteoarthritis on clinical outcome, knee kinetics and muscle co-contraction after opening wedge high tibial osteotomy.* Journal of Orthopaedic Research, 2007. **25**(3): p. 311-318.

52. Takeuchi, R., et al., *Medial opening wedge high tibial osteotomy with early full weight bearing.* Arthroscopy: The Journal of Arthroscopic & Related Surgery, 2009. **25**(1): p. 46-53.

53. El-Azab, H.M., et al., *Limb alignment after open-wedge high tibial osteotomy and its effect on the clinical outcome.* Orthopedics, 2011. **34**(10): p. 767.

54. Fujisawa, Y., K. Masuhara, and S. Shiomi, *The effect of high tibial osteotomy on osteoarthritis of the knee. An arthroscopic study of 54 knee joints.* The Orthopedic clinics of North America, 1979. **10**(3): p. 585-608.

55. Sheehy, L., et al., *Does measurement of the anatomic axis consistently predict hip-knee-ankle angle (HKA) for knee alignment studies in osteoarthritis? Analysis of long limb radiographs from the multicenter osteoarthritis (MOST) study.* Osteoarthritis and Cartilage, 2011. **19**(1): p. 58-64.

56. Insall, J.N., D.M. Joseph, and C. Msika, *HIGH TIBIAL OSTEOTOMY FOR VARUS GONARTHROSIS - A LONG-TERM FOLLOW-UP-STUDY.* Journal of Bone and Joint Surgery-American Volume, 1984. **66A**(7): p. 1040-1048.

57. Hsu, R.W.W., et al., *NORMAL AXIAL ALIGNMENT OF THE LOWER-EXTREMITY AND LOAD-BEARING DISTRIBUTION AT THE KNEE.* Clinical Orthopaedics and Related Research, 1990(255): p. 215-227.

58. Aglietti, P.B., R.; Vena, L.M.; Baldini, A.; Mondaini, A., *High Tibial Valgus Osteotomy for Medial Gonarthrosis.* The journal of Knee Surgery, 2003. **16**(1): p. 6.

59. Takeuchi, R., et al., *Clinical results and radiographical evaluation of opening wedge high tibial osteotomy for spontaneous osteonecrosis of the knee.* Knee Surgery, Sports Traumatology, Arthroscopy, 2009. **17**(4): p. 361-368.

60. Birmingham, T.B., et al., *Medial Opening Wedge High Tibial Osteotomy: A Prospective Cohort Study of Gait, Radiographic, and Patient-Reported Outcomes.* Arthritis & Rheumatism-Arthritis Care & Research, 2009. **61**(5): p. 648-657.

61. Panagiotopoulou, O., *Finite element analysis (FEA): Applying an engineering method to functional morphology in anthropology and human biology.* Annals of Human Biology, 2009. **36**(5): p. 609-623.

62. Halloran, J.P., et al., *Concurrent musculoskeletal dynamics and finite element analysis predicts altered gait patterns to reduce foot tissue loading.* Journal of Biomechanics, 2010. **43**(14): p. 2810-2815.

63. Bendjaballah, M.Z., A. Shirazi-Adl, and D.J. Zukor, *Biomechanics of the human knee joint in compression: reconstruction, mesh generation and finite element analysis.* The Knee, 1995. **2**(2): p. 69-79.

64. Li, G., O. Lopez, and H. Rubash, *Variability of a three-dimensional finite element model constructed using magnetic resonance images of a knee for joint contact stress analysis.* Journal of Biomechanical Engineering-Transactions of the Asme, 2001. **123**(4): p. 341-346.

65.   Yang, N.H., et al., *Effect of Frontal Plane Tibiofemoral Angle on the Stress and Strain at the Knee Cartilage during the Stance Phase of Gait.* Journal of Orthopaedic Research, 2010. **28**(12): p. 1539-1547.

66.   Gardiner, J.C. and J.A. Weiss, *Subject-specific finite element analysis of the human medial collateral ligament during valgus knee loading.* Journal of Orthopaedic Research, 2003. **21**(6): p. 1098-1106.

67.   Pena, E., et al., *Finite element analysis of the effect of meniscal tears and meniscectomies on human knee biomechanics.* Clinical Biomechanics, 2005. **20**(5): p. 498-507.

68.   Pena, E., et al., *A three-dimensional finite element analysis of the combined behavior of ligaments and menisci in the healthy human knee joint.* Journal of Biomechanics, 2006. **39**(9): p. 1686-1701.

69.   Izaham, R., et al., *Finite element analysis of Puddu and Tomofix plate fixation for open wedge high tibial osteotomy.* Injury-International Journal of the Care of the Injured, 2012. **43**(6): p. 898-902.

70.   Blecha, L.D., et al., *How plate positioning impacts the biomechanics of the open wedge tibial osteotomy; a finite element analysis.* Computer Methods in Biomechanics and Biomedical Engineering, 2005. **8**(5): p. 307-13.

71.   Hohe, J., et al., *Three-dimensional analysis and visualization of regional MR signal intensity distribution of articular cartilage.* Medical Engineering & Physics, 2002. **24**(3): p. 219-227.

72.   Fowler, P.J., J.L. Tan, and G.A. Brown, *Medial Opening Wedge High Tibial Osteotomy: How I Do It.* Operative Techniques in Sports Medicine, 2012. **20**(1): p. 87-92.

73.   Kluess, D., et al., *A convenient approach for finite-element-analyses of orthopaedic implants in bone contact: Modeling and experimental validation.* Computer Methods and Programs in Biomedicine, 2009. **95**(1): p. 23-30.

74.   Armstrong, C.G., W.M. Lai, and V.C. Mow, *AN ANALYSIS OF THE UNCONFINED COMPRESSION OF ARTICULAR-CARTILAGE.* Journal of Biomechanical Engineering-Transactions of the Asme, 1984. **106**(2): p. 165-173.

75.   Donzelli, P.S., et al., *Contact analysis of biphasic transversely isotropic cartilage layers and correlations with tissue failure.* Journal of Biomechanics, 1999. **32**(10): p. 1037-1047.

76.   Chia, H.N. and M.L. Hull, *Compressive moduli of the human medial meniscus in the axial and radial directions at equilibrium and at a physiological strain rate.* Journal of Orthopaedic Research, 2008. **26**(7): p. 951-956.

77.   Bischoff, J.E., et al. *Advanced material modeling in a virtual biomechanical knee.* in *Abaqus Users' Conference.* 2008.

78.   Arnoux, P.J., et al., *A Visco-hyperelastic Model With Damage for the Knee Ligaments Under Dynamic Constraints.* Computer Methods in Biomechanics and Biomedical Engineering, 2002. **5**(2): p. 167-174.

79.   Mohamad Nor, N.M., N.A.A. Osman, and O. Atalullah. *Numerical measurement of contact pressure in the tibiofemoral joint during gait.* 2012.

80.   Erdemir, A., et al., *Considerations for reporting finite element analysis studies in biomechanics.* Journal of Biomechanics, 2012. **45**(4): p. 625-633.

81.   Yao, J., et al., *Sensitivities of medial meniscal motion and deformation to material properties of articular cartilage, meniscus and meniscal attachments*

using design of experiments methods. Journal of Biomechanical Engineering-Transactions of the Asme, 2006. **128**(3): p. 399-408.

82. Scanlan, S.F., et al., *Variations in the three-dimensional location and orientation of the ACL in healthy subjects relative to patients after transtibial ACL reconstruction.* Journal of Orthopaedic Research, 2012. **30**(6): p. 910-918.

83. Bendjaballah, M.Z., A. ShiraziAdl, and D.J. Zukor, *Finite element analysis of human knee joint in varus-valgus.* Clinical Biomechanics, 1997. **12**(3): p. 139-148.

84. Yao, J., et al., *Finite element modeling of knee joint contact pressures and comparison to magnetic resonance imaging of the loaded knee.* 2003 Advances in Bioengineering2003, New York: Amer Soc Mechanical Engineers. 247-248.

85. Yang, N.H., P.K. Canavan, and H. Nayeb-Hashemi, *The Effect of the Frontal Plane Tibiofemoral Angle and Varus Knee Moment on the Contact Stress and Strain at the Knee Cartilage.* Journal of Applied Biomechanics, 2010. **26**(4): p. 432-443.

86. Moschella, D., et al., *Wear patterns on tibial plateau from varus osteoarthritic knees.* Clinical Biomechanics, 2006. **21**(2): p. 152-158.

87. Magyar, G., S. Toksvig-Larsen, and A. Lindstrand, *Open wedge tibial osteotomy by callus distraction in gonarthrosis - Operative technique and early results in 36 patients.* Acta Orthopaedica Scandinavica, 1998. **69**(2): p. 147-151.

88. Parker, D.A. and D.G. Viskontas, *Osteotomy for the early varus arthritic knee.* Sports Medicine and Arthroscopy Review, 2007. **15**(1): p. 3-14.

89. Mabrey, J.D. and D.E. McCollum, *HIGH TIBIAL OSTEOTOMY - A RETROSPECTIVE REVIEW OF 72 CASES.* Southern Medical Journal, 1987. **80**(8): p. 975-980.

90. Cashaback, J.G.A. and J.R. Potvin, *Knee muscle contributions to joint rotational stiffness.* Human Movement Science, 2012. **31**(1): p. 118-128.

91. Erdemir, A., et al., *Model-based estimation of muscle forces exerted during movements.* Clinical Biomechanics, 2007. **22**(2): p. 131-154.

92. McLean, S.G., et al., *Knee joint anatomy predicts high-risk in vivo dynamic landing knee biomechanics.* Clinical Biomechanics, 2010. **25**(8): p. 781-788.